

# **From Aminopyridinato Complexes via Metal Containing SiCN Precursor Ceramics to Heterogeneous Recyclable Oxidation Catalysts**

DISSERTATION

zur Erlangung des akademischen Grades eines  
Doktors der Naturwissenschaften (Dr. rer. nat.)  
im Fach Chemie der Fakultät Biologie, Chemie und Geowissenschaften  
der Universität Bayreuth

vorgelegt von  
Dipl. Chem. Christoph Johannes Germund Glatz  
geboren in Weißenburg i. Bay.

Bayreuth, 2009

This thesis fulfils the requirements of the doctoral degree of the faculty of Biology, Chemistry and Geological Sciences at the University of Bayreuth.

Thesis submitted: 22.04.2009

Date of Scientific Colloquium: 17.07.2009

First examiner: Prof. Dr. Rhett Kempe

Second examiner: Prof. Dr. Josef Breu

Third examiner: Prof. Dr. Thomas Hellweg

Chairman: Prof. Dr. Rainer Schobert

The following work has been carried out from May 2006 to April 2009 at the Lehrstuhl für Anorganische Chemie II of the Universität Bayreuth under supervision of Prof. Dr. Rhett Kempe.

***Für meine Eltern***

**„Fümms bö wö tää zää Uu,  
pögiff,  
kwii Ee“**

*Kurt Schwitters*

## Alphabetical list of abbreviations

Ap <sup>BDMVS</sup> H <sub>2</sub>	2,6-Bis-( <i>N,N'</i> -dimethyl-vinylsilyl)-pyridine
Ap <sup>BTMS</sup> H <sub>2</sub>	2,6-Bis-( <i>N,N'</i> -trimethylsilyl)-pyridine
Ap <sub>2</sub> <sup>DMS</sup> H <sub>2</sub>	Dimethyl-bis-( <i>N,N'</i> -4-methyl-2-pyridyl)diaminosilan
Ap <sup>TMA</sup> H	4-Methyl-2-((2',4',6'-trimethylphenyl)-amino)-pyridine
Ap <sup>TMS</sup> H	4-Methyl-2-((trimethylsilyl)-amino)-pyridine
calcd	calculated
cod	1,5-Cyclooctadiene
Cu-SiCN	Copper containing silicon carbonitride
DCP	Dicumylperoxide
dipi	2,6-Diisopropylphenyl-imido
EDS / EDX	Energy dispersive X-ray spectroscopy / energiedispersive Röntgenspektroskopie
Et <sub>3</sub> N	Triethylamine
Et <sub>2</sub> O	Diethylether
GC	Gas chromatography
HDvV	Heisenberg-Dirac-van-Vleck
Me	Methyl
<i>n</i> BuLi	<i>n</i> -Butyllithium
n.d.	not determined
NMR	Nuclear magnetic resonance
ppm	parts per million
SiCN	Silicon carbonitride
SEM / REM	Scanning electron microscopy / Rasterelektronenmikroskopie
TBHP	<i>tert</i> -Butylhydroperoxide
<i>t</i> BuPy	4- <i>tert</i> -Butylpyridine
thf	Tetrahydrofurane
tht	Tetrahydrothiophene

## Table of Contents

<b>1.</b>	<b>Zusammenfassung/Summary .....</b>	<b>1</b>
<b>2.</b>	<b>Introduction.....</b>	<b>7</b>
<b>3.</b>	<b>Overview of Thesis Results.....</b>	<b>11</b>
3.1.	Synthesis and Structure of a Hexameric Silver and Tetrameric Gold aminopyridinates.....	11
3.2.	First Row Transition Metal Aminopyridinates - the Missing Complexes.....	12
3.3.	Novel Cu-SiCN Ceramics via Molecular Design – Part I: Synthesis and Characterisation of Cu-SiCN.....	13
3.4.	Novel Cu-SiCN Ceramics via Molecular Design – Part II: Variation of the Metal Content and Catalytical Activity.....	14
3.5.	Individual contribution to joint publications.....	15
<b>4.</b>	<b>Synthesis and Structure of a Hexameric Silver and Tetrameric Gold Aminopyridinates.....</b>	<b>17</b>
4.1.	Introduction .....	18
4.2.	Results and Discussion .....	18
4.3.	Conclusion .....	24
4.4.	Experimental Section.....	25
4.4.1.	General Procedures Synthesis and Structure .....	25
4.4.2.	Synthesis of the Complexes .....	25
4.4.3.	Acknowledgement.....	27
4.5.	References .....	27
<b>5.</b>	<b>First Row Transition Metal Aminopyridinates - the Missing Complexes .....</b>	<b>30</b>
5.1.	Introduction .....	31
5.2.	Results and Discussion .....	31
5.2.1.	Synthesis and Structural Charactersation .....	31
5.2.2.	Magnetic Properties .....	40
5.3.	Conclusions .....	42
5.4.	Experimental Section.....	43

5.4.1.	General .....	43
5.4.2.	Synthesis of the Complexes .....	43
5.4.3.	Acknowledgements .....	46
5.5.	References .....	46
5.6.	Supplementary Material .....	50

## **6. Novel Cu-SiCN ceramics via molecular design – Part I: Synthesis and characterisation of Cu-SiCN .....51**

6.1.	Introduction .....	52
6.2.	Results and Discussion .....	53
6.2.1.	Metal Complex Synthesis .....	53
6.2.2.	Transmetalation .....	55
6.2.3.	Crosslinking and Ceramisation .....	56
6.3.	Conclusion .....	58
6.4.	Experimental .....	59
6.4.1.	General Remarks .....	59
6.4.2.	Synthesis of the Complexes .....	60
6.4.3.	Transmetalation .....	60
6.4.4.	Crosslinking and Ceramisation .....	61
6.4.5.	Acknowledgement .....	61
6.5.	References .....	61
6.6.	Supplementary Material .....	64

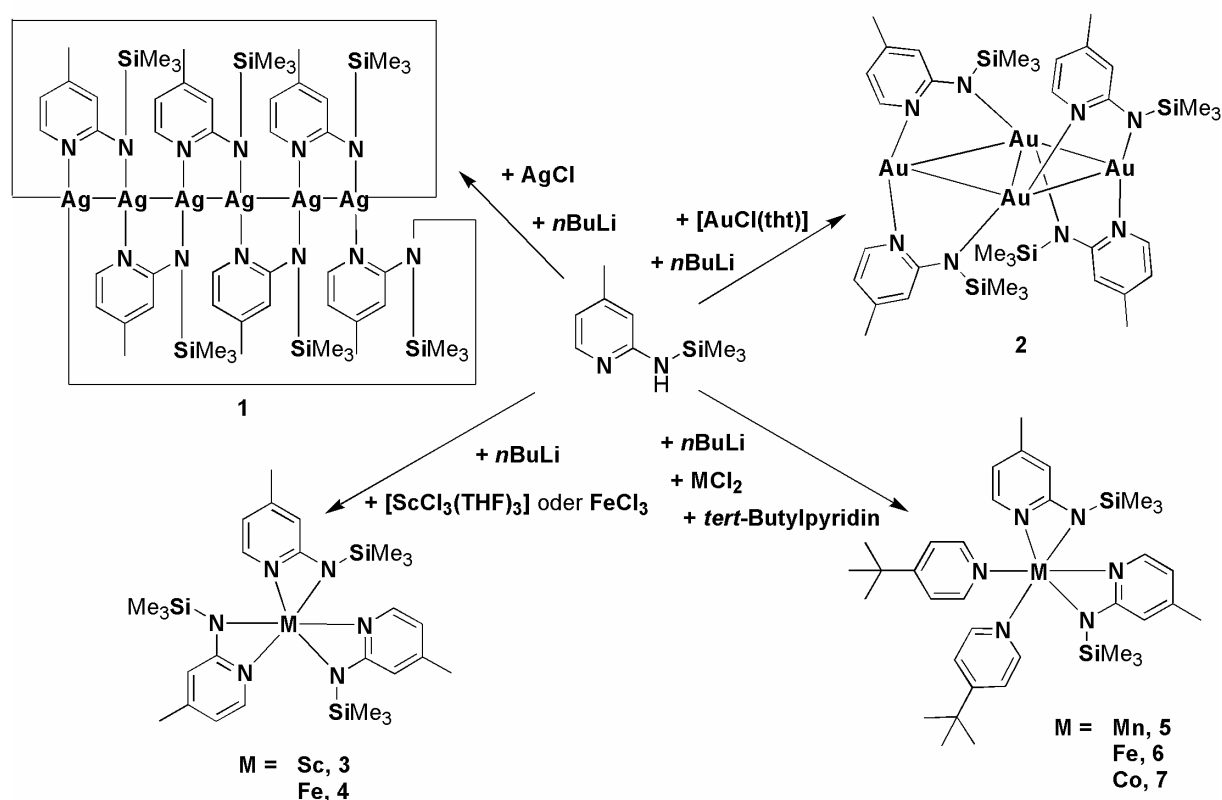
## **7. Novel Cu-SiCN ceramics via molecular design – Part II: Variation of the metal content and catalytical activity .....67**

7.1.	Introduction .....	68
7.2.	Results and Discussion .....	68
7.2.1.	Variation of the Metal Content .....	68
7.2.2.	Catalytical Activity .....	73
7.3.	Conclusion .....	76
7.4.	Experimental Section .....	77
7.4.1.	General Procedures .....	77
7.4.2.	Synthesis of the Ceramic Materials .....	77
7.4.3.	Catalytical Testings .....	78
7.5.	References .....	78

<b>8.</b>	<b>List of Publications .....</b>	<b>80</b>
<b>9.</b>	<b>Danksagung/Acknowledgment .....</b>	<b>83</b>
<b>10.</b>	<b>Declaration/Erklärung .....</b>	<b>87</b>
<b>11.</b>	<b>Appendix .....</b>	<b>88</b>

# 1. Zusammenfassung

Ziel dieser Arbeit ist die gezielte Synthese neuartiger, metallhaltiger Precursorkeramiken, die als heterogene Katalysatoren eingesetzt werden können. Hierzu wurde zunächst eine Reihe an Komplexen von Übergangsmetallen mit 2-Aminopyridinatliganden hergestellt und vollständig charakterisiert. Die Synthese aller Komplexe erfolgte mittels Salzmetathesereaktion.



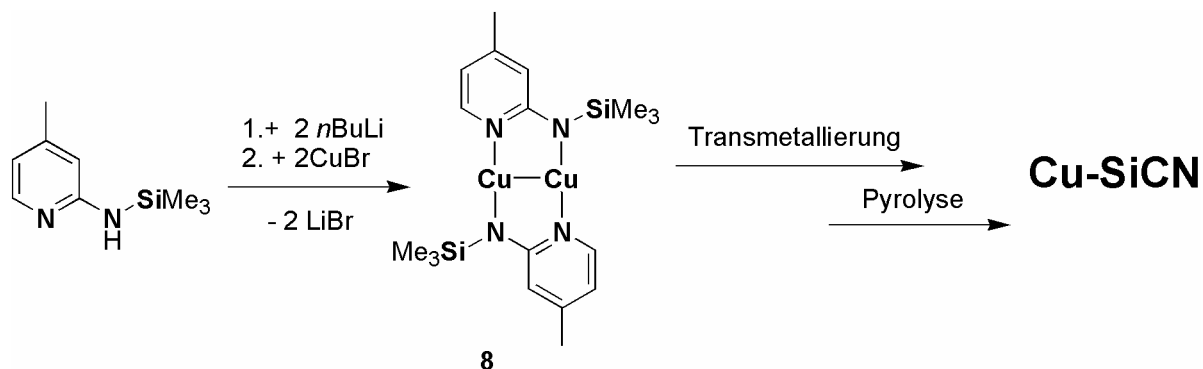
**Schema 1.1.** Allgemeine Synthese von Aminopyridinatkomplexen mittels Salzmetathesereaktion am Beispiel des in der Arbeit verwendeten Liganden  $\text{Ap}^{\text{TMS}}\text{H}$ .

Die auftretende lithiierte Zwischenstufe konnte isoliert und charakterisiert werden. Diese wurde als Ausgangssubstanz zur Synthese von Aminopyridinatokomplexen von verschiedenen Übergangsmetallen eingesetzt, die abhängig vom verwendeten Metall sehr unterschiedliche Strukturen zeigen. Im Fall von Silber wurde ein hochsymmetrischer, hexamerer Komplex (1) erhalten, in dem die Silberatome sesselartig angeordnet sind, wobei die Liganden abwechselnd ober- und unterhalb der Ringebene jeweils zwei Metallatome verbrücken. Hingegen wurde mit Gold ein

Tetramer (2) beobachtet, das in zwei Isomeren vorliegt. Die Liganden wirken auf zur Silberverbindung analoge Weise auch hier verbrückend (siehe Schema 1.1).

Bei der Verwendung von Übergangsmetallen, die in der Regel in höheren Oxidationsstufen vorliegen, koordiniert der Ligand vorzugsweise chelatisierend, sodass diese Verbindungen hochgespannt und damit hochreaktiv sind. Diese Komplexe liegen monomer vor und sind im Fall von dreiwertigen Metallionen homoleptisch ( $\text{Sc}^{3+}$ ,  $\text{Fe}^{3+}$ ), im Fall der meisten zweiwertigen Metallionen ( $\text{Mn}^{2+}$ ,  $\text{Fe}^{2+}$ ,  $\text{Co}^{2+}$ ) hingegen durch zusätzliche Neutralliganden stabilisiert (Schema 1.1). Die Umsetzbarkeit eines Liganden mit solch einer breiten Auswahl an Metallen spricht für seine Vielseitigkeit, und damit auch der Stoffklasse der Aminopyridinate.

Der verwendete Ligand besteht nur aus Elementen, die auch in Siliziumcarbonitridkeramiken (SiCN) enthalten sind. Diese werden aus Polysilazanen durch Vernetzung und anschließender Pyrolyse hergestellt. Aufgrund ihrer Herstellungsweise aus molekularen Vorläufern kann der Einbau von Metallen in die Keramik auf einem molekularen Weg erfolgen. Durch die hohe Reaktivität der Aminopyridinatkomplexe ist eine kovalente Anbindung der Metalle an die NH-Funktionen des Polysilazangerüsts möglich. Am Beispiel eines neu dargestellten Kupferaminopyridinatkomplexes (8, siehe Schema 1.2) wurde mittels NMR-Spektroskopie die Reaktion mit Polysilazanen nachgewiesen.



**Schema 1.2.** Herstellung von kupferhaltigen Precursorkeramiken unter Verwendung eines Kupferaminopyridinatkomplexes.

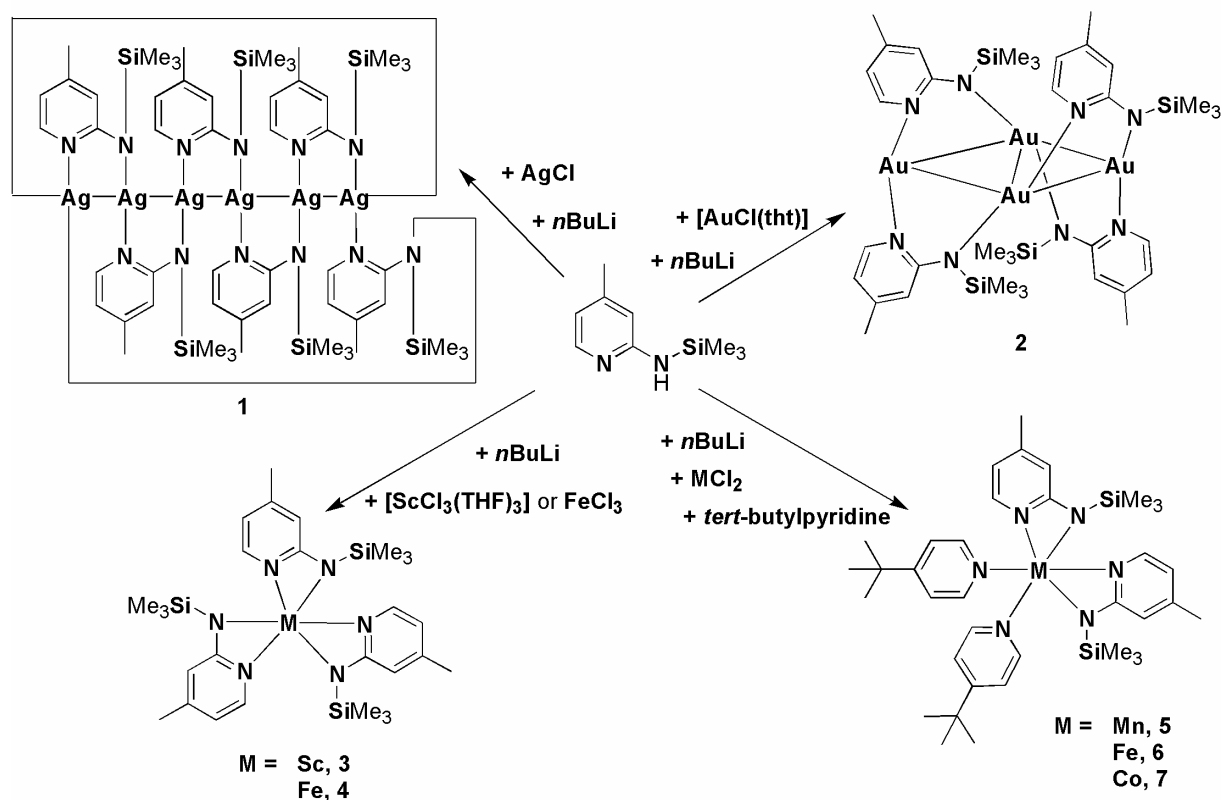
Selbst bei einem sehr hohen Metallgehalt lässt sich noch problemlos eine Keramik herstellen. Die gute keramische Ausbeute ist auf das zielorientierte Ligandendesign zurückzuführen. Mittels Pulverdiffraktometrie, Rasterelektronenmikroskopie (REM) und energiedispersiver Röntgenspektroskopie (EDX) konnte belegt werden, dass die kupferhaltige Keramik elementares und kristallines Kupfer enthält, das in Partikeln

verschiedener Größe vorliegt,. Der molekulare Ansatz zur Herstellung metallhaltiger SiCN-Precursorkeramiken konnte somit erfolgreich umgesetzt werden.

Weiterhin kann der Metallgehalt der Keramik durch Variation der zugegebenen Menge der Aminopyridinatkomponente in einem weiten Bereich gesteuert werden. Dabei sinkt die thermogravimetrisch bestimmte keramische Ausbeute mit steigendem Metallgehalt. Kupfer liegt unterhalb eines gewissen Metallgehalts nicht mehr in kristalliner Form vor. Mittels Festkörper-NMR-Messungen konnte elementares Kupfer auch bei niedrigerem Metallgehalt eindeutig identifiziert werden. Die Partikelgröße variiert bei hohen Kupfergehalten vom Nanometer- bis hin zum Mikrometerbereich, während bei niedrigen Gehalten nur noch Partikel im Nanometerbereich zu finden sind. Alle hergestellten kupferhaltigen Keramiken (Cu-SiCN) sind katalytisch aktiv bezüglich der aeroben selektiven Oxidation von Cycloalkanen zu den entsprechenden Cycloalkanonen. Hierbei besteht eine Abhängigkeit der Selektivität der Oxidation vom Metallgehalt. Je höher der Metallgehalt, desto größer ist die Selektivität. Die Katalysatoren sind rezyklierbar. Die hier vorgestellten Ergebnisse lassen darauf schließen, dass die neue Klasse an metallhaltigen SiCN-Precursorkeramiken auch in Bezug auf weitere Anwendungsgebiete ein hohes Potential besitzt.

## Summary

The objective of this thesis is the synthesis of novel, metal-containing precursor ceramics, which can be employed in heterogeneous catalysis. For this purpose, a series of transition-metal complexes stabilised by 2-aminopyridinato ligands was synthesised and characterised in extenso. The complexes were obtained by using salt metathesis reaction.

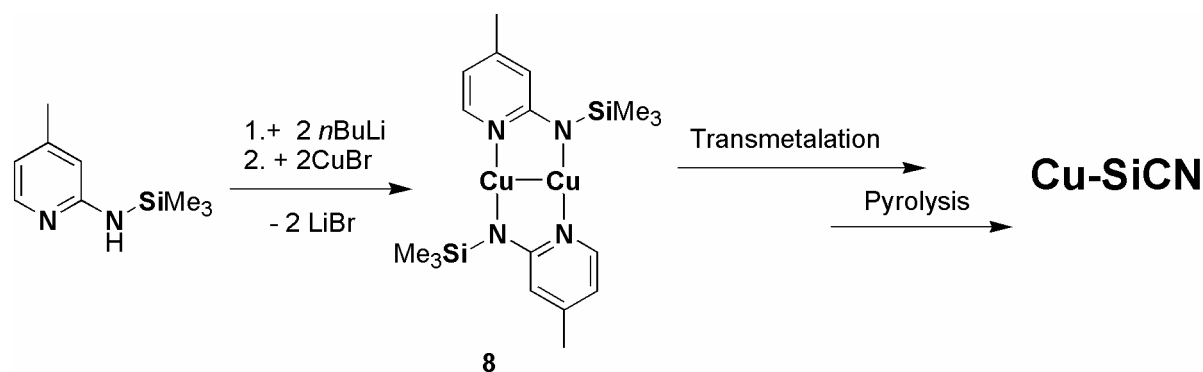


**Scheme 1.1.** General procedure for the synthesis of aminopyridinato complexes exemplified by the ligand Ap<sup>TMS</sup>H, which was used in this thesis.

The occurring lithium intermediate was isolated, characterised and employed as starting material for the synthesis of aminopyridinato complexes of different transition metals. The observed structures differ depending on the used metal. In case of silver a highly symmetrical hexameric complex (1) was obtained, in which each ligand bridges two metal atoms alternating above and below the ring plane. In contrast, when gold was employed a tetrameric complex (2) was obtained, which is present in two isomeric forms. The ligands bridge the metal atoms in an analogous fashion to the silver complex.

When transition metals are used, that usually take higher oxidation states, the ligand prefers to bind in a chelating mode. Therewith, these complexes show highly strained binding modes and thus, are highly reactive. The monomeric complexes are homoleptic in case of three valent metal ions ( $\text{Sc}^{3+}$ ,  $\text{Fe}^{3+}$ ). However, in case of most two valent metal ions ( $\text{Mn}^{2+}$ ,  $\text{Fe}^{2+}$ ,  $\text{Co}^{2+}$ ), the corresponding complexes are stabilised by additional neutral ligands (scheme 1.1). This indicates the high versatility of this ligand and most likely of the aminopyridinates.

The used ligand contains only elements that are also present in silicon-carbonitride ceramics ( $\text{SiCN}$ ), which are produceable from polysilazanes through crosslinking and subsequent pyrolysis. Because of the molecular pathway to these ceramics they are highly tunable and versatile materials. The introduction of metals can be achieved in a molecular fashion. With regard to the high reactivity of aminopyridinato complexes a covalent bond between metal and precursor can be formed. By using a newly synthesised copper-aminopyridinato complex (8, see scheme 1.2), the reaction with polysilazes was evidenced by NMR spectroscopy.



**Scheme 1.2.** Synthesis of copper containing SiCN precursor ceramics by use of a copper aminopyridinato complex.

Ceramics with extremely high metal content are achievable. Due to the targeted ligand design, relatively high ceramic yields were obtained. The presence of different sized, elemental and crystalline copper particles was documented by powder diffraction, scanning electron microscopy (SEM) and energy dispersive X-ray spectroscopy (EDS). This proves the feasibility of this new and molecular approach to metal-containing SiCN precursor ceramics.

Furthermore, the metal content of the ceramic is tunable in a broad range by varying the amount of added aminopyridinato complexes. The ceramic yield decreases with increasing metal content. Below a certain metal content no more crystalline copper

can be found in the ceramics, but still the presence of elemental copper was evidenced by solid-state NMR spectroscopy. Most likely, a homogeneous fine-particle distribution is present when even lower copper contents are achieved. Concerning high copper amounts the particle size varies from nanometer scale up to micrometer scale. In contrast, only nanometer-sized particles are observed at low copper concentration. All synthesised copper-containing SiCN precursor ceramics (Cu-SiCN) are highly active in selective aerobic oxidation reaction of cycloalkanes. With respect to the selectivity of the oxidation reaction this depends on the metal content: the larger the metal content, the higher is the selectivity. The catalysts are recyclable. The results presented in this thesis indicate the great potential of the novel class of metal-containing SiCN precursor ceramics towards other applications.

## 2. Introduction

The term “ceramics” originates from the Greek word “κεραμος”, which denotes clay and the related products. There is no standard obliging definition of the term “ceramic”.<sup>[1]</sup> Usually this term is used for all inorganic, non-metallic materials. In German, these materials are differentiated between glass, binding agents (such as cement, lime, gypsum...) and “Keramik”. In the following, the term “ceramic” is used as a synonym for “Keramik”.

Ceramics can be divided into three classes: silicate ceramics, oxide ceramics and non-oxide ceramics.<sup>[2]</sup> The latter are manufactured by using synthetic resources. This class includes borides, silicides, carbides, nitrides, carbonitrides and many others. These materials show high melting points, extreme hardness and corrosion resistance. These properties originate in the high covalent binding amount.<sup>[3,4]</sup> Conventionally, these ceramics are built up by powder technology. The powders are densified by using additives and yield microstructures, which exhibit definite grains and grain boundaries.<sup>[5]</sup> The macroscopic properties result from the microstructure of a material. Hence, high tunability of the ceramic precursors is desirable. To extend this tunability molecular, oligomeric or polymeric precursors can be employed. Thus, the macroscopic properties and the structure are adjustable by molecular design. The most interesting type of these ceramics is the silicon carbonitride (SiCN) precursor ceramics type, which is manufactured from oligo- or polysilazanes. The general route to these precursor ceramics is shown in Figure 2.1.<sup>[3]</sup> Concerning the molecular structure, these precursors can be modified in many ways and therefore different SiCN ceramics can be obtained.

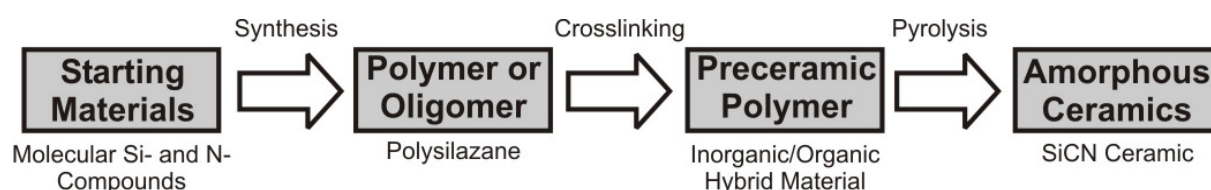


**Figure 2.1.** General route to precursor ceramics.

Currently, alumina and silica are used mainly as catalyst supports in industrial heterogeneous catalysis. But there are some disadvantages like chemical reactivity

and poor thermal conductivity. A SiCN matrix would be attractive owing to its excellent properties like extreme chemical resistance, high thermal stability, creeping stability and long term durability. This balances the efforts of processing SiCN precursor ceramics, which is for example due to the need of an oxygen-free atmosphere during pyrolysis.

To manufacture a catalyst, the metal (mostly transition metal) component has to be introduced into the ceramics. One approach is based on mixing metal powders or alloys with the ceramic precursor and subsequent ceramisation.<sup>[6,7,8]</sup> In order to maintain the advantages of the molecular approach to the SiCN precursor ceramics, a molecular pathway for the introduction of metals would be appropriate. A known method employs ferrocene-based precursors, but the general applicability is limited with regard to the low variety of available precursors.<sup>[9,10]</sup> Furthermore, organometallic compounds like carbonyls have been used but they are extremely toxic and volatile and thus, vaporise during ceramisation.<sup>[11]</sup> A covalent bond between metal and polysilazane would prevent this and provide many advantages like a homogeneous fine-distribution of the metal atoms in the ceramics. For this purpose, metal alkyls like trimethylaluminum<sup>[12]</sup> or early transition-metal amides<sup>[13]</sup> like amidotitanium complexes<sup>[14,15,16,17]</sup> have shown a certain potential for strong interaction with the ceramic precursor and thereby, increasing the ceramic yield. For late transition metals (whose usage would be interesting e.g. in catalysis) the corresponding amido metal complexes are not available or only in rather sophisticated compounds. In addition, late transition-metal alkyls are stable and do not necessarily react with the ceramic precursors. A save and general concept that allows the introduction of a broad variety of transition metals should be based on metal complexes that are able to react with the NH-functions of the polysilazane to form a covalent bond between the metal and the ceramic precursor.

For this reason, the first part of this work was focused on the synthesis of transition-metal complexes suitable for the metal modification of polysilazanes. A great variety of transition metals was addressed. Furthermore, the reactivity of these complexes towards NH-functions of polysilazanes was studied and the processibility of these metal-modified precursors to SiCN ceramics was investigated. The gained material was characterised with a broad variety of methods. Moreover, the obtained ceramics

were tested with regard to their catalytic properties. As assumed before, these new metal-containing SiCN precursor ceramics are highly active heterogeneous catalysts in selective aerobic oxidation reactions and show an enormous potential for further applications.

This thesis covers the synthesis of amido-metal compounds, their reactivity toward polysilzanes, the synthesis and characterisation of new metal-containing SiCN precursor ceramics and their application as heterogeneous catalyst in selective aerobic oxidation reactions.

- [1] W. Kollenberg in *Technische Keramik* (Ed.: W. Kollenberg), Vulkan, Essen **2004**, p. 3.
- [2] W. Kollenberg in *Technische Keramik* (Ed.: W. Kollenberg), Vulkan, Essen **2004**, p. 163.
- [3] E. Kroke, Y.-L. Li, C. Kornetschny, E. Lecomte, C. Fasel, R. Riedel, *Mater. Sci. Eng. R* **2000**, *26*, 97-199.
- [4] W. Kollenberg in *Technische Keramik* (Ed.: W. Kollenberg), Vulkan, Essen **2004**, p. 230.
- [5] J. Bill, F. Aldinger in *Precursor-Derived Ceramics* (Eds.: J. Bill, F. Wakai, F. Aldinger), Wiley-VCH, Weinheim **1999**, pp. 33-58.
- [6] G. Motz, *Adv. Sci. Technol.* **2006**, *50*, 24-30.
- [7] X. Yan, X. Cheng, G. Han, R. Hauser, R. Riedel, *Key Eng. Mater.* **2007**, *353-358*, 1485-1488.
- [8] P. Greil, *Adv. Eng. Mater.* **2000**, *2*, 339-348.
- [9] R. Petersen, D. A. Foucher, B.-Z. Tang, A. Lough, N. P. Raju, J. E. Greedan, I. Manners, *Chem. Mater.* **1995**, *7*, 2045-2053.
- [10] M. Ginzburg, M. J. MacLachlan, S. M. Yang, N. Coombs, T. W. Coyle, N. P. Raju, J. E. Greedan, R. H. Herber, G. A. Ozin, I. Manners, *J. Am. Chem. Soc.* **2002**, *124*, 2625-2639.
- [11] R. Hauser, A. Francis, R. Theismann, R. Riedel, *J. Mat. Sci.* **2008**, *43*, 4042-4049.

- [12] "Mechanical Properties and Performance of Engineering Ceramics and Composites": V. Salles, S. Foucaud, P. Goursat, in *Ceramic Engineering and Science Proceedings, Vol. 28*, Wiley, New York, **2000**, pp. 65-75.
- [13] R. Kempe, *Angew. Chem.* **2000**, *112*, 478-504; *Angew. Chem. Int. Ed.* **2000**, *39*, 468-493.
- [14] G. Motz, J. Hacker, G. Ziegler in *Ceramic Materials for Engines* (Eds.: J. G. Heinrich, F. Aldinger), Wiley-VCH, Weinheim **2001**, pp. 581-585.
- [15] G. Motz, G. Ziegler, *Key Eng. Mater.* **2002**, *206-213*, 475-478.
- [16] G. Motz, J. Hacker, G. Ziegler, in *Ceramic Engineering and Science Proceedings, Vol. 21*, Wiley, New York, **2000**, pp. 307-314.
- [17] N. Hering, K. Schreiber, R. Riedel, O. Lichtenberger, J. Woltersdorf, *Appl. Organomet. Chem.* **2001**, *15*, 879-886.

### 3. Overview of Thesis Results

This thesis comprises four publications, which are presented in chapter 4 to 7.

#### 3.1. Synthesis and Structure of a Hexameric Silver and Tetrameric Gold aminopyridinates

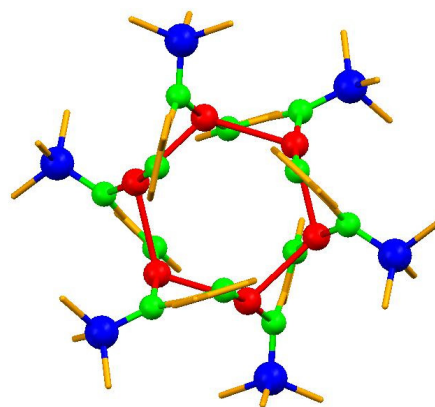


**Figure 3.1.** Top view of the silver aminopyridinate  $[\text{Ag}_6(\text{Ap}^{\text{TMS}})_6]$ .

The ligand 4-Methyl-2-((trimethylsilyl)amino)pyridine ( $\text{Ap}^{\text{TMS}}\text{H}$ ) was synthesised via salt metathesis reaction. Lithiation of  $\text{Ap}^{\text{TMS}}\text{H}$  with  $n\text{-BuLi}$  afforded the transmetalation agent  $[(\text{Ap}^{\text{TMS}})_2\text{Li}_2(\text{OEt}_2)_2]$  (**1**) which was structurally characterised. Reaction of **1** with  $\text{AgCl}$  and  $[\text{AuCl}(\text{tht})]$  ( $\text{tht}$  = tetrahydrothiophene) at low temperatures in thf yielded the corresponding homoleptic aminopyridinates of the heavier group 11 metals, namely  $[(\text{Ap}^{\text{TMS}})_6\text{Ag}_6]$  (**2**) and  $[(\text{Ap}^{\text{TMS}})_4\text{Au}_4]$  (**3a** and **b**) after work-up in hexane. All compounds were characterised by X-ray crystal structure analysis, NMR spectroscopy and elemental analyses. The quality of the structure determination of **3a** allows establishing the connectivity only. The lithium complex **1** shows the expected structure from analogous compounds. The hexameric silver compound shows a new structural motif for silver aminopyridinates. The six-membered ring of silver atoms has a chair conformation. Compounds **3a** and **b** are the first homoleptic gold aminopyridinates and exhibit a rhombic arrangement of the four gold atoms.

### 3.2. First Row Transition Metal Aminopyridinates - the Missing Complexes

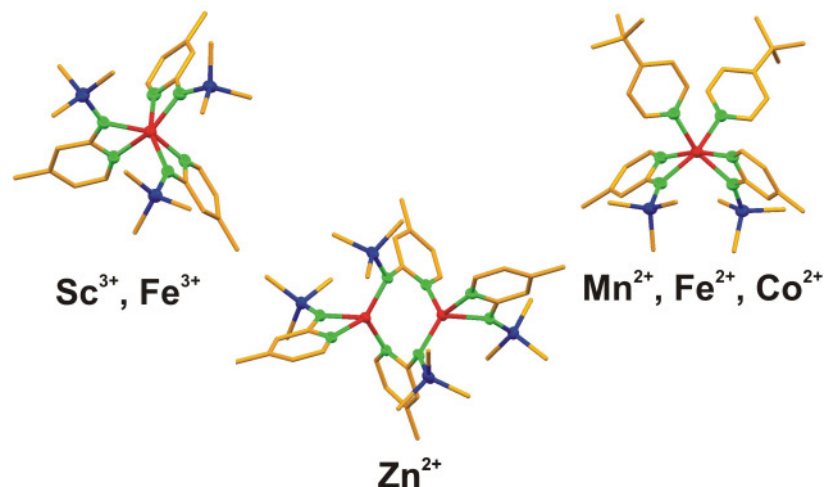


**Figure 3.2.** X-ray structures of transition metal aminopyridinates.

Lithiated 4-methyl-2-((trimethylsilyl)amino)pyridine ( $\text{Ap}^{\text{TMS}}\text{H}$ ) undergoes a salt metathesis reaction with  $[\text{ScCl}_3(\text{thf})_3]$  and  $\text{FeCl}_3$ , at low temperature in thf, to yield the homoleptic complexes  $[\text{Sc}(\text{Ap}^{\text{TMS}})_3]$  (**1**) and  $[\text{Fe}(\text{Ap}^{\text{TMS}})_3]$  (**2**). An analogous reaction with  $\text{MnCl}_2$ ,  $\text{CoCl}_2$  and  $\text{FeCl}_2$  using two equivalents 4-*tert*-butylpyridine (*t*BuPy) as additional donor ligand affords the structurally analogous *cis* complexes  $[\text{Mn}(\text{Ap}^{\text{TMS}})_2(\text{tBuPy})_2]$  (**3**),  $[\text{Co}(\text{Ap}^{\text{TMS}})_2(\text{tBuPy})_2]$  (**4**) and  $[\text{Fe}(\text{Ap}^{\text{TMS}})_2(\text{tBuPy})_2]$  (**5**). If  $\text{FeCl}_2$  is used without *t*BuPy, the highly symmetric trinuclear complex  $[\text{Fe}_3(\text{Ap}^{\text{TMS}})_6\text{Li}_2\text{O}]$  (**6**) is obtained. Furthermore, the use of  $\text{ZnCl}_2$  in a reaction with lithiated  $\text{Ap}^{\text{TMS}}\text{H}$  yields the dimeric complex  $[\text{Zn}_2(\text{Ap}^{\text{TMS}})_4]$  (**7**) in which two  $\text{Ap}^{\text{TMS}}$  ligands bridge the two metals. All complexes have been characterised by X-ray crystal structure analysis. To the best of our knowledge, complexes **1** and **2**, and **5** are the first scandium and iron aminopyridinates, respectively and complex **3** is the first manganese aminopyridinate complex which contains no additional anionic ligand. Complexes **4** and **7** are rare examples of cobalt and zinc aminopyridinates. This study proves that aminopyridinato ligands are highly universal ligands since they are able to stabilise early and late transition metals. Aminopyridinates of every first row transition metal are now available. The magnetic properties of all paramagnetic complexes were investigated. All complexes are high-spin complexes and the trinuclear iron complex **6** exhibits a weak antiferromagnetic coupling.

### 3.3. Novel Cu-SiCN Ceramics via Molecular Design – Part I: Synthesis and Characterisation of Cu-SiCN

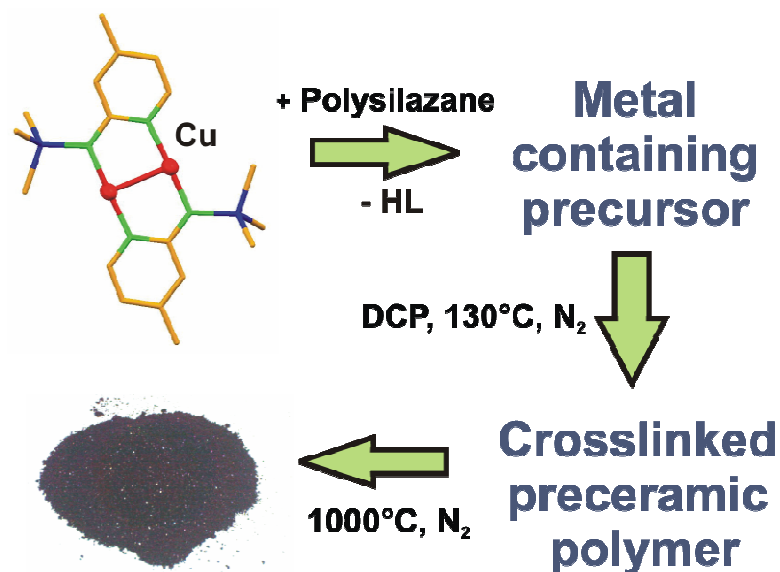


**Figure 3.3.** Molecular pathway to Cu-SiCN ceramics.

A molecular approach to metal containing ceramics is presented. 4-Methyl-2-((trimethylsilyl)amino)pyridine ( $\text{Ap}^{\text{TMSH}}$ ) was used in salt metathesis reactions to obtain copper aminopyridinates. Three obtained copper complexes were characterized by X-ray crystal structure analysis. The copper(I)aminopyridinate  $[\text{Cu}_2(\text{Ap}^{\text{TMS}})_2]$  **3** reacts with poly(organosilazanes) forming a covalent bonding between the Cu atom and the precursor as could be shown for the commercially available ceramic precursor HTT 1800 (Clariant Advanced Materials GmbH, Sulzbach, Germany). This reaction was studied via  $^1\text{H}$  and  $^{13}\text{C}$  NMR spectroscopy. The liberation of the free, protonated ligand  $\text{Ap}^{\text{TMSH}}$  is indirectly indicative of the binding of the copper atoms to the precursor. Cross-linking of the copper-modified poly(organosilazane) and subsequent pyrolysis leads to Cu containing ceramics. SEM measurements of the ceramic material in addition with EDS-mappings showed the presence of particles consisting of elemental copper. Powder diffraction experiments verified the presence of crystalline copper. This study proves the feasibility of this molecular approach to metal containing SiCN precursor ceramics by using silyl-aminopyridinato complexes. Since these complexes are known for nearly all transition metals and lanthanides a rather broad applicability of the concept can be expected.

### 3.4. Novel Cu-SiCN Ceramics via Molecular Design – Part II: The Selective Oxidation of Simple Alkanes Using Air

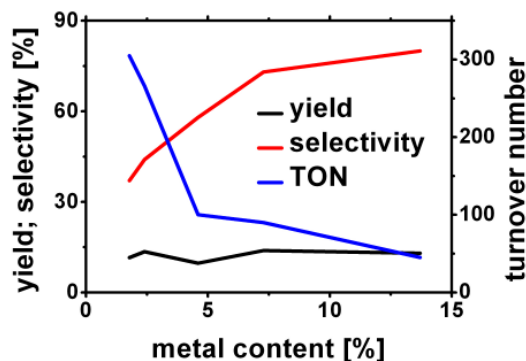


**Figure 3.4.** Yields, selectivities and turn-over-numbers of Cu-SiCN ceramics in aerobic oxidation of cycloalkanes

A series of copper containing SiCN precursor ceramics (Cu-SiCN) was synthesised via molecular design using copper aminopyridinates. This molecular approach allowed the variation of the metal content in a wide range and even high metal contents up to 14% are reachable. These ceramics can be synthesised in very good ceramic yields. Elemental copper is present and depending on the metal content it is detectable by solid-state copper NMR. SEM micrographs clearly indicate the existence of copper particles in all ceramics. The Cu-SiCN ceramics containing higher amounts of copper show a broad distribution of the particle size from micrometer-scale to nanometer-scale. However, only nanometer-scaled particles are found in less copper containing ceramics. Furthermore, a copper particle texture was found within the ceramics, which disappears with decreasing copper content. All ceramics show catalytical activity towards the oxidation of cycloalkanes by using air as oxidant. The selectivity of the reaction raises clearly with increasing copper content, whereas the turnover numbers decrease. The catalysts are recyclable and show only minor catalyst leaching. These results confirm the applicability of this new class of metal-containing ceramics in catalysis.

### 3.5. Individual contribution to joint publications

The results presented here were obtained in collaboration with co-workers and are published, submitted or to be submitted as indicated below. The individual contribution of all authors are specified. The corresponding author is denoted by an asterisk.

#### Chapter 4

This work was published in *Z. Allg. Anorg. Chem.* **2008**, 634, 2897-2902 with the title

**“Synthesis and Structure of a Hexameric Silver and Tetrameric Gold Aminopyridinates”**.

Germund Glatz, Günter Motz, and Rhett Kempe\*

I synthesised all presented compounds. Furthermore, all analyses were carried out by me and the publication was written by me. Günter Motz and Rhett Kempe were involved in scientific discussions, comments and correction of the manuscript.

#### Chapter 5

This work was published in *Eur. J. Inorg. Chem* **2009**, 1385-1392 with the title

**“First Row Transition Metal Aminopyridinates - the Missing Complexes”**.

Germund Glatz, Serhiy Demeshko, Günter Motz, and Rhett Kempe\*

I synthesised all presented compounds. All analyses were carried out by me except the susceptibility measurements, which were done by Serhiy Demeshko. The publication was written by me. Serhiy Demeshko, Günter Motz and Rhett Kempe were involved in scientific discussions, comments and correction of the manuscript.

## Chapter 6

This work is to be submitted with the title

**“Novel Cu-SiCN Ceramics via Molecular Design – Part I: Synthesis and Characterisation of Cu-SiCN”.**

Germund Glatz, Thomas Schmalz, Tobias Kraus, Günter Motz,\* and Rhett Kempe\*

I synthesised and characterised all presented compounds. All experiments concerning transmetalation were carried out by me. The ceramisation experiments were done together with Thomas Schmalz. Tobias Kraus did the SEM and EDX experiments as well as thermogravimetical analyses. The publication was written by me. Thomas Schmalz, Günter Motz and Rhett Kempe were involved in scientific discussions, comments and correction of the manuscript.

## Chapter 7

This work is to be submitted with the title

**“Novel Cu-SiCN Ceramics via Molecular Design – Part II: The Selective Oxidation of Simple Alkanes Using Air”.**

Germund Glatz, Thomas Schmalz, Tobias Kraus, Frank Haarmann, Günter Motz,\* and Rhett Kempe\*

The metal modification of the precursors and all experiments concerning catalytical activity were done by me. The ceramisation experiments were carried out together with Thomas Schmalz. Tobias Kraus did the SEM and EDX experiments as well as thermogravimetical analyses. Frank Haarmann did the solid-state copper NMR experiments. The publication was written by me. Thomas Schmalz, Frank Haarmann, Günter Motz and Rhett Kempe were involved in scientific discussions, comments and correction of the manuscript.

## 4. Synthesis and Structure of a Hexameric Silver and Tetrameric Gold Aminopyridinates

Germund Glatz,<sup>a</sup> Günter Motz,<sup>b</sup> Rhett Kempe<sup>a,\*</sup>

[a] Lehrstuhl für Anorganische Chemie II, Universität Bayreuth, 95440 Bayreuth, Germany, e-mail: kempe@uni-bayreuth.de

[b] Lehrstuhl Keramische Werkstoffe, Universität Bayreuth, 95440 Bayreuth, Germany

*Dedicated to Dr. habil. Werner Hanke in Recognition and Gratitude for his Work done for this Journal over the Last Decades*

**Keywords:** Gold; Lithium; Silver; Aminopyridinato ligands

Published in:

*Zeitschrift für Allgemeine und Anorganische Chemie* **2008**, 634, 2897-2902.

**Abstract.** 4-Methyl-2-((trimethylsilyl)amino)pyridine (Ap<sup>TMS</sup>H) was synthesized via a salt metathesis reaction. Lithiation of Ap<sup>TMS</sup>H with *n*-BuLi afforded the transmetallation agent [(Ap<sup>TMS</sup>)<sub>2</sub>Li<sub>2</sub>(OEt<sub>2</sub>)<sub>2</sub>] (**1**) which was structurally characterized. Reaction of **1** with AgCl and [AuCl(tht)] (tht = tetrahydrothiophene) at low temperatures in thf yielded homoleptic aminopyridinates of the heavier group 11 metals, namely [(Ap<sup>TMS</sup>)<sub>6</sub>Ag<sub>6</sub>] (**2**) and [(Ap<sup>TMS</sup>)<sub>4</sub>Au<sub>4</sub>] (**3a** and **b**) after work-up in hexane. All compounds were characterized by X-ray crystal structure analysis. The quality of the structure determination of **3a** allows establishing the connectivity only. The lithium complex **1** shows the expected structure from analogous compounds. The hexameric silver compound shows a new structural motif for silver aminopyridinates. The six-membered ring of silver atoms has a chair conformation. Compounds **3a** and **b** are the first homoleptic gold aminopyridinates and exhibit a rhombic arrangement of the four gold atoms.

## 4.1. Introduction

Aminopyridinates of late transition metals are far less investigated than those of early transition metals [1]. Silver and Gold complexes very often show highly aggregated structures or clusters of great beauty [2-5]. Thus, we became interested in silver and gold aminopyridinates. Gold amides are rare and the first base free a homoleptic silyl amide  $[\text{Au}(\mu\text{-N}(\text{SiMe}_3)_2)]_4$  was reported rather recently [6]. Silver and gold complexes are highly sensitive towards reduction on reaction with lithium alkyls or amides, especially if no stabilizing phosphanes are present. In order to avoid reduction, electrochemical methods [7], soft bases [8] or special starting materials [9, 10] are often applied. Because of synthesis problems, there are only a few homoleptic silver aminopyridinates, namely dinuclear [7, 8], tetranuclear [7, 11] and polymeric [7, 12, 13] ones. In contrast, there are no homoleptic gold aminopyridinate described in the literature to the best of our knowledge. Remarkable few, just three examples of heteroleptic gold aminopyridinates are documented [9, 10, 14], of which only one has been characterized by X-ray crystal structure analysis [9]. Here we report on the synthesis and structure of an unique highly symmetric hexameric silver aminopyridinate and the first homoleptic gold aminopyridinate. Silver and gold complexes stabilized by structurally similar alkyl and not amido ligand namely the trimethylsilyl substituted 6-methylpyridine ligand gave selectively dimeric structures [15, 16].

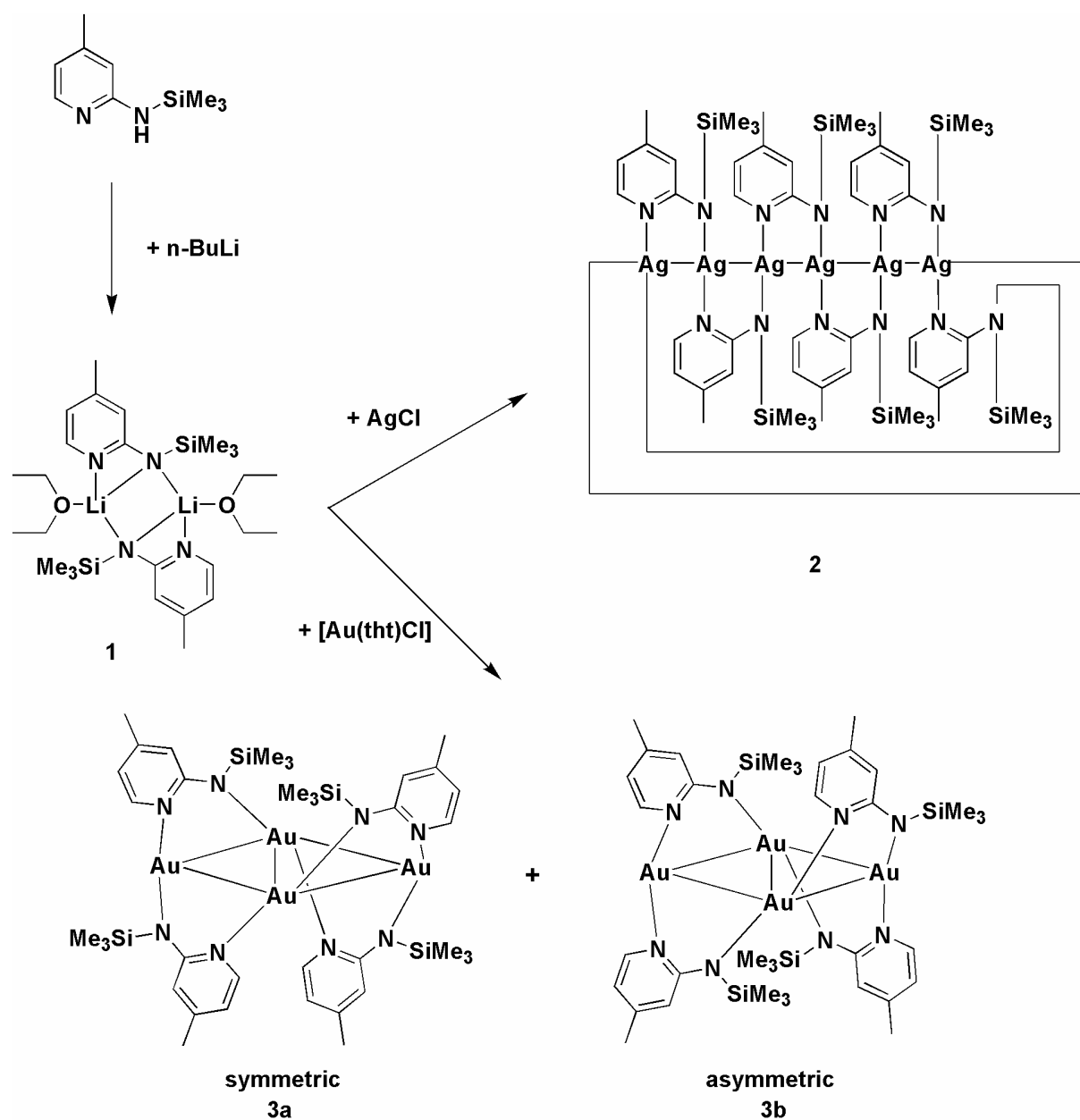
## 4.2. Results and Discussion

4-Methyl-2-((trimethylsilyl)amino)pyridine ( $\text{Ap}^{\text{TMS}}\text{H}$ ) was obtained following a published procedure [17]. The product was isolated in very good yields and purity after filtration and distillation.

The reaction of one equivalent  $\text{Ap}^{\text{TMS}}\text{H}$  with one equivalent of *n*-BuLi in  $\text{Et}_2\text{O}$  followed by concentration of the mother liquor yielded crystalline  $[(\text{Ap}^{\text{TMS}})_2\text{Li}_2(\text{OEt}_2)_2]$  (**1**) in very good yields (Scheme 1).

The  $^1\text{H-NMR}$  spectrum shows three signals at 7.79, 6.45 and 6.06 ppm belonging to the aromatic hydrogens of the deprotonated aminopyridine. The methyl group of the ligand shows a singlet at 1.94 ppm and the trimethylsilyl group shows a signal at 0.94

ppm. Additional signals at 0.91 (triplet) and 3.17 (quartet) can be assigned to the coordinated ether molecule. The  $^{29}\text{Si}$  spectrum shows one signal at -8.53 ppm.



**Scheme 1.** Synthesis of 1-3.

The observed single signal set is indicative of either a mononuclear or a highly symmetric polynuclear structural ensemble. Structurally similar lithium compounds show monomeric [11, 18-21], dimeric [11, 20, 22-27], heptameric [11, 28] or octameric [28-31] structures in the solid state. The solid state structure of **1** was determined by X-ray crystal structure analysis (Figure 1). This complex consists of two lithium centres which are coordinated tetrahedrally. Each aminopyridinato ligand is bridging the two metal atoms. Furthermore the amido nitrogen coordinates both

lithium atoms so that each ligand is acting as a chelating ligand at the same time. Each metal atom is coordinated by the oxygen atom of a diethyl ether ligand. The distance between the metal atoms is 2.532(7) Å and is in good agreement to the distances reported from dimeric lithium aminopyridinates (2.382 [20]-2.828 Å [24]).

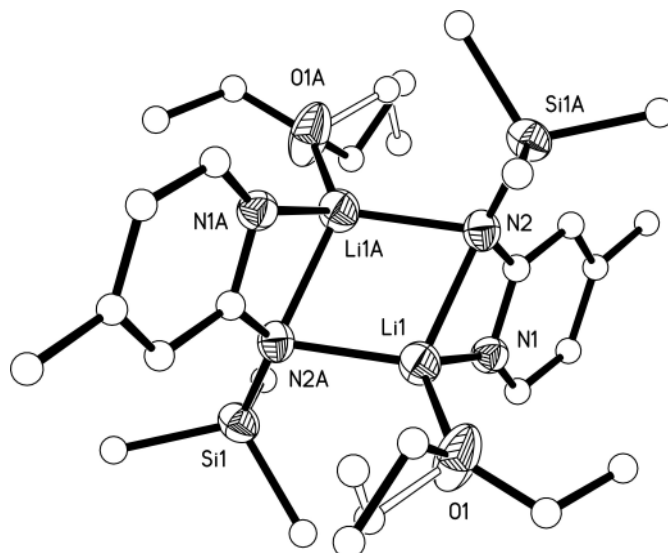


**Figure 1.** Molecule structure of **1** (ORTEP view; for clarity, only non carbon atoms are drawn as 50% probability ellipsoids). Selected bond lengths/Å and angles/°: Li1-O1 1.957(4), Li1-N1 2.046(4), Li1-N2 2.93(4), Li1-N2A-2.083(4), Li1-Li1 2.532(7), N2-Li1-N1 67.15(12), N1-Li1-O1 122.29(18), N1-Li1-N2A 112.30(17), N2-Li1-N2A 105.36(16) Li1-N2-Li1 74.64(16) O1-Li1-N2 124.51(19) O1-Li1-N2A 115.79(18).

The bond lengths Li-N<sub>pyridine</sub> are nearly equal to the Li-N<sub>Amido</sub> distances with 2.083(4) and 2.093(4) Å, respectively. This is in the range of Li-N distances known for aminopyridinates (1.901 [30]-2.289 Å [11]). The distance between lithium and the oxygen atom of the coordinating diethyl ether molecule is 1.957(4) Å. Lithium Aminopyridinates containing coordinated diethyl ether compounds show distances from 1.903 to 2.013 Å [11, 20, 31].

The reaction of one equivalent of **1** with one equivalent AgCl in Et<sub>2</sub>O/thf yielded after workup in hexane a beige powder of [(Ap<sup>TMS</sup>)<sub>6</sub>Ag<sub>6</sub>] (**2**) in moderate yield. The <sup>1</sup>H-NMR spectrum shows a single signal set. The expected signals of the ligand at 7.15, 6.20 and 5.46 ppm (aromatic protons) as well as two signals at 1.81 and 0.45 ppm belong to the methyl and trimethylsilyl group, respectively. The <sup>29</sup>Si spectrum shown one signal at -1.94 ppm. The molecular structure of **2** determined by X-ray crystal structure analysis is shown in Figure 2.

**Table 1:** Data of the X-ray crystal structure analyses

Compound	1	2	3
Formula	C <sub>16</sub> H <sub>50</sub> Li <sub>2</sub> N <sub>4</sub> O <sub>2</sub> Si <sub>2</sub>	C <sub>54</sub> H <sub>90</sub> Ag <sub>6</sub> N <sub>12</sub> Si <sub>6</sub>	C <sub>36</sub> H <sub>60</sub> Au <sub>4</sub> N <sub>8</sub> Si <sub>4</sub>
<i>F</i> <sub>w</sub>	520.76	1723.14	1505.12
Crystal system	triclinic	trigonal	monoclinic
Space group	<i>P</i> -1	<i>R</i> -3	<i>P</i> 2 <sub>1</sub> / <i>n</i>
<i>a</i> /Å	9.1640(11)	14.7880(11)	14.1670(5)
<i>b</i> /Å	10.0180(12)	14.7880(11)	13.5760(6)
<i>c</i> /Å	10.8040(13)	29.6560(12)	24.4830(9)
<i>α</i> /°	114.903(9)	90	90
<i>β</i> /°	109.669(9)	90	95.915(3)
<i>γ</i> /°	97.949(10)	120	90
<i>V</i> /Å <sup>3</sup>	800.32(17)	5616.5(6)	4683.8(3)
<i>Z</i>	1	3	4
<i>d</i> (calcd)/g/cm <sup>3</sup>	1.080	1.528	2.134
<i>μ</i> /mm <sup>-1</sup>	0.137	1.674	12.626
2 <i>θ</i> range/°	4.62-51.88	3.46-51.73	2.89-52.17
<i>ωR</i> <sup>2</sup> (all data)	0.1466	0.1053	0.0898
<i>R</i> value	0.0511	0.0530	0.0404

The silver atoms of this compound form a six-membered ring showing a chair conformation similar to that described for cyclohexane. Only one crystallographic independent silver atom and ligand are present.

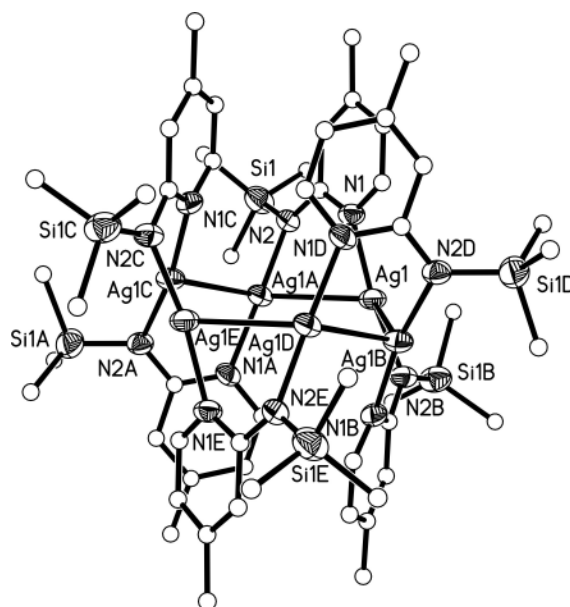


**Figure 2.** Molecular structure of **2** (ORTEP view; for clarity, only non carbon atoms are drawn as 50% probability ellipsoids). Selected bond lengths/Å and angles/°: Ag1-Ag1A 2.9099(8), Ag1-Ag1B 2.9099(8), Ag1-N1 2.117(6), Ag1-N2 2.095(7), Ag1A-Ag1-Ag1B 117.821(12), N2-Ag1-N1 170.2(3).

The silver atoms are coordinated by one N<sub>amido</sub> and one N<sub>pyridine</sub> atom from two different ligands. The ligands bridge the silvers alternating above and below the six-membered silver ring. The Ag-Ag distance is 2.9099(8) Å and represents the average found for silver aminopyridinates (2.74-2.98 Å) [7, 8, 11, 12]. The N<sub>pyridine</sub>-Ag and the

$N_{\text{amido}}\text{-Ag}$  bonds do not differ significantly (2.095(7) Å for Ag1-N2 and 2.117(6) for Ag1-N1) and are at the short end of the range reported in the literature (2.10-2.33 Å) [7, 8, 11, 12]. Complex **2** shows a new structural type for silver aminopyridinates since until now such complexes were known to be polymeric [7, 12, 13], dimeric [7, 8] or tetrameric [11]. A few examples of six-membered silver rings stabilized by other classes of ligands are known [32-34]. The synthesis of aminopyridinates using AgCl as a starting material is documented only once [11].

Initially AuCl was used to obtain gold(I) aminopyridinates. The reaction of (**1**) yielded gold precipitates only in a variety of solvents and at different temperatures. In order to avoid gold precipitation, [AuCl(tht)] was employed as starting material because it has been successfully used in a salt metathesis reaction with a lithium compound [35].

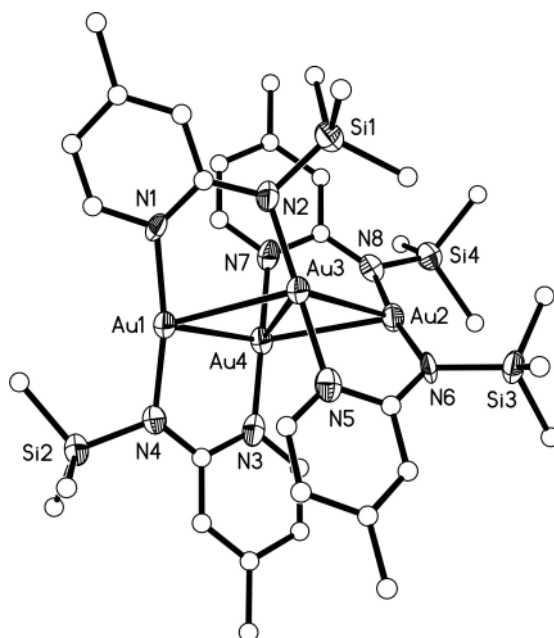


**Figure 3.** Molecule structure of **3** (ORTEP view; for clarity, only non carbon atoms are drawn as 50% probability ellipsoids). Selected bond lengths/Å and angles/°: Au1-N1 2.057(11), Au1-N4 2.045(11), Au2-N6 2.036(10), Au2-N8 2.044(12), Au3-N2 2.023(11), Au3-N5 2.048(12), Au4-N3 2.018(12), Au4-N7 2.016(12), Au1-Au3 2.9685(7), Au1-Au4 2.8684(7), Au3-Au4 3.1172(7), Au2-Au3 3.1270(8), Au2-Au4 2.9374(7), Au1-Au3-Au2 112.25(2), Au1-Au4-Au2 121.34(2), Au3-Au1-Au4 64.533(18), Au3-Au2-Au4 61.770(17).

At low temperatures and under exclusion of light a homoleptic gold aminopyridinates  $[(\text{Ap}^{\text{TMS}})_4\text{Au}_4]$  (**3a** and **b**) are formed. After workup with hexane and concentration of the mother liquor a beige powder of a mixture of **3a** and **b** in overall moderate yields was obtained. The presence of two different species in solution is indicative by  $^1\text{H}$ -NMR spectroscopy in the temperature range from -65 °C to 60 °C. If emanating from



The X-ray crystal structure of **3b** revealed that three ligands are oriented in one direction and one in the opposite direction. Two gold atoms are coordinated by one N<sub>pyridine</sub> and one N<sub>amido</sub> donor, one is coordinated by two N<sub>pyridine</sub> and one by two N<sub>amido</sub> donor functions. The structural motif of this complex is known from gold amidinates [36-39] and triazenides [40]. To the best of our knowledge there are only three known gold aminopyridinates [9, 10, 14] and only one of them is characterized by X-ray crystal structure analysis [9]. The Au-N distances in compound **3b** vary from 2.016(12) Å (N7-Au4) to 2.057(11) Å (N1-Au1) which is comparable with the distances reported of the known and structurally characterized gold aminopyridinate (2.054 to 2.093 Å) [9], the gold amidinates (2.000 to 2.085 Å) [36-39, 41] and triazenides (2.018 to 2.066 Å) [40]. The Au-Au distances are 2.8684(8), 2.9374(7), 2.9685(7), 3.1172(7) and 3.1270(8) Å for Au1-Au4, Au2-Au4, Au1-Au3, Au3-Au4 and Au2-Au3, respectively, which are as well in the range of the structurally known aminopyridinates (2.973 Å) [9], amidinates (2.646 to 3.103 Å) [36-39, 41] and triazenides (2.848 to 3.319 Å) [40]. The two sets of Au-Au-Au angles in the rhomb are 61.770(17)° (Au4-Au2-Au3) and 64.533(18)° (Au4-Au1-Au3) as well as 112.25(2)° (Au1-Au3-Au2) and 121.34(2)° (Au1-Au4-Au2). The angles reported for similar structures range from 63.47° to 71.47° and from 108.51° to 118.27° [36-40]. Thus, there is a larger rhombic distortion **3a,b** in comparison to the compounds reported in the literature suggesting a stronger fifth Au-Au interaction along the short diagonal in the rhomb.

### 4.3. Conclusion

Ap<sup>TMS</sup>H reacts with *n*-BuLi to form a dimeric lithium aminopyridinate. Salt metathesis reaction of this lithium salt with AgCl yields a hexameric silver aminopyridinate. An analogous reaction using AuCl gave metallic gold. Application of [AuCl(tht)] under exclusion of light yielded the first homoleptic gold aminopyridinates.

## 4.4. Experimental Section

### 4.4.1. General Procedures Synthesis and Structure

All reactions and manipulations with air sensitive compounds were performed under dry argon, using standard Schlenk and glovebox techniques. All reactions containing AgCl or [AuCl(tht)] and the following workup were performed under exclusion of light. Non halogenated solvents were distilled from sodium benzophenone ketyl and halogenated solvents from P<sub>2</sub>O<sub>5</sub>. Deuterated solvents were obtained from Cambridge Isotope Laboratories and were degassed, dried using molecular sieves and distilled prior to use.

Starting materials: 4-methyl-2-((trimethylsilyl)amino)pyridine (Ap<sup>TMS</sup>H) and [AuCl(tht)] were synthesized using literature methods. All other chemicals were purchased from commercial vendors and used without further purification if not otherwise mentioned in the synthetic procedure. NMR spectra were obtained using either a Bruker ARX 250 or Varian INNOVA 300 or a Varian INNOVA 400 spectrometer. Chemical shifts are reported in ppm relative to the residual protons of the deuterated solvent. X-ray crystal structure analyses were performed by using a STOE-IPDS II equipped with an Oxford Cryostream low-temperature unit. Structure solution and refinement were accomplished using SIR97 [42], SHELXL-97 [43] and WinGX [44]. Crystallographic details are summarized in Table 1. CCDC-713161 (compound **1**), -713162 (compound **2**), and -713163 (compound **3**) contain the supplementary crystallographic data for this publication. These data can be obtained free of charge at [www.ccdc.cam.ac.uk/conts/retrieving.html](http://www.ccdc.cam.ac.uk/conts/retrieving.html) (or from the Cambridge Crystallographic Data Centre, 12 Union Road, Cambridge CB2 1EZ, UK; Fax: + 44-1223-336-033; e-mail: [deposit@ccdc.cam.ac.uk](mailto:deposit@ccdc.cam.ac.uk)). Elemental analyses were carried out by Vario elementar EL III.

### 4.4.2. Synthesis of the Complexes

**Synthesis of 1:** A solution of Ap<sup>TMS</sup>H (1.803 g, 10 mmol) in 10 mL of Et<sub>2</sub>O was treated with 6.25 mL (1.6 M, 10 mmol) of *n*-BuLi in hexanes at -40 °C and stirred for 30 min. After stirring for 1 h at room temperature this mixture turned from colourless

to pale yellow and was allowed to stand. Colourless crystals formed overnight. Reducing the volume to 2 mL and filtration yielded a white powder. Crystals suitable for X-ray structure analysis were grown from a saturated solution of 1 in Et<sub>2</sub>O in a freezer at -30 °C. Yield: 2.316 mg (8.9 mmol, 89%). Anal. Found for C<sub>25</sub>H<sub>50</sub>Li<sub>2</sub>N<sub>4</sub>O<sub>2</sub>Si<sub>2</sub> (*M<sub>r</sub>*=520.75): C, 59.83; H, 9.73; N, 11.19%. Calcd: C, 59.97; H, 9.68; N, 10.76%.

<sup>1</sup>H NMR (C<sub>6</sub>D<sub>6</sub>, 296 K): δ = 0.43 (s, 18H, TMS), 0.91 (t, 12H, CH<sub>3</sub>), 1.94 (s, 6H, ar-CH<sub>3</sub>), 3.17 (q, 8H, CH<sub>2</sub>-O) 6.06 (d, 2H), 6.45 (s, 2H), 7.79 (s, 2H). <sup>13</sup>C NMR (C<sub>6</sub>D<sub>6</sub>, 296 K): δ = 2.71, 15.10, 21.66, 65.85, 110.63, 116.15, 147.44, 148.116, 172.17. <sup>29</sup>Si NMR (C<sub>6</sub>D<sub>6</sub>, 296 K): δ = -8.53.

**Synthesis of 2:** A solution of Ap<sup>TMS</sup>H (361 mg, 2 mmol) in 10 mL of Et<sub>2</sub>O was treated with 1.25 mL (1.6 M, 2 mmol) of *n*-BuLi in hexanes at -40 °C and stirred for 30 min. After stirring for 1 h at room temperature, this mixture was added to a suspension of AgCl (287 mg, 2 mmol) in 10 mL THF at -40 °C. The colour turned from colourless to pale brown. After stirring overnight at room temperature, the solvent was removed. The residue was extracted twice with 10 mL of hexane and filtered. Concentration of the mother liquor yielded a beige powder. Crystals suitable for X-ray analysis were obtained by slow evaporation of the mother liquor. Yield: 0.125 mg (0.44 mmol, 22%). Anal. Found for C<sub>54</sub>H<sub>90</sub>Ag<sub>6</sub>N<sub>12</sub>Si<sub>6</sub> (*M<sub>r</sub>*=1723.10): C, 38.04; H, 5.35; N, 9.70%. Calcd: C, 37.64; H, 5.26; N, 9.75%.

<sup>1</sup>H NMR (C<sub>6</sub>D<sub>6</sub>, 296 K): δ = 0.45 (s, 54H, TMS), 1.81 (s, 18H, ar-CH<sub>3</sub>), 5.46 (s, 6H), 6.20 (s, 6H), 7.15 (s, 6H). <sup>13</sup>C NMR (C<sub>6</sub>D<sub>6</sub>, 296 K): δ = 3.11, 21.32, 111.57 116.92, 147.52, 149.45, 183.21. <sup>29</sup>Si NMR (C<sub>6</sub>D<sub>6</sub>, 296 K): δ = -1.94.

**Synthesis of 3:** A solution of Ap<sup>TMS</sup>H (361 mg, 2 mmol) in 40 mL of Et<sub>2</sub>O was treated with 1.25 mL (1.6 M, 2 mmol) of *n*-BuLi in hexanes at 0 °C and stirred for 30 min. After stirring overnight at room temperature this mixture was added to a suspension of [AuCl(tht)] (641 mg, 2 mmol) in 30 mL toluene at -40 °C and the colour turned from white to purple. After stirring overnight at room temperature the solvent was removed. The residue was extracted twice with 15 mL of hexane and filtered. The pale yellow solution was concentrated and was allowed to crystallize in a freezer at -30 °C. After a few days colourless crystals were obtained. Further concentration yielded a beige powder. Total yield: 0.224 g (0.15 mmol, 30%). Anal. Found for C<sub>36</sub>H<sub>60</sub>Au<sub>4</sub>N<sub>8</sub>Si<sub>4</sub> (*M<sub>r</sub>*=1505.12): C, 29.09; H, 4.21; N, 7.28%. Calcd: C, 28.73; H, 4.02; N, 7.44%.

**3a:**  $^1\text{H NMR}$  ( $\text{C}_6\text{D}_6$ , 296 K):  $\delta = 0.47$  (s, 36H, TMS), 1.68 (s, 12H, ar- $\text{CH}_3$ ), 5.66 (d, 4H), 6.41 (s, 4H), 8.14 (d, 4H).  $^{13}\text{C NMR}$  ( $\text{C}_6\text{D}_6$ , 296 K):  $\delta = 3.48$ , 21.32, 112.32, 117.96, 146.40, 150.18, 165.36.  $^{29}\text{Si NMR}$  ( $\text{C}_6\text{D}_6$ , 296 K):  $\delta = 1.38$ .

**3b:**  $^1\text{H NMR}$  ( $\text{C}_6\text{D}_6$ , 296 K):  $\delta = 0.54$  (s, 18H, TMS), 0.65 (s, 9H, TMS), 0.66 (s, 9H, TMS), 1.62 (s, 3H, ar- $\text{CH}_3$ ), 1.66 (s, 3H, ar- $\text{CH}_3$ ), 1.71 (s, 6H, ar- $\text{CH}_3$ ), 5.40 (d, 1H), 5.48 (d, 1H), 5.57 (d, 1H), 5.76 (d, 1H), 6.37 (s, 1H), 6.39 (s, 1H), 6.52 (s, 1H), 6.58 (s, 1H), 7.73 (d, 1H), 8.18 (d, 1H), 8.23 (d, 1H), 8.26 (d, 1H).  $^{13}\text{C NMR}$  ( $\text{C}_6\text{D}_6$ , 296 K):  $\delta = 1.76$ , 3.68, 3.92, 3.97, 14.70, 21.21, 23.40, 32.31, 111.74, 111.82, 112.52, 112.85, 145.92, 146.60, 146.68, 146.74, 148.41, 148.84, 149.06, 150.03, 164.55, 165.06, 166.17, 166.68.  $^{29}\text{Si NMR}$  ( $\text{C}_6\text{D}_6$ , 296 K):  $\delta = -0.59$ , -0.31, 0.38, 4.23.

#### 4.4.3. Acknowledgement

Financial support from the DFG (SPP 1181 „Nanoskalige anorganische Materialien durch molekulares Design“) is acknowledged.

#### 4.5. References

- [1] R. Kempe, *Eur. J. Inorg. Chem.* **2003**, 791-803.
- [2] J. Strähle, *Metal Clusters in Chemistry* **1999**, 1, 535-560.
- [3] Y. Yang, P. R. Sharp, *J. Am. Chem. Soc.* **1994**, 116, 6983-6984.
- [4] D. Rais, J. Yau, D. M. P. Mingos, R. Vilar, A. J. P. White, D. J. Williams, *Angew. Chem. Int. Ed.* **2001**, 40, 3464-3467; *Angew. Chem.* **2001**, 117, 3572-3575.
- [5] H.-W. Lerner, G. Margraf, J. W. Bats, M. Wagner, *Chem. Commun.* **2005**, 4545-4547.
- [6] S. D. Bunge, O. Just, W. S. Rees, Jr., *Angew. Chem. Int. Ed.* **2000**, 39, 3082-3084; *Angew. Chem.* **2000**, 112, 3199-3200.
- [7] I. Beloso, J. Castro, J. A. Garcia-Vazquez, P. Perez-Lourido, J. Romero, A. Sousa, *Inorg. Chem.* **2005**, 44, 336-351.
- [8] C.-F. Lee, S. M. Peng, *J. Chin Chem. Soc.* **1991**, 38, 559-564.
- [9] E. M. Barranco, O. Crespo, M. C. Gimeno, P. G. Jones, A. Laguna, *Eur. J. Inorg. Chem.* **2004**, 4820-4827.
- [10] M. Burgos, O. Crespo, M. C. Gimeno, P. G. Jones, A. Laguna, *Eur. J. Inorg. Chem.* **2003**, 2170-2174.

- [11] L. M. Engelhardt, G. E. Jacobsen, P. C. Junk, C. L. Raston, B. W. Skelton, A. H. White, *J. Chem. Soc., Dalton Trans.* **1988**, 1001-1020.
- [12] J.-H. Liao, P.-L. Chen, C.-C. Hsu, *J. Phys. Chem. Solids* **2001**, *62*, 1629-1642.
- [13] E. Uhlig, M. Madler, *Z. Naturforsch.* **1965**, *20b*, 598-599.
- [14] S. Komiya, Y. Mizuno, *Nippon Kagaku Kaishi* **1988**, *4*, 591-596.
- [15] R. I. Papasergio, C. L. Raston, A. H. White, *J. Chem. Soc., Dalton Trans.* **1987**, 3085-3091.
- [16] T. R. van den Ancker, S. K. Bhargava, F. Mohr, S. Papadopoulos, C. L. Raston, B. W. Skelton, A. H. White, *J. Chem. Soc., Dalton Trans.* **2001**, 3069-3072.
- [17] R. Kempe, P. Arndt, *Inorg. Chem.* **1996**, *35*, 2644-2649.
- [18] K. O. Xavier, E. Smolensky, M. Kaphon, S. M. Aucott, J. D. Woolins, M. S. Eisen, *Eur. J. Inorg. Chem* **2004**, 4795-4802.
- [19] S. T. Liddle, W. Clegg, *J. Chem. Soc., Dalton Trans.* **2001**, 402-408.
- [20] N. M. Scott, T. Schareina, O. Tok, R. Kempe, *Eur. J. Inorg. Chem.* **2004**, 3297-3304.
- [21] D. Barr, W. Clegg, R. E. Mulvey, R. Snaith, *Chem. Commun.* **1984**, 469-470.
- [22] D. Barr, W. Clegg, R. E. Mulvey, R. Snaith, *Chem. Commun.* **1984**, 700-701.
- [23] J. Baldamus, M. L. Cole, U. Helmstedt, E.-M. Hey-Hawkins, C. Jones, P.C. Junk, F. Lange, N.A. Smithies, *J. Organomet. Chem.* **2003**, *665*, 33-42.
- [24] N. Feeder, R. Snaith, E. H. Wheatley, *Eur. J. Inorg. Chem.* **1998**, 879-883.
- [25] M. Polamo, M. Leskela, *Dalton Trans.* **1996**, 4345-4349.
- [26] W. Clegg, S. T. Liddle, *Acta Cryst. E* **2004**, *E60*, m1587-m1589.
- [27] R. Kempe, A. Spannenberg, S. Brenner, *Z. Kristallogr.* **1996**, *211*, 567-568.
- [28] D. R. Armstrong, W. Clegg, R. P. Davies, D. J. Linton, P. R. Raithby, R. Snaith, A. E. H. Wheatley, *Angew. Chem. Int Ed.* **1999**, *38*, 3367-3370; *Angew. Chem.* **1999**, *111*, 3568-3570.
- [29] S. M. Boss, M. P. Coles, V. Eyre-Brook, F. Garcia, R. Haigh, P. B. Hitchcock, M. McPartlin, J. V. Morey, H. Naka, P. R. Raithby, H. A. Sparkes, C. W. Tate, A. E. H. Wheatley, *Dalton Trans* **2006**, 5574-5582.
- [30] S. M. Boss, J. M. Cole, R. Haigh, R. Snaith, A. E. W. Wheatley, *Organometallics* **2004**, *23*, 4527-4530.
- [31] C. Jones, P. C. Junk, S. G. Leary, N. A. Smithies, *Dalton Trans.* **2000**, 3186-3190.

- [32] C.-W. Liu, I.-J. Shang, C.-M. Hung, J.-C. Wang, T.-C. Keng, *J. Chem. Soc. Dalton Trans.* **2002**, 1974-1979.
- [33] B. Djordevic, O. Schuster, H. Schmidtbour, *Inorg. Chem.* **2005**, *44*, 673-676.
- [34] P. Reiss, D. Fenske, *Z. Anorg. Allg. Chem.* **2000**, *626*, 2245-2247.
- [35] R. Uson, A. Laguna, M. Laguna, *Inorg. Synth.* **1989**, *26*, 85-91.
- [36] E. Hartmann, J. Strähle, *Z. Naturforsch., B* **1989**, *44*, 1-4.
- [37] A. A. Mohamad, H. E. Abdou, M. D. Irwin, J. M. López-de-Luzuriaga, J. P. Fackler Jr., *J. Cluster Sci.* **2003**, *14*, 253-266.
- [38] H. E. Abdou, A. A. Mohamad, J. M. López-de-Luzuriaga, J. P. Fackler Jr., *J. Cluster Sci.* **2004**, *15*, 397-411.
- [39] H. E. Abdou, A. A. Mohamad, J. P. Fackler Jr., *Inorg. Chem.* **2007**, *46*, 141-146.
- [40] J. Beck, J. Strähle, *Angew. Chem.* **1986**, *98*, 106-107; *Angew. Chem. Int. Ed.* **1986**, *25*, 95-96.
- [41] D. Fenske, G. Baum, A. Zinn, K. Dehnicke, *Z. Naturforsch. B* **1990**, *45*, 1273-1277.
- [42] A. Altomare, M. C. Burla, M. Camalli, G. L. Cascarano, C. Giacovazzo, A. Guagliardi, A. G. G. Moliterni, G. Polidori, R. Spagna, *J. Appl. Crystallogr.* **1999**, *32*, 115-119.
- [43] G. M. Sheldrick, *SHELX-97*, Program for Crystal Structure Analysis (Release 97n2), Institut für Anorganische Chemie der Universität Göttingen, Germany, **1998**.
- [44] L. J. Farrugia, *J. Appl. Crystallogr.* **1999**, *32*, 837-838.

## 5. First Row Transition Metal Aminopyridinates - the Missing Complexes

Germund Glatz,<sup>[a]</sup> Serhiy Demeshko,<sup>[b]</sup> Günter Motz,<sup>[c]</sup> Rhett Kempe<sup>\*,[a]</sup>

[a] Lehrstuhl für Anorganische Chemie II, Universität Bayreuth, 95440 Bayreuth, Germany, e-mail: kempe@uni-bayreuth.de

[b] Institut für Anorganische Chemie, Georg - August - Universität Göttingen, Tammannstraße 4, 37077 Göttingen.

[c] Lehrstuhl Keramische Werkstoffe, Universität Bayreuth, 95440 Bayreuth, Germany.

**Keywords:** N Ligands / Cobalt / Iron / Manganese / Scandium / Zinc

Published in:

*European Journal of Inorganic Chemistry* **2009**, 1385-1392.

**Abstract.** Lithiated 4-methyl-2-((trimethylsilyl)amino)pyridine ( $\text{Ap}^{\text{TMS}}\text{H}$ ) undergoes a salt metathesis reaction with  $[\text{ScCl}_3(\text{thf})_3]$  and  $\text{FeCl}_3$  at low temperature in *thf*, to yield the homoleptic complexes  $[\text{Sc}(\text{Ap}^{\text{TMS}})_3]$  (**1**) and  $[\text{Fe}(\text{Ap}^{\text{TMS}})_3]$  (**2**). An analogous reaction with  $\text{MnCl}_2$ ,  $\text{CoCl}_2$  and  $\text{FeCl}_2$  using two equivalents 4-*tert*-butylpyridine (*t*BuPy) as additional donor ligand affords the structurally analogous *cis* complexes  $[\text{Mn}(\text{Ap}^{\text{TMS}})_2(\text{tBuPy})_2]$  (**3**),  $[\text{Co}(\text{Ap}^{\text{TMS}})_2(\text{tBuPy})_2]$  (**4**) and  $[\text{Fe}(\text{Ap}^{\text{TMS}})_2(\text{tBuPy})_2]$  (**5**). If  $\text{FeCl}_2$  is used without *t*BuPy, the highly symmetric trinuclear complex  $[\text{Fe}_3(\text{Ap}^{\text{TMS}})_6\text{Li}_2\text{O}]$  (**6**) is obtained. Furthermore, the use of  $\text{ZnCl}_2$  in a reaction with lithiated  $\text{Ap}^{\text{TMS}}\text{H}$  yields the dimeric complex  $[\text{Zn}_2(\text{Ap}^{\text{TMS}})_4]$  (**7**) in which two  $\text{Ap}^{\text{TMS}}$  ligands bridge the two metals. All compounds were characterised by X-ray crystal structure analysis. To the best of our knowledge, complexes **1** and **2**, and **5** are the first scandium and iron aminopyridinates, respectively, and complex **3** is the first manganese aminopyridinate complex which contains no additional anionic ligand. Complexes **4** and **7** are rare examples of cobalt and zinc aminopyridinates. This study proves that aminopyridinato ligands are highly universal ligands since they are able to stabilize early and late transition metals. Aminopyridinates of every first

transition metal row metal are now available. The magnetic properties of all paramagnetic complexes were investigated. All complexes are high-spin complexes and the trinuclear iron complex **6** exhibits a weak antiferromagnetic coupling.

## 5.1. Introduction

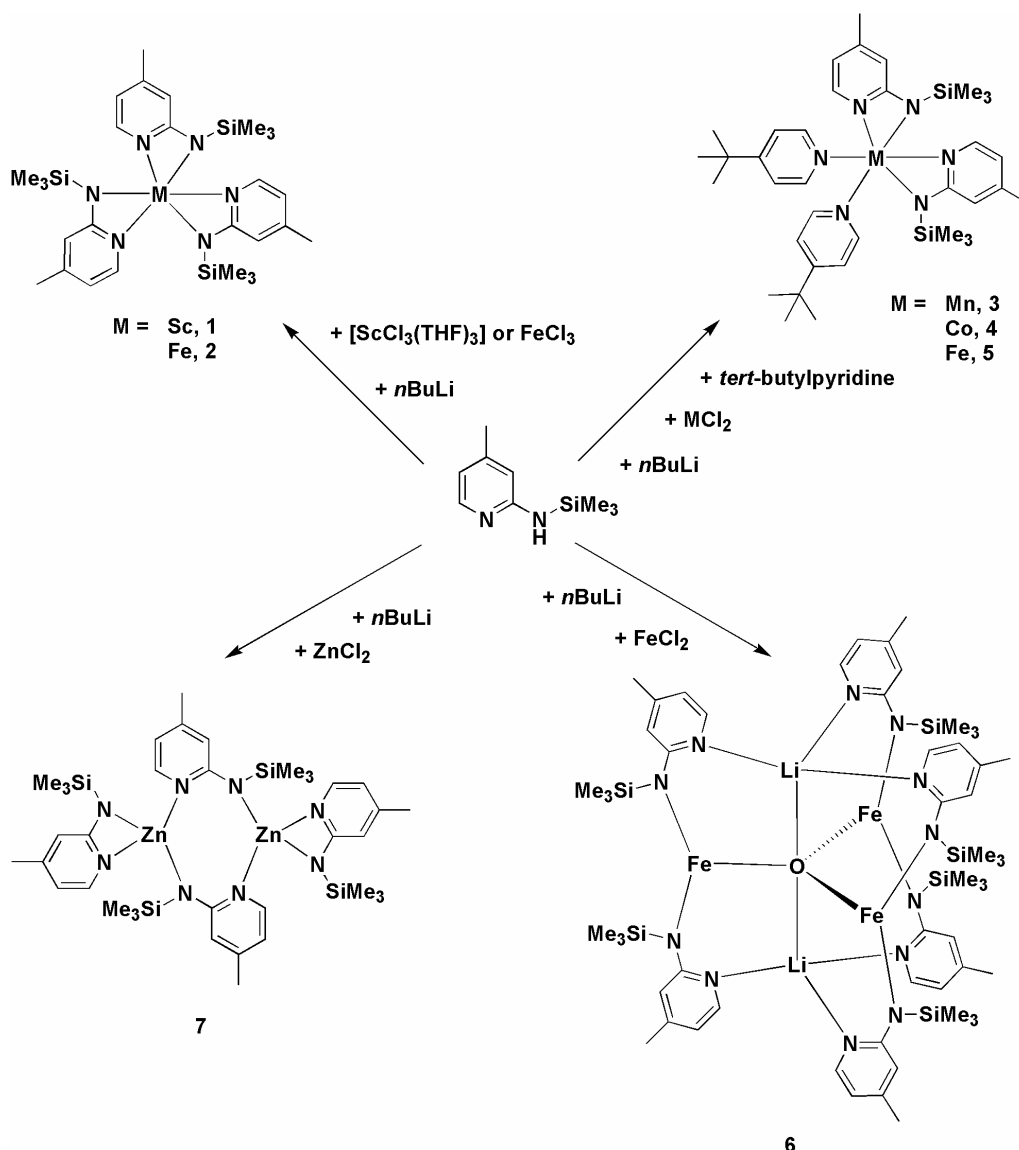
Aminopyridinates of the first row transition metals have been investigated for years.<sup>[1-3]</sup> Such complexes are mostly known for early transition metals like titanium, vanadium and chromium,<sup>[4-10]</sup> and only a few examples are known for the later first row transition metals like cobalt,<sup>[11]</sup> nickel,<sup>[12]</sup> copper<sup>[13,14]</sup> and zinc.<sup>[15]</sup> To the best of our knowledge, there are no known examples of aminopyridinate complexes for scandium and iron. A variety of related complexes are known for manganese,<sup>[16]</sup> cobalt,<sup>[17,18]</sup> nickel,<sup>[19]</sup> copper<sup>[20,21]</sup> and zinc,<sup>[22,23]</sup> but the ligands used are better described as pyridine-substituted sulfonamides rather than aminopyridinates because only the pyridine nitrogen of the ligand binds to the metal atom in many cases. Additionally, some complexes containing residual anionic non-aminopyridinate fragments such as a cyclopentadienyl fragment<sup>[24,25]</sup> (manganese), ethyl<sup>[13]</sup>, methyl<sup>[15]</sup> or  $\mu^4$ -oxo group<sup>[26]</sup> (zinc) are known. We decided to investigate whether it is possible to isolate stable aminopyridinate complexes of all first row transition metals using deprotonated, silyl substituted aminopyridines since we plan to use such complexes to prepare metal-containing SiCN ceramics and would prefer not to introduce other elements (beside the wanted metal) which are not part of the ceramic precursor. Herein we report on the synthesis and structural characterisation of  $\text{Ap}^{\text{TMS}}$  complexes of scandium, manganese, iron, cobalt and zinc and some aspects of the magnetic behaviour of the paramagnetic compounds.

## 5.2. Results and Discussion

### 5.2.1. Synthesis and Structural Characterisation

4-Methyl-2-((trimethylsilyl)amino)pyridine ( $\text{Ap}^{\text{TMSH}}$ ) was obtained following a published procedure.<sup>[27]</sup> The product was isolated in very good yields and purified by distillation.  $[\text{ScCl}_3(\text{thf})_3]$  was synthesised according to a literature procedure.<sup>[28]</sup> The

synthesis of all compounds presented here is shown in Scheme 1. A mixture of three equivalents  $\text{Ap}^{\text{TMS}}\text{H}$  and three equivalents  $n\text{BuLi}$  in  $\text{Et}_2\text{O}$  was treated with one equivalent of  $[\text{ScCl}_3(\text{thf})_3]$  or  $\text{FeCl}_3$  in  $\text{thf}$ . After workup,  $[\text{Sc}(\text{Ap}^{\text{TMS}})_3]$  (**1**) was obtained as a white powder in moderate yields. In the case of iron, a deep purple precipitate of  $[\text{Fe}(\text{Ap}^{\text{TMS}})_3]$  (**2**) was obtained in moderate yields. Crystalline **1** and **2** could be obtained by concentration of the mother liquor followed by storage at  $-30\text{ }^\circ\text{C}$ . The  $^1\text{H}$  NMR spectrum of **1** exhibits singlets at 0.37 and 1.76 ppm for the trimethylsilyl group and the methyl group attached to the pyridine ring, respectively.



Scheme 1: Synthesis of 1-7.

Additional signals at 5.82, 6.33 and 7.55 ppm belong to the three aromatic protons. The  $^{29}\text{Si}$  NMR spectrum shows one signal at  $-5.62$  ppm. The X-ray crystal structure

analyses of complexes **1** and **2** show that they are monomeric in the solid state (Figures 1 and 2, respectively), with the metal coordinated by three ligands in a distorted octahedral fashion. All ligands are  $\eta^2$ -coordinating. The  $N_{\text{pyridine}}\text{-Sc}$  bond lengths vary from 2.220(5) (N3–Sc1) to 2.245(4) Å (N5–Sc1) and the  $N_{\text{amido}}\text{-Sc}$  bond lengths from 2.169(4) (N4–Sc1) to 2.182(4) Å (N6–Sc1), with just a small difference between the two different nitrogen donor types.<sup>[29]</sup> The Sc–N distances in complex **1** lie in between those for a pure Sc– $N_{\text{amido}}$  bond (2.000 Å)<sup>[30]</sup> and a pure Sc– $N_{\text{pyridine}}$  bond (2.309 Å).<sup>[31]</sup> This can be understood as a “mixture” of both amidopyridine and aminopyridinate binding modes<sup>[29]</sup> and a significant delocalisation of the anionic function of the ligand at the  $N_{\text{amido}}$  atom. The N–Sc–N bond angles vary from 61.81 (N6–Sc1–N5) to 62.31° (N2–Sc1–N1) and reveal the highly strained binding mode of the aminopyridinate ligands.

In the case of iron, the  $N_{\text{pyridine}}\text{-Fe}$  bond length range from 2.147(3) (N3–Fe1) to 2.191(3) Å (N5–Fe1) and the  $N_{\text{amido}}\text{-Fe}$  distances from 2.037(3) (N6–Fe1) to 2.054(3) Å (N4–Fe1). A pure iron(III)– $N_{\text{amido}}$  bond is about 1.918 Å,<sup>[32]</sup> whereas the iron(III)–pyridine distances vary from 1.984<sup>[33]</sup> to 2.274 Å<sup>[34]</sup> and depend on temperature and spin state.<sup>[33]</sup> The N–Fe distances in complex **2** are therefore indicative of a dominant amidopyridine binding mode. The Fe–N bond angles range from 63.74 (N5–Fe1–N6) to 64.14° (N3–Fe1–N4).

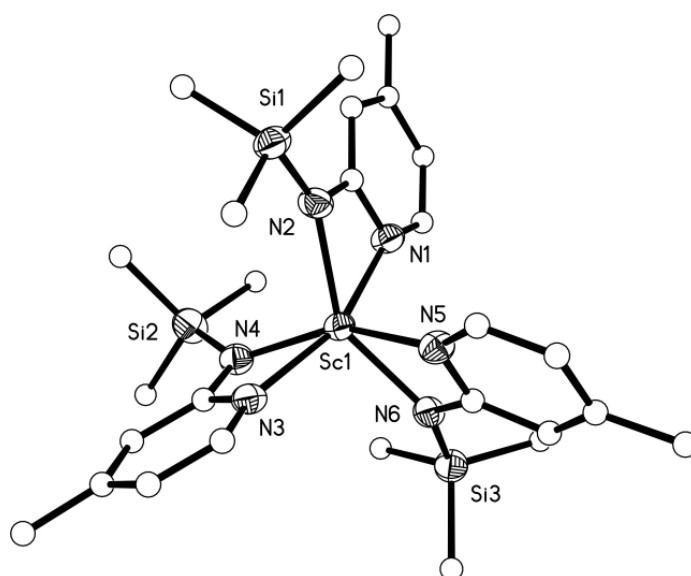
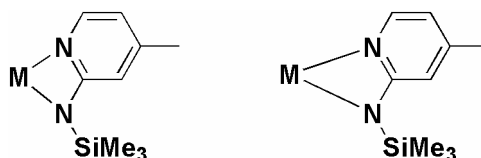


Figure 1. Molecule structure of **1** (ORTEP view; for clarity, only non carbon atoms are drawn as 50% probability ellipsoids). Selected bond lengths [Å] and angles [°]: Sc1–N1 2.225(4), Sc1–N2 2.174(4), Sc1–N3 2.220(5), Sc1–N4 2.169(4), Sc1–N5 2.245(4), Sc1–N6 2.182(4), N1–Sc1–N2 62.31(15), N3–Sc1–N4 62.22(16), N5–Sc1–N6 61.81(15).

The N-M-N angles of the homoleptic trivalent metal aminopyridinates ( $\text{Sc}^{3+}$ ,  $\text{Fe}^{3+}$ ,  $\text{Ti}^{3+}$ ,<sup>[4]</sup>  $\text{Cr}^{3+}$ <sup>[4]</sup>) decrease with increasing effective ionic radius of the metal (Table 1). This can be explained geometrically: the N-C-N angle and C-N bond lengths of the ligand can be assumed to be rigid, which leads, in case of increasing M-N bond lengths (which is due to a larger effective ionic radius), to a decrease of the chelating angle (Scheme 2).



Scheme 2. Influence of M-N bond length on the N-M-N chelating angle. A short M-N distance leads to a relatively large chelating angle (left hand) and a large M-N distance leads to a small chelating angle (right hand).

The smallest angles are observed in case of scandium, which has the largest effective ionic radius of the trivalent metals (mean angle:  $62.11^\circ$ ). Titanium has a smaller effective ionic radius, which leads to a larger mean bond angle ( $64.07^\circ$ ). The largest N-M-N bond angles are found for chromium (mean angle:  $65.98^\circ$ ). It can therefore be concluded that the smaller the metal ion, the larger the N-M-N bond angle. The only metal ion that does not match this sequence perfectly is iron(III), possibly due to the large difference between the mean  $\text{M-N}_{\text{pyridine}}$  and the mean  $\text{M-N}_{\text{amido}}$  bond lengths (see Table 1)

Table 1. Effective ionic radii and mean bond angle of homoleptic trivalent metal complexes.

Metal ion	Effective ionic radius	Mean N-M-N bond angle	Mean M-N distance	Mean $\text{M-N}_{\text{pyridine}}$ distance	Mean $\text{M-N}_{\text{amido}}$ distance
$\text{Sc}^{3+}$	88.5	62.1	2.21	2.23	2.18
$\text{Ti}^{3+}$ <sup>[4]</sup>	81	64.1	2.12	2.15	2.09
$\text{Fe}^{3+}$	78.5	64.0	2.11	2.17	2.04
$\text{Cr}^{3+}$ <sup>[4]</sup>	75.5	66.0	2.06	2.04	2.07

$\text{MnCl}_2$ ,  $\text{CoCl}_2$  and  $\text{FeCl}_2$  were used as starting material to obtain manganese(II), cobalt(II) and iron(II) aminopyridinate. Two equivalents of 4-*tert*-butylpyridine (*t*BuPy) were employed as an additional neutral donor ligand in order to obtain an octahedral coordination sphere. After workup,  $[\text{Mn}(\text{Ap}^{\text{TMS}})_2(\text{tBuPy})_2]$  (**3**) was obtained as a highly air-sensitive orange precipitate and  $[\text{Co}(\text{Ap}^{\text{TMS}})_2(\text{tBuPy})_2]$  (**4**) as a ochre-green precipitate, both in moderate yields. In the case of iron(II)  $[\text{Fe}(\text{Ap}^{\text{TMS}})_2(\text{tBuPy})_2]$  (**5**) could be isolated as a dark red crystalline material in very good yields. Single crystals

of **3**, **4** and **5** were obtained by concentration of the mother liquor followed by storage at -30 °C. The molecular structures of **3**, **4** and **5** were determined by X-ray analysis (Figures 3, 4 and 5, respectively). Further crystallographic details can be found in Table 3.

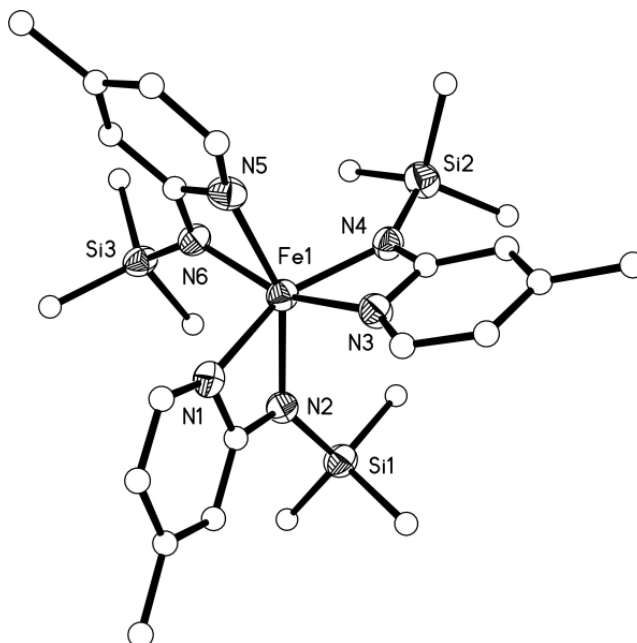


Figure 2. Molecule structure of **2** (ORTEP view; for clarity, only non carbon atoms are drawn as 50% probability ellipsoids). Selected bond lengths [Å] and angles [°]: Fe1–N1 2.166(3), Fe1–N2 2.042(3), Fe1–N3 2.147(3), Fe1–N4 2.054(3), Fe1–N5 2.191(3), Fe1–N6 2.037(3), N1–Fe1–N2 64.06(10), N3–Fe1–N4 64.14(10), N5–Fe1–N6 63.74(10).

Compounds **3**, **4** and **5** are isostructural monomeric complexes containing two  $\eta^2$ -chelating ligands as well as two additional neutral *t*BuPy ligands in a *cis* arrangement. The N–M–N aminopyridinate bond angles vary from 59.86(15) (N1–Co1–N2) to 62.02(9)° (N3–Fe1–N4) and reveal a strained binding mode of the aminopyridinate ligands, which leads to a distorted octahedral coordination of the metal atom. The  $N_{\text{amido}}\text{--M}$  bond lengths are significantly shorter (2.1927(15) and 2.1998(16) Å for **3**, 2.209(4) and 2.217(5) Å for **4**, 2.139(2) and 2.149(2) Å for **5**) than the corresponding  $N_{\text{pyridine}}\text{--M}$  distances [2.2997(16) and 2.3240(16) Å for **3**, 2.284(5) and 2.310(5) Å for **4**, 2.227(2) and 2.245(2) Å for **5**], which indicates a localisation of the anionic function of the ligand at the amido N atom.

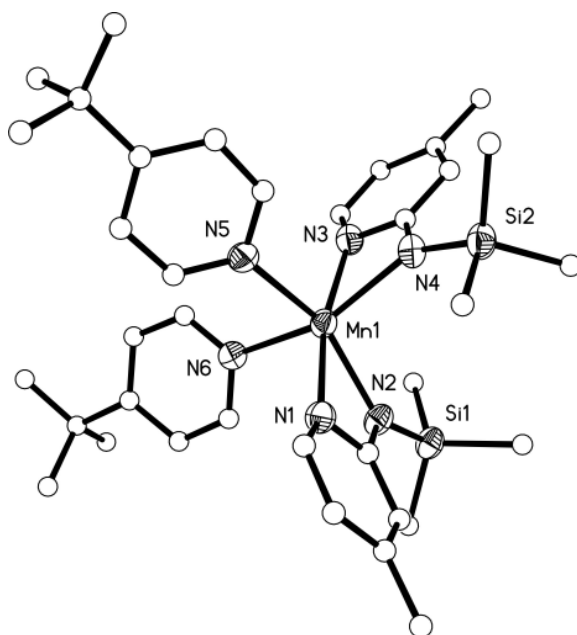


Figure 3. Molecule structure of **3** (ORTEP view; for clarity, only non carbon atoms are drawn as 50% probability ellipsoids). Selected bond lengths [Å] and angles [°]: Mn1–N1 2.3077(16), Mn1–N2 2.1927(15), Mn1–N3 2.2997(16), Mn1–N4 2.1998(16), Mn1–N5 2.3240(15), Mn1–N6 2.3179(16), N1–Mn1–N2 60.20(5), N3–Mn1–N4 60.18(6), N5–Mn1–N6 87.99(6).

The *t*BuPy ligands are arranged in a nearly ideal *cis* positions with angles ranging from 87.54(8) (N5–Fe1–N6) to 88.26(17)° (N5–Co1–N6). In the case of manganese, a structurally related aminopyridinate-cyclopentadienido complex exhibits similar Mn–N bond lengths (2.183 to 2.285 Å) and a similar N–Mn–N bond angle (60.52°)<sup>[24]</sup>

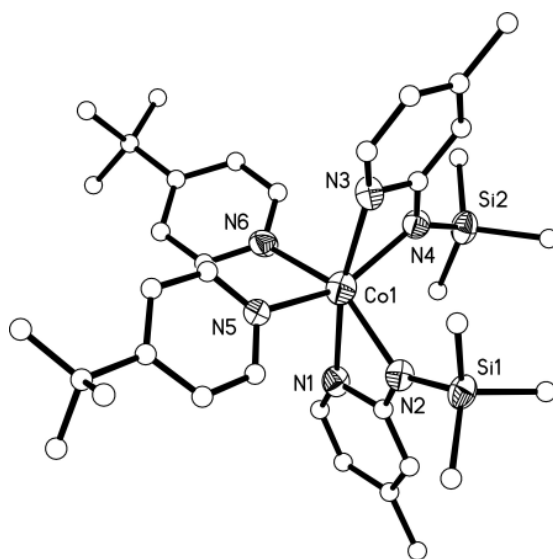


Figure 4. Molecule structure of **4** (ORTEP view; for clarity, only non carbon atoms are drawn as 50% probability ellipsoids). Selected bond lengths [Å] and angles [°]: Co1–N1 2.310(5), Co1–N2 2.209(4), Co1–N3 2.284(5), Co1–N4 2.217(5), Co1–N5 2.328(5), Co1–N6 2.330(4), N1–Co1–N2 59.86(15), N3–Co1–N4 60.40(17), N5–Co1–N6 88.26(17).

The Co–N distances in compound **4** are similar to those in the only known cobalt aminopyridinate (1.998 to 2.355 Å) but the bite angle is smaller [59.86(15) in comparison to 62.7 and 63.8°].<sup>[11]</sup> Pure N<sub>amido</sub>–Fe<sup>II</sup> bonds usually vary from 1.892<sup>[35]</sup> to 2.085 Å<sup>[36]</sup> and are shorter than the bonds found in complex **5**, which suggests a mixture of both pure N<sub>amido</sub>–Fe and pure N<sub>pyridine</sub>–Fe bonds. The N<sub>pyridine</sub>–Fe<sup>II</sup> distances in **5** lie in the range of bond lengths found in the literature (1.992–2.307 Å).<sup>[37,38]</sup>

According to the trend described for the homoleptic trivalent metal aminopyridinates, a similar behaviour can be proposed for the series Mn<sup>2+</sup>, Fe<sup>2+</sup>, Co<sup>2+</sup> and Ni<sup>2+</sup>. The structurally analogous *cis* complexes should exhibit smaller chelating angles for larger metal ions and this is indeed observed for manganese(II), iron(II) and nickel(II)<sup>[12]</sup> complexes (see Table 2). The only exception is the cobalt complex which shows an unexpectedly small N–M–N bond angle. This small angle is in accordance with the relatively long M–N bond length (compared to the other M<sup>2+</sup> aminopyridinates).

Table 2: Effective ionic radii and mean bond angle of homoleptic trivalent metal complexes.

Metal ion	Effective ionic radius <sup>[39]</sup>	Mean N–M–N bond angle	Mean M–N distance
Mn <sup>2+</sup>	97	60.2	2.25
Fe <sup>2+</sup>	92	62.0	2.19
Co <sup>2+</sup>	88.5	60.1	2.26
Ni <sup>2+</sup> [12]	83	63.1	2.11

If the reaction for iron(II) is carried out without additional donor ligands, the yellow highly air-sensitive complex **6** is obtained in moderate yield. The molecular structure of **6** was determined by X-ray structure analysis (Figure 6). A highly symmetric trinuclear complex with a central (interstitial) five-coordinate oxygen atom bridging three iron and two lithium atoms is observed in the solid state. All iron atoms are coordinated by two N<sub>amido</sub> nitrogen atoms from the Ap<sup>TMS</sup> ligands and the central oxygen atom. The lithium atoms are coordinated tetrahedrally in a distorted fashion by three N<sub>pyridine</sub> donors and the central oxygen atom. The Fe–N distance (2.021(3) Å) lies in the range of known pure Fe<sup>II</sup>–N<sub>amido</sub> distances (1.892–2.307 Å).<sup>[35,36]</sup>

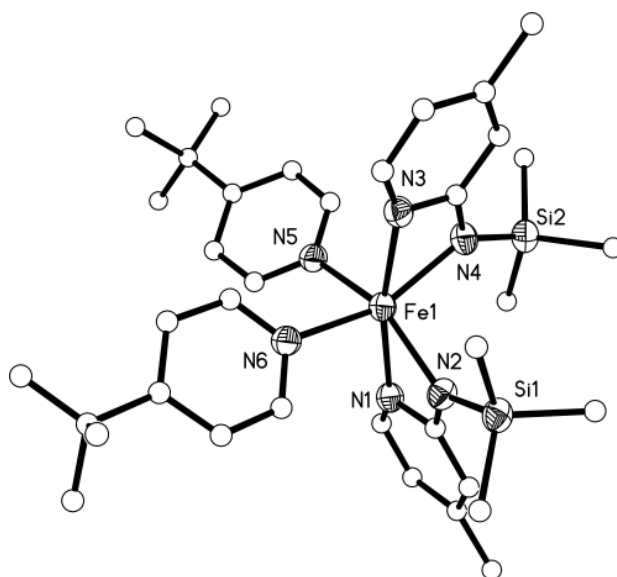


Figure 5. Molecule structure of **5** (ORTEP view; for clarity, only non carbon atoms are drawn as 50% probability ellipsoids). Selected bond lengths [Å] and angles [°]: Fe1–N1 2.245(2), Fe1–N2 2.139(2), Fe1–N3 2.227(2), Fe1–N4 2.149(2), Fe1–N5 2.248(2), Fe1–N6 2.244(2), N1–Fe1–N2 61.90(8), N3–Fe1–N4 61.02(9), N5–Fe1–N6 87.54(8).

Futhermore, the Li–N bond length is similar to those found in the literature (1.901–2.289 Å),<sup>[13,40]</sup> as are the Fe–O [1.9504(7) Å] and Li–O [2.005(8) Å] distances (literature: 1.840–2.100 Å<sup>[41,42]</sup> and 1.784–2.386 Å<sup>[43,44]</sup> for Fe–O and Li–O, respectively). The O1–Fe1–N2 bond angle is 124.46(9)° and the N2–Fe–N2 angle is 111.08(18)° thereby revealing the trigonal coordination of the iron atom.

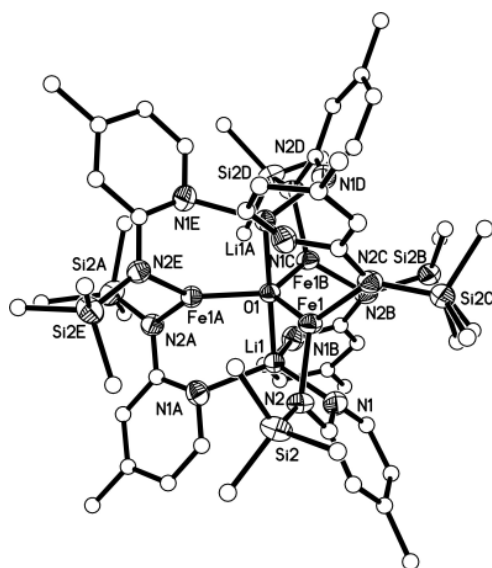


Figure 6. Molecule structure of **6** (ORTEP view; for clarity, only non carbon atoms are drawn as 50% probability ellipsoids). Selected bond lengths [Å] and angles [°]: Fe1–O1 1.9504(7), Fe1–N2 2.021(3), Li1–O1 2.005(8), Li1–N1 2.094(4), O1–Fe1–N2 124.46(9), N2–Fe1–N2 111.08(18), N1–Li1–O1 102.2(2), N1–Li1–N1 115.65(16).

Zinc(II) was employed in a reaction with two equivalents of lithiated Ap<sup>TMS</sup> to yield complex **7**. After workup, compound **7** was obtained as a white crystalline powder in moderate yields.

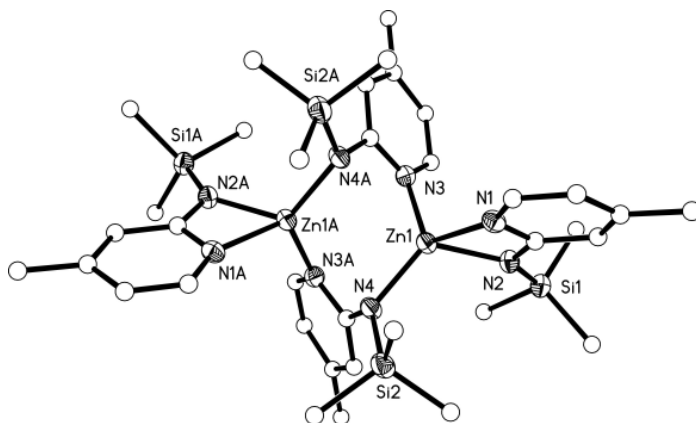


Figure 7. Molecule structure of **7** (ORTEP view; for clarity, only non carbon atoms are drawn as 50% probability ellipsoids). Selected bond lengths [Å] and angles [°]: Zn1–N1 2.102(2), Zn1–N2 2.063(2), Zn1–N3 2.030(2), Zn1–N4 1.9752(19), N1–Zn1–N2 65.43(8), N3–Zn1–N4 120.40(8)

The molecular structure of **7** was determined by X-ray analysis (Figure 7), shows that this complex is a dimer. A similar zinc aminopyridinate complex, in which two ligands bind to the metal in a strained  $\eta^2$  coordination mode and the other two ligands bridge the zinc atoms, has been reported.<sup>[15]</sup> Interestingly, this latter exhibits an inversion centre in its solid state structure, whereas complex **7** has  $C_2$  symmetry.

Table 3. Data of the X-ray crystal structure analyses

Complex	1	2	3	4
Formula	C <sub>27</sub> H <sub>45</sub> N <sub>6</sub> ScSi <sub>3</sub>	C <sub>27</sub> H <sub>45</sub> FeN <sub>6</sub> Si <sub>3</sub>	C <sub>36</sub> H <sub>56</sub> MnN <sub>6</sub> Si <sub>2</sub>	C <sub>36</sub> H <sub>56</sub> CoN <sub>6</sub> Si <sub>2</sub>
$F_w$	582.92	593.81	683.99	687.98
Crystal system	triclinic	monoclinic	triclinic	Triclinic
Space group	<i>P</i> -1	<i>P</i> 2 <sub>1</sub> / <i>c</i>	<i>P</i> -1	<i>P</i> -1
<i>a</i> [Å]	9.6560(14)	17.6410(11)	11.5160(8)	11.5280(11)
<i>b</i> [Å]	11.2060(16)	12.1910(8)	13.2530(9)	13.2620(11)
<i>c</i> [Å]	16.006(2)	16.1570(11)	13.6260(9)	13.6540(13)
$\alpha$ [°]	101.535(11)	90	88.737(5)	88.632(7)
$\beta$ [°]	97.703(11)	104.601(5)	79.573(5)	79.496(8)
$\gamma$ [°]	91.443(12)	90	73.192(5)	73.040(7)
<i>V</i> [Å <sup>3</sup> ]	1679.2(4)	3362.5(4)	1956.9(2)	1962.3(3)
<i>Z</i>	2	4	2	2
<i>T</i> (K)	133(2)	191(2)	191(2)	191(2)
<i>d</i> (calcd) [g/cm <sup>3</sup> ]	1.153	1.173	1.161	1.164
$\mu$ [mm <sup>-1</sup> ]	0.351	0.580	0.430	0.530
2 $\theta$ range [°]	3.72-51.07	2.60-51.99	3.04-52.22	3.03-51.75
$\omega R^2$ (all data)	0.0853	0.0944	0.1140	0.1219
<i>R</i> value	0.0526	0.0524	0.0408	0.0528

Table 3 (continued).

Complex	5	6	7
Formula	C <sub>36</sub> H <sub>56</sub> FeN <sub>6</sub> Si <sub>2</sub>	C <sub>54</sub> H <sub>90</sub> Fe <sub>3</sub> Li <sub>2</sub> N <sub>12</sub> OSi <sub>6</sub>	C <sub>36</sub> H <sub>60</sub> N <sub>8</sub> Si <sub>4</sub> Zn <sub>2</sub>
<i>F</i> <sub>w</sub>	684.90	1273.35	848.02
Crystal system	triclinic	trigonal	Monoclinic
Space group	<i>P</i> -1	<i>P</i> 6 <sub>3</sub> 22	<i>C</i> 2/ <i>c</i>
<i>a</i> [Å]	11.4380(11)	16.1790(9)	24.5640(8)
<i>b</i> [Å]	13.1750(14)	16.1790(9)	9.4770(5)
<i>c</i> [Å]	13.6440(14)	17.7250(10)	19.2960(11)
$\alpha$ [°]	88.374(8)	90	90
$\beta$ [°]	79.004(8)	90	92.175(5)
$\gamma$ [°]	73.192(8)	120	90
<i>V</i> [Å <sup>3</sup> ]	1931.3(3)	4018.1(4)	4488.7(4)
<i>Z</i>	2	2	4
<i>T</i> [K]	133(2)	133(2)	133(2)
<i>d</i> (calcd) [g/cm <sup>3</sup> ]	1.178	1.052	1.255
$\mu$ [mm <sup>-1</sup> ]	0.484	0.661	1.209
2 $\theta$ range [°]	3.04-52.00	2.90-51.90	3.32-52.25
$\omega R^2$ (all data)	0.1052	0.1125	0.0678
<i>R</i> value	0.0473	0.0534	0.0319

The two different coordination modes of the ligands would suggest that two separate signal sets should be observed for each ligand in the NMR experiments. However, in the case of **7** only one set of signals was observed in the <sup>1</sup>H, <sup>13</sup>C and <sup>29</sup>Si NMR for all aminopyridinato ligands. These data are indicative of rapid ligand exchange processes. The Zn–N distances vary from 1.9752(19) (Zn1–N4) to 2.102(2) Å (Zn1–N1) and are similar to the Zn–N bond lengths of the known zinc aminopyridinate (1.943 to 2.127 Å), as are as the N–Zn–N bond angles [65.43(8) and 120.40(8)° in comparison to 65.12 and 123.14°].<sup>[15]</sup> The distance between the zinc atoms (3.270 Å) allows us to conclude that there is no interaction between the zinc atoms.

### 5.2.2. Magnetic Properties

Complexes **2** to **6** are paramagnetic. Measurements of the magnetic susceptibility were therefore carried out to characterise their magnetic behaviour. All measurements were performed at a field of 0.5 T.

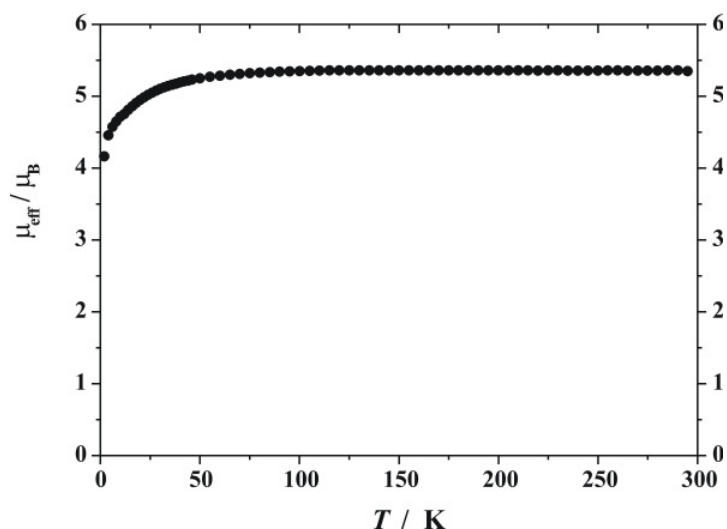


Figure 8. Dependency of the effective magnetic moment  $\mu_{\text{eff}}$  of **5** from the temperature at a field of 0.5 T

Complex **2** is a high-spin iron(III) complex with an  $\mu_{\text{eff}}$  value of  $5.63 \mu_{\text{B}}$  at 297 K. The effective magnetic moment of complex **3** and **4** at 250 K is  $5.88$  and  $4.80 \mu_{\text{B}}$ , respectively. Both these complexes are also high-spin.

The high effective magnetic moment of complex **4** indicates a large spin-orbit coupling. The magnetic moment of complexes **3**, **4** and **5** remains stable upon lowering the temperature and shows only Curie paramagnetism. Complex **5** is a high spin iron(II) complex with an effective magnetic moment of  $5.35 \mu_{\text{B}}$  and does not show spin-crossover behaviour in the temperature range investigated (Figure 8).

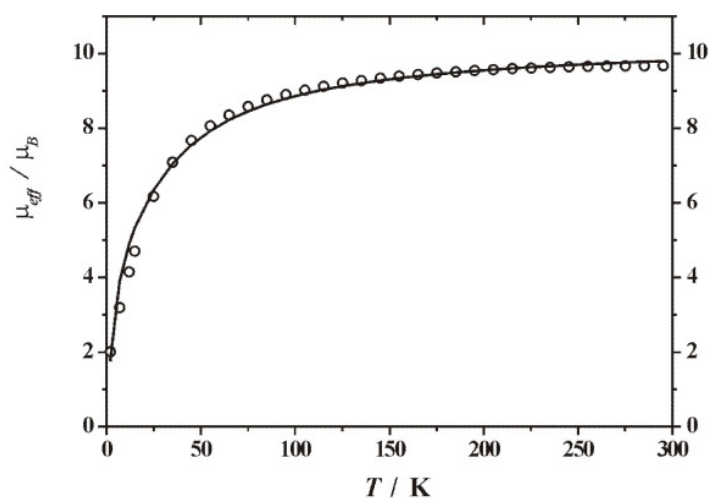


Figure 9. Dependency of the effective magnetic moment  $\mu_{\text{eff}}$  of **6** from the temperature at a field of 0.5 T (circles: experimental data, simulation: solid line)

Complex **6** has a effective magnetic moment of  $9.68 \mu_B$  at room temperature, which indicates the existence of three separated iron(II) atoms with  $S = 4/2$ . This temperature-dependence is indicative of Curie law behaviour with a weak antiferromagnetic coupling between the iron centres, which lowers the effective magnetic moment to a remaining value of  $2.01 \mu_B$  at 2 K (Figure 9). The experimental data for trinuclear complex **6** was modelled by fitting to the appropriate Heisenberg-Dirac-van-Vleck (HDvV) spin Hamiltonian for isotropic exchange coupling and Zeeman splitting [Equation (1)].<sup>[45]</sup>

$$\hat{H} = -2J \sum \hat{S}_i \hat{S}_j + g\mu_B B \sum \hat{S}_{iz} \quad (1)$$

A Curie-Weiss-type paramagnetic impurity ( $\rho$ ) with spin  $S = 4/2$  and temperature-independent paramagnetism (*TIP*) were included according to  $\chi = (1 - \rho)\chi + \rho\chi_{\text{mono}} + \text{TIP}$ .<sup>[46]</sup> The calculated curve fit is shown as a solid line in Figure 9. The best fit parameters are  $g = 2.48$ ,  $J = -2.7 \text{ cm}^{-1}$ ,  $PI = 5.0 \%$  (fixed) and  $\text{TIP} = 2.0 \times 10^{-4} \text{ cm}^3 \text{ mol}^{-1}$  (fixed).

### 5.3. Conclusions

We have presented the missing complexes of the first row transition metal aminopyridinates and have been able to show that one specific aminopyridinato ligand is able to stabilise all first row transition metal metals, which indicates the high versatility of this ligand and most likely of the ligand class. Homoleptic complexes were obtained for scandium(III) and iron(III), whereas manganese(II), iron(II) and cobalt(II) form structurally analogous *cis* complexes upon coordination of additional neutral ligands. All paramagnetic complexes are high-spin and show Curie paramagnetism.

If no additional neutral N ligands were added, iron(II) forms a highly symmetric trinuclear complex containing three weakly antiferromagnetically coupled high-spin metal centres. Zinc(II) yielded a dimeric complex which exhibits  $C_2$  symmetry.

## 5.4. Experimental Section

### 5.4.1. General

All reactions and manipulations with air-sensitive compounds were performed under dry argon, using standard Schlenk and glovebox techniques. Non-halogenated solvents were distilled from sodium benzophenone ketyl and halogenated solvents from P<sub>2</sub>O<sub>5</sub>. Deuterated solvents were obtained from Cambridge Isotope Laboratories and were degassed, dried with molecular sieves and distilled prior to use. All chemicals were purchased from commercial sources and used without further purification unless mentioned otherwise in the synthetic procedure. NMR spectra were recorded with either a Varian INOVA 300 or a Varian INOVA 400 spectrometer. Chemical shifts are reported in ppm relative to the deuterated solvent. Elemental analyses were carried out on a Vario elemental EL III. Magnetic data were measured with a Quantum-Design MPMS-5S SQUID magnetometer equipped with a 5-T magnet in the range from 295-2 K. The powdered samples were contained in a gel bucket and fixed in a non-magnetic sample holder. Each raw data file for the measured magnetic moment was corrected for the diamagnetic contribution of the sample holder and the gel bucket. The molar susceptibility was corrected using Pascal constants and the increment method according to Haberditzl.<sup>[47]</sup>

### 5.4.2. Synthesis of the Complexes

**Synthesis of 1:** A solution of Ap<sup>TMS</sup>H (2.705 g, 15 mmol) in 80 mL of Et<sub>2</sub>O was treated with 9.375 mL (1.6 M, 15 mmol) of *n*BuLi in hexanes at 0 °C and stirred for 30 min. After stirring overnight at room temperature the mixture turned from colourless to pale yellow. It was then added to a solution of [ScCl<sub>3</sub>(thf)<sub>3</sub>] (1.838 g, 5 mmol) in 60 mL of thf at 0 °C. The colour remained pale yellow. The solution was again stirred overnight at room temperature. After removing the solvent, the residue was extracted with 60 mL of hexane, filtered and concentrated. Colourless crystals of **1** were obtained after storage in a freezer at -30 °C. Further concentration of the mother liquor yielded **1** as a white precipitate. Yield 1.065 g (1.8 mmol, 37%). C<sub>27</sub>H<sub>45</sub>N<sub>6</sub>Si<sub>3</sub>Sc (582.90): calcd. C 55.63; H 7.78, N 14.42; found C 55.14, H 8.19, N 14.55. <sup>1</sup>H NMR (C<sub>6</sub>D<sub>6</sub>, 296 K): δ = 0.37 (s, 27 H, TMS), 1.76 (s, 9 H, ar-CH<sub>3</sub>), 5.82 (d, J<sub>H,H</sub> = 5,7 Hz, 3

H), 6.33 (s, 3 H), 7.55 (d,  $J_{\text{H,H}} = 5,7$  Hz, 3 H) ppm.  $^{13}\text{C}$  NMR ( $\text{C}_6\text{D}_6$ , 296 K):  $\delta = 1.66$ , 21.90, 110.85, 113.55, 143.72, 151.38, 170.68 ppm.  $^{29}\text{Si}$  NMR ( $\text{C}_6\text{D}_6$ , 296 K):  $\delta = -5.62$  ppm.

**Synthesis of 2:** A solution of  $\text{Ap}^{\text{TMS}}\text{H}$  (1.082 g, 6 mmol) in 15 mL of  $\text{Et}_2\text{O}$  was treated with 3.25 mL (1.6 M, 6 mmol) of  $n\text{BuLi}$  in hexanes at  $-50$  °C and stirred for 30 min. After stirring overnight at room temperature the mixture turned from colourless to pale yellow. It was then added to a suspension of  $\text{FeCl}_3$  (0.324 g, 2 mmol) in 15 mL of thf at  $-50$  °C. The colour turned first red then dark purple. The solution was again stirred overnight at room temperature. After removing the solvent, the residue was extracted twice with 15 mL of hexane, filtered and concentrated. Dark purple crystals of **2** were obtained after storage at  $-30$  °C. Further concentration of the mother liquor yielded **2** as a dark purple precipitate. Yield 0.707 g (1.2 mmol, 40%).  $\text{C}_{27}\text{H}_{45}\text{N}_6\text{Si}_3\text{Fe}$  (593.79): calcd. C 54.61, H 7.64, N 14.15; found C 54.33, H 8.01, N 14.10.  $\mu_{\text{B}} = 5.44$  (270 K, 0.5 T).

**Synthesis of 3:** A solution of  $\text{Ap}^{\text{TMS}}\text{H}$  (3.606 g, 20 mmol) in 50 mL of  $\text{Et}_2\text{O}$  was treated with 12.5 mL (1.6 M, 20 mmol) of  $n\text{BuLi}$  in hexanes at  $0$  °C and stirred for 30 min. After stirring overnight at room temperature the mixture turned from colourless to pale yellow. It was then added to a suspension of  $\text{MnCl}_2$  (1.258 g, 10 mmol) and *tert*-butylpyridine (2.9 mL, 20 mmol) in 100 mL of thf at  $0$  °C. The solution was again stirred overnight at room temperature and the colour changed to orange. After removing the solvent, the residue was extracted with 100 mL of hexane, filtered and concentrated. Light orange crystals of **3** were obtained after storage at  $-30$  °C. Further concentration of the mother liquor yielded **3** as a orange precipitate. Yield 1.470 g (2.1 mmol, 22%).  $\text{C}_{36}\text{H}_{56}\text{N}_6\text{Si}_2\text{Mn}$  (683.98): calcd, C 63.22, H 8.25, N 12.29; found C 62.97, H 8.32, N 12.35.  $\mu_{\text{B}} = 5.88$  (250 K, 0.5 T).

**Synthesis of 4:** A solution of  $\text{Ap}^{\text{TMS}}\text{H}$  (1.803 g, 10 mmol) in 50 mL of  $\text{Et}_2\text{O}$  was treated with 6.25 mL (1.6 M, 10 mmol) of  $n\text{BuLi}$  in hexanes at  $0$  °C and stirred for 30 min and then overnight at room temperature. The mixture turned from colourless to pale yellow. It was then added to a suspension of  $\text{CoCl}_2$  (0.650 g, 5 mmol) and *tert*-butylpyridine (1.47 mL, 10 mmol) in 20 mL of thf at  $0$  °C. The solution was again stirred overnight at room temperature, whereupon the coloured changed to dark

green. After removing the solvent, the residue was extracted with 100 mL of hexane, filtered and concentrated. Ochre-green crystals of **4** were obtained after storage in a freezer at -30 °C. Further concentration of the mother liquor yielded **4** as a ochre-green precipitate. Yield 1.731 g (2.5 mmol, 50%). C<sub>36</sub>H<sub>56</sub>N<sub>6</sub>Si<sub>2</sub>Co (687.97): calcd. C 62.85, H 8.20, N 12.22; found C 62.42, H 8.15, N 12.59.  $\mu_B = 4.80$  (250 K, 0.2 T).

**Synthesis of 5:** A solution of Ap<sup>TMS</sup>H (1.803 g, 10 mmol) in 50 mL of Et<sub>2</sub>O was treated with 6.25 mL (1.6 M, 10 mmol) of *n*BuLi in hexanes at 0 °C and stirred overnight at room temperature. The mixture turned from colourless to pale yellow. It was then added to a suspension of FeCl<sub>2</sub> (0.630 g, 5 mmol) and *tert*-butylpyridine (1.47 mL, 10 mmol) in 50 mL of thf at 0 °C. The solution was again stirred overnight at room temperature and the colour changed to dark red-brown. After removing the solvent, the residue was extracted with 100 mL of hexane, filtered and concentrated. Dark red crystals of **5** were obtained after storage at -30 °C. Further concentration of the mother liquor yielded **5** as a dark red precipitate. Yield 2.720 g (4.0 mmol, 80%). C<sub>36</sub>H<sub>56</sub>N<sub>6</sub>Si<sub>2</sub>Fe (684.90): calcd. C 63.13, H 8.24, N 12.27; found C 62.65, H 8.70, N 12.34.  $\mu_B = 5.35$  (295 K, 0.5 T).

**Synthesis of 6:** A solution of Ap<sup>TMS</sup>H (1.443 g, 8 mmol) in 20 mL of Et<sub>2</sub>O was treated with 5 mL (1.6 M, 8 mmol) of *n*BuLi in hexanes at 0 °C and stirred overnight at room temperature. The mixture turned from colourless to pale yellow. A suspension of FeCl<sub>2</sub> (0.507 g, 4 mmol) in 20 mL of thf was stirred overnight, then the solution of the lithiated ligand was added at 0 °C and the mixture again stirred overnight at room temperature, whereupon the colour changed to very dark black-green. After removing the solvent, the residue was extracted with 50 mL hexane, filtered and concentrated. Yellow-brown crystals of **6** were obtained after a few days at room temperature. Further concentration of the mother liquor yielded **1** as a yellow-brown precipitate. Yield 0.602 g (0.5 mmol, 35%). C<sub>54</sub>H<sub>90</sub>Fe<sub>3</sub>Li<sub>2</sub>N<sub>12</sub>OSi<sub>6</sub> (1272.43): calcd: C 50.93, H 7.13, N 13.21; found C 50.76, H 6.87, N 12.97.  $\mu_B = 9.68$  (295 K, 0.5 T).

**Synthesis of 7:** A solution of Ap<sup>TMS</sup>H (3.606 g, 20 mmol) in 40 mL of Et<sub>2</sub>O was treated with 12.5 mL (1.6 M, 20 mmol) of *n*BuLi in hexanes at 0 °C and stirred for 30 min. This mixture turned from colourless to pale yellow after stirring overnight at room temperature. It was then added to a solution of ZnCl<sub>2</sub> (1.363 g, 10 mmol) in 20 mL of

thf at 0 °C. The colour remained pale yellow. The solution was stirred again overnight at room temperature. After removing the solvent, the residue was extracted with 40 mL of hexane, filtered and concentrated. Colourless crystals of **7** were obtained after storage in a freezer at -30 °C. Further concentration of the mother liquor yielded **7** as a white precipitate. Yield 1.215 g (1.4 mmol, 29%). C<sub>36</sub>H<sub>60</sub>N<sub>8</sub>Si<sub>4</sub>Zn<sub>2</sub> (848.04): calcd. C 50.99, H 7.13, N 13.21; found C 51.18, H 7.55, N 12.99. <sup>1</sup>H NMR (C<sub>6</sub>D<sub>6</sub>, 296 K): δ = 0.34 (s, 36 H, TMS), 1.81 (s, 12H, ar-CH<sub>3</sub>), 6.01 (d, J<sub>H,H</sub> = 4,2 Hz, 4 H), 6.52 (s, 4 H), 7.74 (d, J<sub>H,H</sub> = 4,2 Hz, 4 H) ppm. <sup>13</sup>C NMR (C<sub>6</sub>D<sub>6</sub>, 296 K): δ = 2.13, 21.55, 112.92, 115.70, 146.13, 150.40, 168.98 ppm. <sup>29</sup>Si NMR (C<sub>6</sub>D<sub>6</sub>, 296 K): δ = -2.09 ppm.

X-ray crystal structure analyses were performed with a STOE-IPDS II equipped with an Oxford Cryostream low-temperature unit. Structure solution and refinement were accomplished using SIR97,<sup>[48]</sup> SHELXL-97<sup>[49]</sup> and WinGX<sup>[50]</sup>. Crystallographic details are summarised in Table 3. CCDC-706703 (for **1**), -706704 (for **2**), -706705 (for **3**), -706706 (for **4**), -706707 (for **5**), -706708 (for **6**), -706709 (for **7**), contain the supplementary crystallographic data for this publication. These data can be obtained free of charge from The Cambridge Crystallographic Data Centre via [www.ccdc.cam.ac.uk/data\\_request/cif](http://www.ccdc.cam.ac.uk/data_request/cif).

### 5.4.3. Acknowledgements

Financial support from the DFG (SPP 1181 "Nanoskalige anorganische Materialien durch molekulares Design") is gratefully acknowledged.

## 5.5. References

- [1] R. Kempe, *Eur. J. Inorg. Chem.* **2003**, 791-803.
- [2] R. Kempe, H. Noss H, T. Irrgang *J. Organomet. Chem.* **2002**, 647, 12-20.
- [3] R. Kempe, *Angew. Chem.* **2000**, 112, 478-504; *Angew. Chem. Int. Ed. Engl* **2000**, 39, 468-493.
- [4] A. Spannenberg, A. Tillack, P. Arndt, R. Kirmse, R. Kempe, *Polyhedron* **1998**, 17, 845-850.
- [5] E. Smolensky, M. Kapon, M. S. Eisen, *Organometallics* **2005**, 24, 5495-5498.
- [6] E. Smolensky, M. Kapon, J. D. Williams, M. S. Eisen, *Organometallics* **2005**, 24, 3255-3265.
- [7] R. Kempe, *Z. Krist. NCS* **1997**, 212, 477.

- [8] J. J. H. Edema, S. Gambarotta, A. Meetsma, A. L. Spek, N. Veldman, *Inorg. Chem.* **1991**, *30*, 2062-2066.
- [9] F. A. Cotton, E. A. Hillard, C. A. Murillo, X. Wang, *Inorg. Chem.* **2003**, *42*, 6063-6070.
- [10] F. A. Cotton, R. H. Niswander, J. C. Sekutowski, *Inorg. Chem.* **1978**, *17*, 3541-3545.
- [11] H. K. Lee, C. H. Lam, S. L. Li, Z.-Y. Zhang, T. C. W. Mak, *Inorg. Chem.* **2001**, *40*, 4691-4695.
- [12] S. Deeken, S. Proch, E. Casini, H. F. Braun, C. Mechtler, C. Marschner, G. Motz, R. Kempe, *Inorg. Chem.* **2006**, *45*, 1871-1879.
- [13] L. M. Engelhardt, G. E. Jacobsen, W. Y. Patalinghug, B. W. Skelton, C. L. Raston, A. H. White, *J. Chem. Soc. Dalton Trans.* **1991**, 2859-2868.
- [14] H. Aghabozorg, S. Gambarotta, C. Bensimon, *J. Sci. I. R. Iran* **1994**, *5*, 158-162.
- [15] S. J. Birch, S. R. Boss, S. C. Cole, M. P. Coles, R. Haigh, P. B. Hitchcock, A. E. H. Wheatley, *Dalton Trans.* **2004**, 3568-3574.
- [16] M. Jain, S. Mehra, P. C. Trivedi, R. V. Singh, *Metal-Based Drugs* **2002**, *9*, 53-60.
- [17] S. Cabaleiro, J. Castro, J. A. García-Vázquez, J. Romero, A. Sousa, *Polyhedron* **2000**, *19*, 1607-1614.
- [18] I. Beloso, J. Castro, J. A. García-Vázquez, P. Pérez-Lourido, J. Romero, A. Sousa, *Polyhedron* **2006**, *25*, 2673-2682.
- [19] S. Cabaleiro, J. Castro, E. Vázquez-López, J. A. García-Vázquez, J. Romero, A. Sousa, *Polyhedron* **1999**, *18*, 1669-1674.
- [20] H.-Y. Cheng, P.-H. Cheng, C.-F. Lee, S.-M. Peng, *Inorg. Chim. Acta* **1991**, *181*, 145-147.
- [21] C.-F. Lee, S.-M. Peng, *J. Chin. Chem. Soc.* **1991**, *38*, 559-564.
- [22] S. Cabaleiro, J. Castro, J. Romero, J. A. García-Vázquez, A. Sousa, *Acta Cryst. C* **2000**, *C56*, 293-295.
- [23] I. Beloso, J. Castro, J. A. García-Vázquez, P. Pérez-Lourido, J. Romero, A. Sousa, *Polyhedron* **2003**, *22*, 1099-1111.
- [24] C. S. Alvarez, S. R. Boss, J. C. Burley, S. M. Humphry, R. A. Layfield, R. A. Kowenicki, M. McPartlin, J. M. Rawson, A. E. H. Wheatley, P. T. Wood, D. S. Wright, *Dalton Trans.* **2004**, 3481-3487.

- [25] C. S. Alvarez, A. D. Bond, D. Cave, M. E. G. Mosquera, E. A. Harron, R. A. Layfield, M. McPartlin, J. M. Rawson, P. T. Wood, D. S. Wright, *Chem. Commun.* **2002**, 2980-2981.
- [26] R. P. Davies, D. J. Linton, P. Schooler, R. Snaith, A. E. H. Wheatley, *Chem. Eur. J.* **2001**, 7, 3696-3704.
- [27] R. Kempe, P. Arndt, *Inorg. Chem.* **1996**, 35, 2644-2649.
- [28] L. E. Manzer, *Inorg. Synth.* **1982**, 21, 135.140.
- [29] S. Deeken, G. Motz, R. Kempe, *Z. Allg. Anorg. Chem.* **2007**, 633, 320-325.
- [30] C. Meermann, P. Sirsch, K. W. Tornroos, R. Anwander, *Dalton Trans.* **2006**, 1041-1050.
- [31] M. E. G. Skinner, B. R. Tyrrell, B. D. Ward, P. Mountford, *J. Organomet. Chem.* **2002**, 647, 145.150.
- [32] M. B. Hursthouse, P. F. Rodesiler, *J. Chem. Soc., Dalton Trans.* **1972**, 2100-2102.
- [33] Y. Ohgo, T. Ikeue, M. Nakamura, *Inorg. Chem.* **2002**, 41, 1698-1700.
- [34] W. Chiang, D. Vanegen, M. E. Thompson, *Polyhedron* **1996**, 15, 2369-2376.
- [35] T. Komuro, H. Kawaguchi, K. Tatsumi, *Inorg. Chem.* **2002**, 41, 5083-5090.
- [36] M. D. Fryzuk, D. B. Leznoff, E. S. F. Ma, S. J. Rettig, V. G. Young Jr., *Organometallics* **1998**, 17, 2313-2323.
- [37] C. R. Goldsmith, R. T. Jonas, A. P. Cole, T. D. P. Stack, *Inorg. Chem.* **2003**, 41, 4642-4652.
- [38] B. Weber, E. Kaps, *Heteroat. Chem.* **2005**, 16, 391-397.
- [39] R. D. Shannon, *Acta Cryst.* **1976**, A32, 751-767.
- [40] S. M. Boss, J. M. Cole, R. Haigh, R. Snaith, A. E. W. Wheatley, *Organometallics* **2004**, 23, 4527-4530.
- [41] C.-C. Wu, S. A. Hunt, P. K. Gantzel, P. Gütllich, D. N. Hendrickson, *Inorg. Chem.* **1997**, 36, 4717-4733.
- [42] A. Abinati, F. Calderazzo, F. Marchetti, S. A. Mason, B. Melai, G. Pampaloni, S. Rizzato, *Inorg. Chem. Commun.* **2007**, 10, 902-905.
- [43] M. Veith, O. Schutt, V. Huch, *Angew. Chem. Int. Ed. Engl.* **2000**, 39, 601-604; *Angew. Chem.* **2000**, 112, 614-617.
- [44] J. Gracia, A. Martin, M. Mena, M. del C. Morales-Varela, J.-M. Poblet, C. Santamaria, *Angew. Chem. Int. Ed. Engl.* **2003**, 42, 927-930; *Angew. Chem.* **2003**, 115, 957-960.

- [45] O. Kahn, *Molecular Magnetism*, Wiley-VCH Publishers Inc., New York **1993**.
- [46] Simulation of the experimental magnetic data with a full-matrix diagonalisation of exchange coupling and Zeeman splitting was performed with the *JulX* program developed by E. Bill (Max-Planck Institute for Bioinorganic Chemistry, Mülheim/Ruhr, Germany).
- [47] a) W. Haberditzl, *Angew. Chem.* **1966**, *78*, 277-312; *Angew. Chem. Int. Ed. Engl.* **1966**, *5*, 288-298; b) W. Haberditzl, *Magnetochemie*, Akademie-Verlag **1968**.
- [48] A. Altomare, M. C. Burla, M. Camalli, G. L. Cascarano, C. Giacovazzo, A. Guagliardi, A. G. G. Moliterni, G. Polidori, R. Spagna, *J. Appl. Crystallogr.* **1999**, *32*, 115-119.
- [49] G. M. Sheldrick, SHELX-97, Program for Crystal Structure Analysis (Release 97-2), Institut für Anorganische Chemie der Universität, Göttingen, Germany, **1998**.
- [50] L. J. Farrugia, *J. Appl. Crystallogr.* **1999**, *32*, 837-838.

## 5.6. Supplementary Material

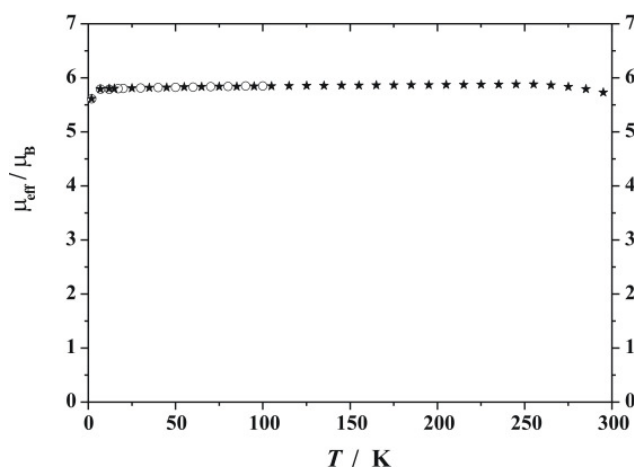


**Figure S1.** Dependency of the effective magnetic moment  $\mu_{\text{eff}}$  of 3 from the temperature at a field of 0.5 T [measured from 100 to 2 K (circles) and from 2 to 295 K (stars)].

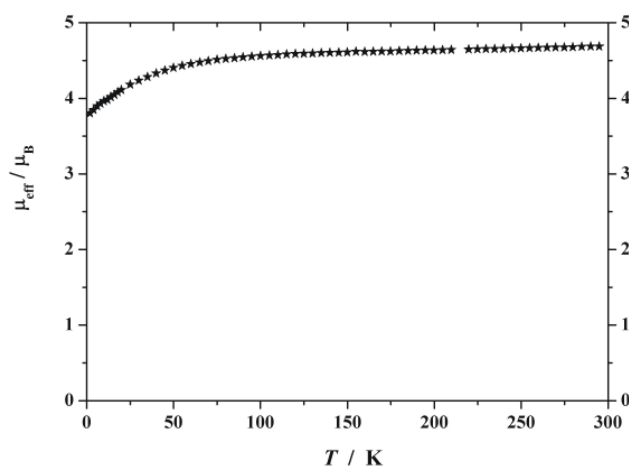


**Figure S2.** Dependency of the effective magnetic moment  $\mu_{\text{eff}}$  of 4 from the temperature at a field of 0.2 T (stars).

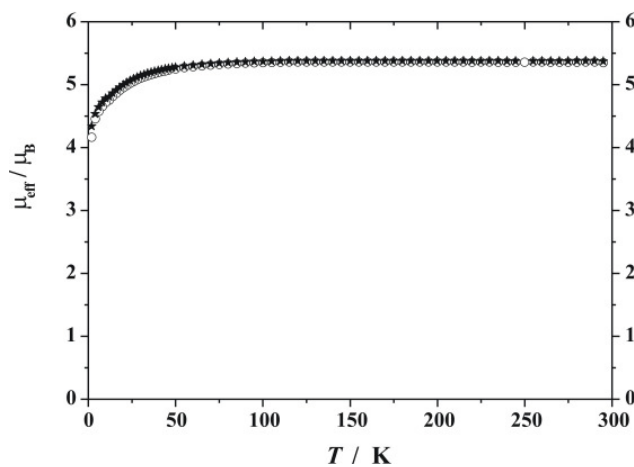


**Figure S3.** Dependency of the effective magnetic moment  $\mu_{\text{eff}}$  of 5 from the temperature at a field of 0.2 T (stars) and 0.5 T (circles)

## 6. Novel Cu-SiCN ceramics via molecular design – Part I: Synthesis and characterisation of Cu-SiCN

Germund Glatz,<sup>[a]</sup> Thomas Schmalz,<sup>[b]</sup> Tobias Kraus,<sup>[b]</sup> Günter Motz,<sup>\*,[b]</sup> and  
Rhett Kempe<sup>\*,[a]</sup>

[a] Anorganische Chemie II, Universität Bayreuth, Universitätsstraße 30, 95440  
Bayreuth, Germany

[b] Lehrstuhl Keramische Werkstoffe, Universität Bayreuth, Ludwig-Thoma-Straße  
36b, 95440 Bayreuth, Germany

**Keywords:** Aminopyridinato ligands; Preceramic polymer; Cu-SiCN; Metal  
modification; Precursor ceramics

To be submitted

**Abstract.** A molecular approach to metal containing ceramics is presented. 4-Methyl-2-((trimethylsilyl)amino)pyridine ( $\text{Ap}^{\text{TMS}}\text{H}$ ) was used in salt metathesis reactions to obtain copper aminopyridinates. The obtained copper complexes 1, 2 and 3 were characterized by X-ray crystal structure analysis. The aminopyridinato copper complex 3 reacts with poly(organosilazanes) forming a covalent bonding between the Cu atom and the precursor as could be shown for the commercially available ceramic precursor HTT 1800 (Clariant Advanced Materials GmbH, Sulzbach, Germany). This reaction was studied via  $^1\text{H}$  and  $^{13}\text{C}$  NMR spectroscopy. The liberation of the free, protonated ligand  $\text{Ap}^{\text{TMS}}\text{H}$  is indirectly indicative of the binding of the copper atoms to the precursor. Cross-linking of the copper modified poly(organosilazane) and subsequent pyrolysis leads to the Cu containing ceramic. SEM measurements of the ceramic material in addition with EDS-mappings showed the presence of particles consisting of elemental copper. Powder diffraction experiments verified the presence of crystalline copper. This study proves the feasibility of this molecular approach to metal enforced SiCN precursor ceramics by using silyl-aminopyridinato complexes. Since these complexes are known for nearly all transition metals and lanthanides a rather broad applicability of the concept can be expected.

## 6.1. Introduction

A lot of research interest during the last years has been focused on SiCN precursor ceramics [1-5 and references therein]. High temperature stability, corrosion resistance or long term durability are provided by amorphous SiCN precursor ceramics derived from poly(organosilazanes). Because of the molecular pathway to these ceramics they are highly tunable and versatile materials [6-10]. An extension of the property profiles like improved electrical and thermal conductivity should be gained by the introduction of transition metals in the ceramic. One approach is to mix metal powders or alloys with the ceramic precursor and to ceramize this material [6,11-15]. Molecular pathways to introduce transition metals have been described for ferrocene functionalised ceramic precursors but the general applicability is limited due to the low variety of available precursors [16-18]. A more general molecular approach is the use of organometallic compounds like iron and cobalt carbonyls [19]. Unfortunately, metal carbonyls are very volatile and extremely toxic and may vaporise during the ceramic formation at high temperature. Metal alkyls like trimethylaluminum [20] or early transition metal amides [21] like amidotitanium complexes [8-10,22] have shown a certain potential to stronger interact with the ceramic precursor and increase ceramic yield. For late transition metals (which would be interesting e.g. for catalysis) the corresponding amido metal complexes are not available or only in rather sophisticated compounds. In addition late metal alkyls are stable and do not necessarily react with the ceramic precursors. A save and general concept which allows the introduction of a broad variety of transition metals should be based on metal complexes that are able to react with the NH functions of the precursor to form a covalent bond between the metal and the ceramic precursor. Furthermore, these metal complexes should show high solubility in a variety of organic solvents, especially in those solvents which are used to dissolve the ceramic precursors. Moreover, the compounds should not contain “alien” elements, elements that are not wanted to be found in the ceramic afterwards. Additionally, this class of compounds should be easy to synthesise in a multi-gram scale and be available of a broad range of different metals. These issues can be addressed by using aminopyridinato complexes [23-29]. We report herein on the synthesis and

characterisation of novel copper aminopyridinates, which were used for metal modification of the commercially available ceramic precursor HTT 1800 (Clariant Advanced Materials GmbH, Sulzbach, Germany). The reaction of the metal compound with the preceramic polymer was investigated by NMR spectroscopy. After ceramisation of the metal modified precursor, the ceramic was characterised using SEM, EDS and powder diffraction. The processing scheme for the synthesis of the novel Cu-SiCN ceramics via molecular design is shown in Figure 1.

## 6.2. Results and Discussion

### 6.2.1. Metal Complex Synthesis

In order to obtain copper aminopyridinates for metal modification of poly(organosilazanes)  $\text{CuBr}_2$  was reacted with two equivalents of lithiated 4-methyl-2-trimethylsilylamino pyridine ( $\text{Ap}^{\text{TMS}}$ ). After workup in hexane dark blue crystals of  $[\text{Cu}_3\text{Ap}^{\text{TMS}}_4]$  (**1**) were isolated, which is a mixed-valent copper complex. As a byproduct a tetrameric Cu(I) complex  $[\text{Cu}_4\text{ApTMS}_4]$  (**2**) was obtained. It can be concluded that  $[\text{Li}_2(\text{Ap}^{\text{TMS}})_2(\text{OEt}_2)_2]$  acts towards Cu(II) as a reducing agent. Hence, the yields of **1** and **2** were moderate. To avoid reduction and to improve the yield  $\text{CuBr}$  was employed in a reaction with lithiated  $\text{Ap}^{\text{TMS}}$ . After workup in hexane a light green powder of  $[\text{Cu}_2\text{Ap}^{\text{TMS}}_2]$  (**3**) was obtained in very good yields (Figure 1, top). All molecular structures were determined by X-ray crystal structure analysis (see supporting information).  $[\text{Cu}_2\text{Ap}^{\text{TMS}}_2]$  shows a close structural relationship to a known copper aminopyridinate [30]. The synthesis of **3** can be scaled up to multi-gram scale without yield loss. Hence compound **3** is an ideal candidate for metal modification of poly(organosilazanes).



## 6.2.2. Transmetalation

Complex **3** was employed as transmetalation agent in a reaction with HTT 1800. If transmetalation with the poly(organosilazane) takes place the protonated ligand  $\text{Ap}^{\text{TMS}}\text{H}$  should be liberated. The driving force of this reaction could be the low coordination number of copper in **3**. Additionally, the ceramic precursor provides an excess of N-donors to which copper can bind datively and covalently (see Figure 1).

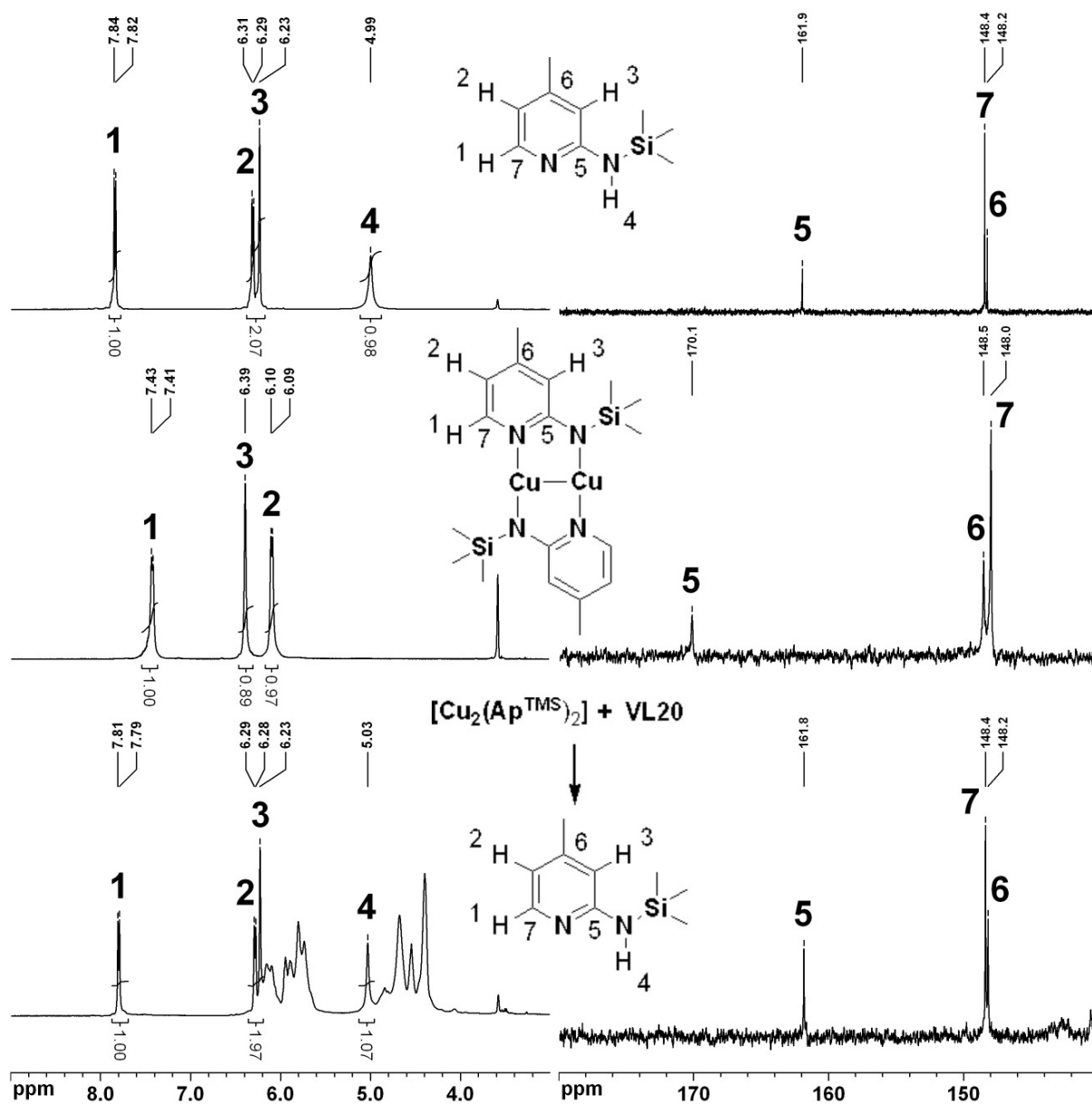


Figure 3.  $^1\text{H}$ - (left) and  $^{13}\text{C}$ -NMR spectra (right) of  $\text{Ap}^{\text{TMS}}\text{H}$ , compound **3** and after reaction of **3** with HTT 1800 (from top to bottom).

To verify that transmetalation takes place  $^1\text{H}$  and  $^{13}\text{C}$  NMR experiments were carried out. For comparability all spectra were recorded in  $\text{thf-d}^8$ . There are some

characteristic differences between the NMR spectra of the protonated ligand and those of compound **3**. On top of Figure 2 there are the  $^1\text{H}$  (left) and the  $^{13}\text{C}$  NMR (right) spectra of  $\text{Ap}^{\text{TMS}}\text{H}$ . In the middle the corresponding spectra of complex **3** and on bottom of the reaction mixture of **3** and HTT 1800 are shown. Signal 1 belongs to the proton located in 6-position of the pyridine ring. This signal at 7.83 ppm (protonated ligand) shifts significantly upfield to 7.42 ppm (complex **3**). Signals 2 and 3 exchange the position, relative to each other, when ligand and complex spectra are compared. Obviously, the signal of the proton attached to the nitrogen disappears in the spectrum of complex **3**. When complex **3** is reacted with the ceramic precursor, all the characteristic signals of the protonated ligand appear which evidences the presence of the ligand as proposed before (Figure 2, bottom left). The additional signals, which can be obtained in the spectrum of the reaction mixture, correspond to the ceramic precursor. According to the spectra the reaction goes to total completeness. The same results can be concluded from the  $^{13}\text{C}$  NMR spectra (Figure 2, right hand). This is an indirect evidence for the formation of covalent chemical bonds between copper atoms and the precursor.

### 6.2.3. Crosslinking and Ceramisation

Firstly, the metal modified precursor was crosslinked by using dicumylperoxide (DCP) as initiator for hydrosilylation and polymerisation reactions at  $130^\circ\text{C}$ . Subsequent pyrolysis at  $1000^\circ\text{C}$  for 30 min in a  $\text{N}_2$  atmosphere lead to the Cu-SiCN ceramic. A ceramic yield of 61% was determined by thermogravimetical measurements. This indicates the possibility of ceramisation of the metal modified precursor. If assumed, that the liberated ligand ( $\text{Ap}^{\text{TMS}}\text{H}$ ) is completely eliminated during ceramisation and only the copper remains in the ceramic, a theoretical yield of 53% would be expected. The higher ceramic yield confirms not only the disposition of copper in the ceramic material but it indicates also that the  $\text{Ap}^{\text{TMS}}$  ligand contributes significantly to the ceramic yield. In order to quantify the ceramic composition, elemental analysis of the ceramic was performed (see Table 1). As shown in Table 1 the copper content increases significantly during ceramisation and lies in the expected range. The pyrolysis process of silazanes is characterized by the release of methane and hydrogen, which reduces the C and H content in the resulting ceramic remarkably.

Table 1. Elemental composition of the Cu containing precursor and of the resulting Cu-SiCN ceramic. All values are given in [wt.%].

	metal containing precursor (calc.)	Cu-SiCN ceramic (after pyrolysis at 1000 °C)
<b>C</b>	34.0	15.0
<b>H</b>	7.5	0.7
<b>N</b>	17.4	21.8
<b>Si</b>	29.8	44.4
<b>Cu</b>	11.3	13.7
<b>O</b>	–	3.4

A possible formation of volatile copper compounds during the ceramisation is prevented due to the covalent copper-precursor bond, which was formed during transmetalation reaction.

SEM micrographs of the Cu-SiCN ceramic (Figure 3) show the presence of particles of different sizes (from  $\mu\text{m}$ -scale down to sizes of about a few hundred nanometers) formed during ceramisation. The associated EDS-mappings clearly indicate that these particles consist of elemental copper. The “in-situ” reduction of copper(I) to elemental copper results from the reductive atmosphere consisting of the pyrolysis gases methane and hydrogen. The unexpected agglomeration to Cu-particles in  $\mu\text{m}$ -scale is due to the pyrolysis temperature of 1000 °C which is close to the melting temperature of copper (1083 °C). Hence, the copper atoms are quite mobile and can agglomerate. As it can be seen in Figure 3 the Cu-EDS-mapping fits perfectly to the particles that can be found in the SEM image. The Si-mapping shows the presence of silicon-free areas exactly at the position of the copper particles. The overlap mapping picture points out this clearly. Hence, it can be concluded that the particles do not consist of any copper compound (e.g. nitride, carbide, silicide) but of elemental copper. In order to prove the presence of crystalline elemental copper in the ceramic material a powder diffractogram of the milled ceramic powder was performed (Figure 3). The three prominent peaks can clearly be assigned to *fcc*-centred elemental copper ( $2\theta$  values [°]: exp.: 43.46, 50.59, 74.25; lit. [31]: 43.32, 50.45, 74.13). The ceramic matrix is amorphous and thus, cannot be seen in the diffractogram. Both methods, SEM and powder diffraction, reveal the presence of elemental copper particles in the ceramic material.

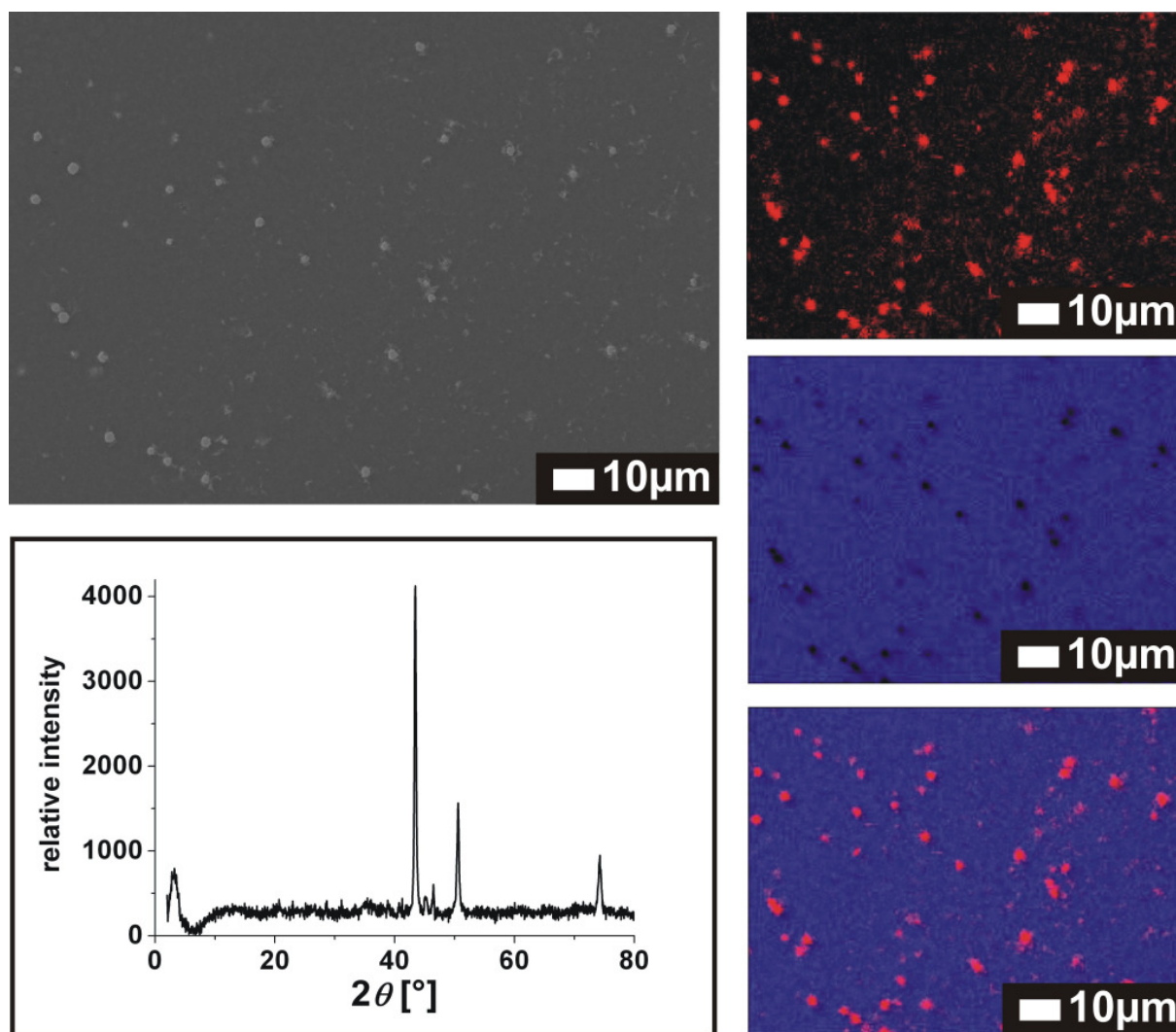


Figure 4. SEM image (top left), accordant Cu-EDS-mapping (top right), Si-EDS-mapping (middle right), overlap of both mappings (bottom right) and powder diffractogram of the ceramic (bottom left). All magnitudes of the images are 2000x.

### 6.3. Conclusion

Novel copper aminopyridinato complexes were synthesised and characterised. The dinuclear compound **3** was employed (due to the easy and cheap availability) in the metal modification of the polycarbosilazane HTT 1800. This reaction was investigated using NMR spectroscopy and goes smoothly to completeness. Covalent bonding between the metal centre and the precursor has been formed, which underlines the versatility of aminopyridinates metal modification of poly(organosilazanes). The gained metal enforced ceramic was investigated using SEM, EDS and powder diffraction. The results show the formation of crystallites and particles in different

sizes, which consist of elemental copper. Further investigations will focus on catalytic properties depending of the metal content.

## 6.4. Experimental

### 6.4.1. General Remarks

All reactions and manipulations with air-sensitive compounds were performed under dry argon, using standard Schlenk and glovebox techniques. Solvents were distilled from sodium benzophenone ketyl. Deuterated solvents were obtained from Cambridge Isotope Laboratories and were degassed, dried using molsieves and distilled prior to use.

The following starting material, 4-methyl-2-((trimethylsilyl)amino)pyridine ( $\text{Ap}^{\text{TMSH}}$ ) was synthesized using literature methods [32]. All other chemicals were purchased from commercial vendors and used without further purification if not otherwise mentioned in the synthetic procedure. NMR spectra were obtained using either a Varian INNOVA 300 or a Varian INNOVA 400 spectrometer. Chemical shifts are reported in ppm relative to the deuterated solvent. X-ray crystal structure analyses were performed by using a STOE-IPDS II equipped with an Oxford Cryostream low-temperature unit. Structure solution and refinement were accomplished using SIR97 [33], SHELXL-97 [34] and WinGX [35]. Crystallographic details are summarised in the supplementary material. CCDC-721155 (compound 1), -721156 (compound 2), -721157 (compound 3) contain the supplementary crystallographic data for this publication. These data can be obtained free of charge at [www.ccdc.cam.ac.uk/conts/retrieving.html](http://www.ccdc.cam.ac.uk/conts/retrieving.html) (or from the Cambridge Crystallographic Data Centre, 12 Union Road, Cambridge CB2 1EZ, UK; Fax: + 44-1223-336-033; e-mail: [deposit@ccdc.cam.ac.uk](mailto:deposit@ccdc.cam.ac.uk) ).

Elemental analyses were carried out by Vario elementar EL III except the elemental analysis of the ceramic. This was carried out by Mikroanalytisches Labor Pascher, Remagen, Germany. Magnetic data were measured with a Quantum-Design MPMS-5S SQUID magnetometer equipped with a 5 Tesla magnet in the range from 295 K to 2 K. The powdered samples were contained in a gel bucket and fixed in a non-magnetic sample holder. Each raw data file for the measured magnetic moment was

corrected for the diamagnetic contribution of the sample holder and the gel bucket. The molar susceptibility was corrected using Pascal constants and the increment method according to Haberditzl [36]. Crosslinking and ceramisation was carried out under nitrogen (Nabertherm R70/9). For SEM investigations, the ceramic material was embedded in an epoxy resin with added TiN particles and polished to a thickness of  $\sim 10 \mu\text{m}$ . The SEM measurements were performed with a Zeiss 1540EsB Cross beam, equipped with a Thermo Noran System Six EDS-system. The Powder diffractogram was recorded with a STOE STADI P.

#### 6.4.2. Synthesis of the Complexes

Synthesis of  $[(\text{Ap}^{\text{TMS}})_2\text{Cu}_2]$  (**3**): A solution of  $\text{Ap}^{\text{TMS}}\text{H}$  (1.803 g, 10 mmol) in 25 mL of diethylether ( $\text{Et}_2\text{O}$ ) was treated with 6.25 mL (1.6 M, 10 mmol) of *n*-BuLi in hexanes at  $0^\circ\text{C}$  and stirred for 30 min. After stirring for 1 h at room temperature this mixture was added to a suspension of CuBr (1.435 g, 10 mmol) in 140 mL THF at  $0^\circ\text{C}$  and the colour turned from dark green to pale green. After stirring overnight at room temperature the solvent was removed. The residue was extracted twice with 40 mL of hexane and filtered. Removing the solvent under reduced pressure yielded a pale green powder. Crystalline material was obtained after slow evaporation of a solution of **3** in hexane. Yield: 2.148 g (8.84 mmol, 88%). Anal. Found for  $\text{C}_{18}\text{H}_{30}\text{Cu}_2\text{N}_4\text{Si}_2$  ( $M_r=485.72$ ): C 44.30, H 6.56, N 11.49%. Calcd: C 44.51, H 6.23, N 11.53%.  $^1\text{H}$  NMR (400 MHz,  $\text{THF-d}^8$ ,  $\delta$ ): 0.31 (s, 18H, TMS), 2.11 (s, 6H, ar- $\text{CH}_3$ ), 6.09 (d,  $J = 7.6$  Hz, 2H, Ar-H), 6.39 (s, 2H, Ar-H), 7.42 (d,  $J = 7.6$  Hz, 2H, Ar-H);  $^{13}\text{C}$  NMR (400MHz,  $\text{THF-d}^8$ ,  $\delta$ ): 2.15, 21.40, 111.61, 116.41, 147.99 148.53, 170.13;  $^{29}\text{Si}$  NMR (300 MHz,  $\text{THF-d}^8$ ,  $\delta$ ): -0.58.

#### 6.4.3. Transmetalation

The poly(organosilazane) HTT 1800 (6.435 g) was reacted with 4.86 g (10 mmol) of complex **3** in 10 mL of  $\text{Et}_2\text{O}$ . Furthermore, 129 mg (0.48 mmol) dicumylperoxide was added. During 30 min the reaction mixture turned from pale yellow to dark brown. The solvent was removed in vacuo yielding a viscous brown oil. The NMR experiments were performed without addition of dicumylperoxide.

#### 6.4.4. Crosslinking and Ceramisation

The gained viscous brown oil was taken into an oven under nitrogen. The temperature was raised to 130 °C with a heating rate of 3 K/min. After holding for 30 min it was allowed to cool to room temperature. The aluminium bowl was removed from the solidified preceramic polymer and the temperature was raised to 1000 °C (heating rate 3 K/min to 300 °C; 1 K/min to 700 °C; 3 K/min to 950 °C; 1 K/min to 1000 °C) and held for 30 min. Afterwards the sample was allowed to cool to room temperature. The gained ceramic material was milled. Some fragments were taken out before and embedded in an epoxy resin for SEM investigations. A powder diffractogram was taken from the milled ceramic.

Further experimental details can be taken from the supporting information

#### 6.4.5. Acknowledgement

Financial support from the DFG (SPP 1181 “Nanoskalige anorganische Materialien durch molekulares Design”) and the Fonds der Chemischen Industrie is acknowledged. We thank A. M. Dietel for lab assistance, Dr. S. Demeshko for measuring magnetic susceptibilities, Dr. Ute Hörmann for preparing the samples for SEM investigations and Dr. Wolfgang Milius for powder diffraction measurements. Furthermore, we thank Clariant Advanced Materials GmbH for providing the precursor HTT 1800.

#### Supporting Information Available

Thermal ellipsoid plots of compound 1,2 and 3; X-ray data table. X-ray crystallographic files for compound 1,2 and 3. A Plot of magnetic moment of compound 1 against temperature. Detailed synthesis of compounds 1 and 2. This material is available free of charge via the internet at <http://pubs.acs.org>

#### 6.5. References

- [1] L. V. Interrante, K. Moraes, Q. Liu, N. Lu, A. Puerta, L. G. Sneddon, *Pure Appl. Chem.* **2002**, *74*, 2111-2117.
- [2] R. Riedel, G. Mera, R. Hauser, A. Klonczynski, *J. Ceram. Soc. Jpn.* **2006**, *114*, 425-444.

- [3] R. M. Laine, A. Sellinger, "Si-containing ceramic precursors" in *Chemistry of Organic Silicon Compounds* (Eds.: Z. Rappoport, Y. Apeloig), Wiley, Chichester, **1998**, vol. 2 (Pt. 3), pp. 2245-2316.
- [4] E. Kroke, Y.-L. Li, C. Konetschny, E. Lecomte, C. Fasel, R. Riedel, *Mater. Sci. Eng. R*, **2000**, *26*, 97-199.
- [5] A. Lukacs, *Am. Ceram. Soc. Bull.* **2007**, *86*, 9301-9306.
- [6] G. Motz, *Advances in Science and Technology* **2006**, *50*, 24-30.
- [7] G. Motz, T. Kabelitz, G. Ziegler, *Key Engineering Materials* **2004**, *264-268*, 481-484.
- [8] G. Motz, J. Hacker, G. Ziegler, "Design of SiCN - precursors for various applications" in *Ceramic Materials for Engines* (Eds.: J. G. Heinrich, F. Aldinger), Wiley-VCH, Weinheim, **2001**, pp. 581-585.
- [9] G. Motz, G. Ziegler, *Key Engineering Materials* **2002**, *206-213*, 475-478.
- [10] G. Motz, J. Hacker, G. Ziegler, "Special modified silazanes for coatings, fibers and CMC's" in *Ceramic Engineering and Science Proceedings*, Wiley, **2000**, vol. 21 (4, 24th Annual Conference on Composites, Advanced Ceramics, Materials and Structures: B), pp. 307-314.
- [11] X. Yan, X. Cheng, G. Han, R. Hauser, R. Riedel, *Key Engineering Materials* **2007**, *353-358*, 1485-1488.
- [12] X. Yan, X. Cheng, C. Li, R. Hauser, R. Riedel, *Mater. Sci. Forum* **2007**, *546-549*, 2269-2272.
- [13] H.-Y. Ryu, R. Raj, *J. Am. Ceram. Soc.* **2007**, *90*, 295-297.
- [14] P. Greil, *J. Eur. Ceram. Soc.* **1998**, *18*, 1905-1914.
- [15] P. Greil, *Adv. Eng. Mater.* **2000**, *2*, 339-348.
- [16] R. Petersen, D. A. Foucher, B.-Z. Tang, A. Lough, N. P. Raju, J. E. Greedan, I. Manners, *Chem. Mater.* **1995**, *7*, 2045-53.
- [17] R. Petersen, D. A. Foucher, A. Lough, N. Coombs, I. Manners, *Phosphorus, Sulfur Silicon Relat. Elem.* **1994**, *93-94*, 359-360.
- [18] M. Ginzburg, M. J. MacLachlan, S. M. Yang, N. Coombs, T. W. Coyle, N. P. Raju, J. E. Greedan, R. H. Herber, G. A. Ozin, I. Manners, *J. Am. Chem. Soc.* **2002**, *124*, 2625-39.
- [19] R. Hauser, A. Francis, R. Theismann, R. Riedel, *J. Mat. Sci.* **2008**, *43*, 4042-4049.

- [20] V. Salles, S. Foucaud, P. Goursat, "Ultrafine powders doped with aluminium in SiCN system" in *Ceramic Engineering and Science Proceedings*, Wiley, **2000**, vol. 28 (2, Mechanical Properties and Performance of Engineering Ceramics and Composites III), pp. 65-75.
- [21] R. Kempe, *Angew. Chem.* **2000**, *112*, 478-504; *Angew. Chem. Int. Ed.* **2000**, *39*, 468-493.
- [22] N. Hering, K. Schreiber, R. Riedel, O. Lichtenberger, J. Woltersdorf, *Appl. Organomet. Chem.* **2001**, *15*, 879-886.
- [23] R. Kempe, *Eur. J. Inorg. Chem.* **2003**, 791-803.
- [24] G. Glatz, G. Motz, R. Kempe, *Z. Anorg. Allg. Chem.* **2008**, *634*, 2897-2902.
- [25] G. Glatz, S. Demshko, G. Motz, R. Kempe, *Eur. J. Inorg. Chem.* **2009**, 1385-1392.
- [26] S. Deeken, S. Proch, E. Casini, H. F. Braun, C. Mechtler, C. Marschner, G. Motz, R. Kempe, *Inorg. Chem.* **2006**, *45*, 1871-1879.
- [27] A. Spannenberg, P. Arndt, R. Kempe, *Angew. Chem., Int. Ed.* **1998**, *37*, 832-835; *Angew. Chem.* **1998**, *110*, 824-827.
- [28] S. Deeken, T. Irrgang, R. Kempe, *Z. Krist. NCS* **2006**, *221*, 93-94.
- [29] A. Spannenberg, A. Tillack, P. Arndt, R. Kirmse, R. Kempe, *Polyhedron* **1998**, *17*, 845-850.
- [30] L. M. Engelhardt, G. E. Jacobsen, P. C. Junk, C. L. Raston, B. W. Skelton, A. H. White, *J. Chem. Soc., Dalton Trans.* **1988**, 1001-1020.
- [31] H. E. Swanson, E. Tatge in: *Standard X-Ray Diffraction Powder Patterns*, NBS Circular 539, **1953**, vol. 1, p.11.
- [32] R. Kempe, P. Arndt, *Inorg. Chem.* **1996**, *35*, 2644-2649.
- [33] A. Altomare, M.C. Burla, M. Camalli, G.L. Cascarano, C. Giacovazzo, A. Guagliardi, A.G.G. Moliterni, G. Polidori, R. Spagna, *J. Appl. Crystallogr.* **1999**, *32*, 115-119.
- [34] G. M. Sheldrick, SHELX-97, Program for Crystal Structure Analysis (Release 97-2), Institut für Anorganische Chemie der Universität Göttingen, Germany, **1998**.
- [35] L.J. Farrugia, *J. Appl. Crystallogr.* **1999**, *32*, 837-838.
- [36] a) W. Haberditzl, *Angew. Chem.* **1966**, *78*, 277-312; *Angew. Chem. Int. Ed. Engl.* **1966**, *5*, 288-298; b) W. Haberditzl, *Magnetochemie*, Akademie-Verlag 1968.

## 6.6. Supplementary Material

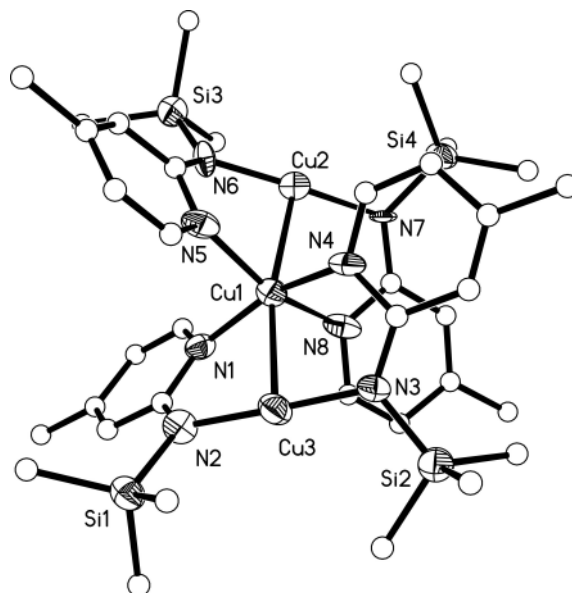


**Figure S1.** Molecule structure of **1** (ORTEP view; for clarity, only non carbon atoms are drawn as 50% probability ellipsoids). Selected bond lengths [Å] and angles [°]: Cu1-Cu2 2.576(2), Cu1-Cu3 2.562(2), Cu1-N1 1.950(9), Cu1-N4 1.983(9), Cu1-N5 1.979(10), Cu1-N8 2.014(9), Cu2-N6 1.851(8), Cu2-N7 1.863(8), Cu3-N2 1.840(9), Cu3-N3 1.841(9), Cu3-Cu1-Cu2 168.56(8), N2-Cu3-N3 175.6(4), N6-Cu2-N7 176.6(4).

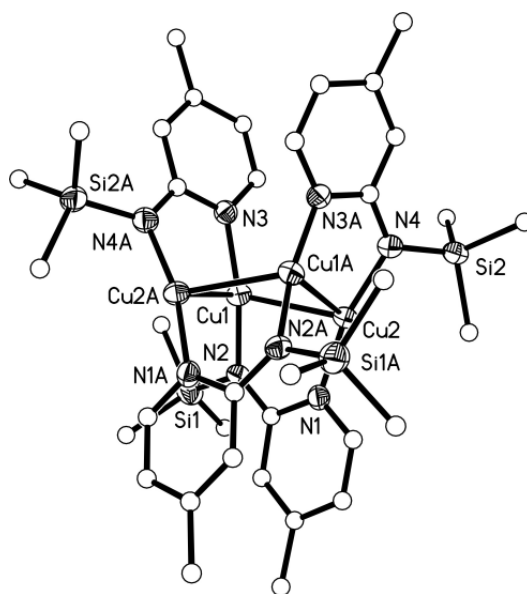


**Figure S2.** Molecular structure of **2** (ORTEP view; for clarity, only non carbon atoms are drawn as 50% probability ellipsoids). Selected bond lengths [Å] and angles [°]: Cu1-Cu2 2.5932(13), Cu1-Cu2A 2.6467(10), Cu1-N2 1.888(4), Cu1-N3 1.901(4), Cu2-N1 1.878(4), Cu2-N4 1.863(4), Cu1-Cu2-Cu1A 79.55(4), Cu2-Cu1-Cu2A 96.68(4), N2-Cu1-N3 165.25(16), N4-Cu2-N1 166.28(16).

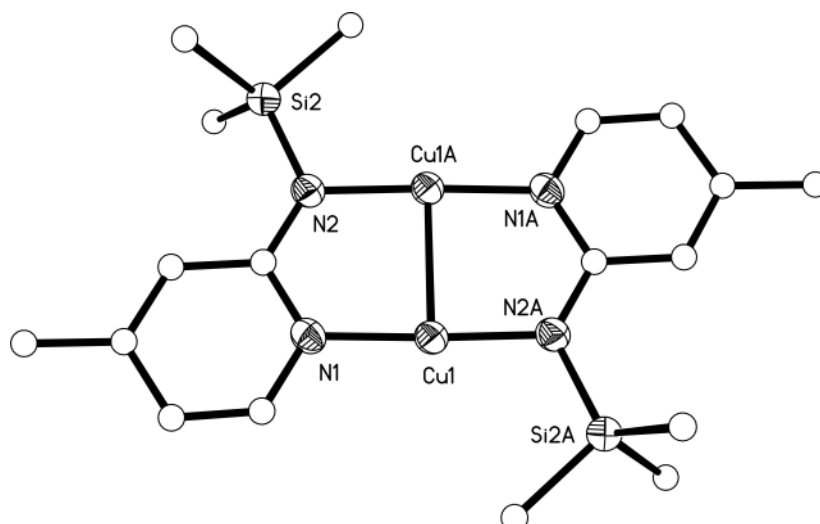


**Figure S3.** Molecule structure of 3 (ORTEP view; for clarity, only non carbon atoms are drawn as 50% probability ellipsoids). Selected bond lengths [Å] and angles [°]: Cu1-N1 1.880(3), Cu1-N2 1.872(3), Cu1-Cu1 2.4143(8), N1-Cu1-N2A 177.83(12), N1-Cu1-Cu1 88.65(8), N2-Cu1-Cu1 89.18(8).

**Table S1.** Data of the X-ray crystal structure analyses

Compound	1	2	3
Formula	$C_{36}H_{60}Cu_3N_8Si_4$	$C_{36}H_{60}Cu_4N_8Si_4$	$C_{18}H_{30}Cu_2N_4Si_2$
$F_w$	907.90	971.44	485.72
crystal system	monoclinic	monoclinic	triclinic
space group	$P2_1/n$	$C2/c$	$P-1$
$a$ [Å]	10.3860(15)	18.254(4)	7.1050(9)
$b$ [Å]	18.738(3)	18.545(4)	7.1490(9)
$c$ [Å]	23.079(3)	14.003(5)	11.7500(15)
$\alpha$ [°]	90	90	105.584(10)
$\beta$ [°]	95.045(11)	99.80(3)	91.627(10)
$\gamma$ [°]	90	90	103.728(10)
$V$ [Å <sup>3</sup> ]	4474.1(11)	4671(2)	555.75(12)
$Z$	4	4	1
$d$ (calcd) [g cm <sup>-3</sup> ]	1.348	1.381	1.451
$\mu$ [mm <sup>-1</sup> ]	1.555	1.933	2.030
$2\theta$ range [°]	2.80-49.21	4.47-52.17	3.62-52.14
$\omega R^2$ (all data)	0.1174	0.0739	0.0783
$R$ value	0.0467	0.0377	0.0305

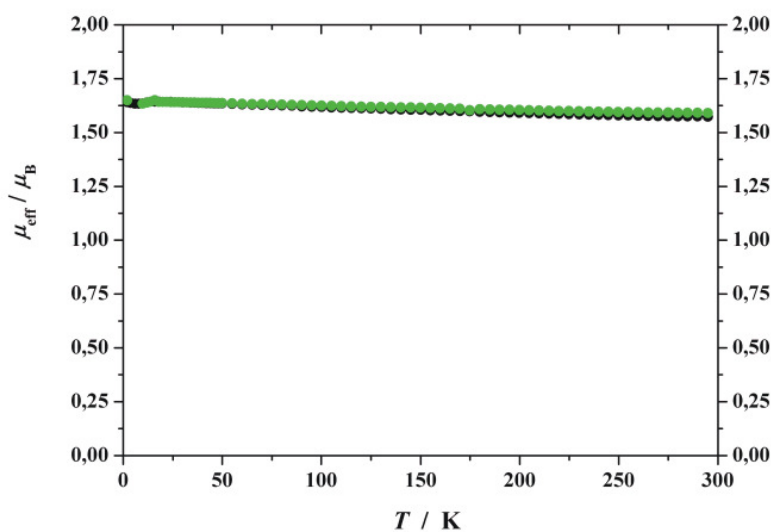


**Figure S4.** Dependency of the effective magnetic moment  $\mu_{\text{eff}}$  of 1 from the temperature at a field of 0.2 (green circles) and 0.5 T (black circles).

### Synthesis of complexes

Synthesis of  $[(\text{Ap}^{\text{TMS}})_4\text{Cu}_3]$  (1): A solution of  $\text{Ap}^{\text{TMS}}\text{H}$  (361 mg, 2 mmol) in 10 mL of diethylether ( $\text{Et}_2\text{O}$ ) was treated with 1.25 mL (1.6 M, 2 mmol) of  $n\text{-BuLi}$  in hexanes at  $-40^\circ\text{C}$  and stirred for 30 min. After stirring for 1 h at room temperature this mixture was added to a suspension of  $\text{CuBr}_2$  (223 mg, 1 mmol) in 10 mL THF at  $-40^\circ\text{C}$  and the colour turned from brownish to greenish. After stirring overnight at room temperature the solvent was removed. The residue was extracted twice with 15 mL of hexane and filtered afterwards. The dark blue solution was concentrated and filtered again leaving a beige crystalline solid. The filtrate was concentrated again and was allowed to crystallize in a freezer. After a few days dark blue crystals were obtained. Yield: 0.157 g (0.17 mmol, 52%). Anal. Found for  $\text{C}_{36}\text{H}_{60}\text{Cu}_3\text{N}_8\text{Si}_4$  ( $M_r=907.90$ ): C 47.72, H 6.58, N 12.29%. Calcd: C 47.63, H 6.66, N 12.34%.  $\mu_{\text{B}}$  (295 K)=1.59.

As a byproduct a few beige crystals (suitable for X-ray analysis) of  $[(\text{Ap}^{\text{TMS}})_4\text{Cu}_4]$  (2) were obtained and could be separated via picking.

## 7. Novel Cu-SiCN ceramics via molecular design – Part II: The Selective Oxidation of Simple Alkanes Using Air

Germund Glatz,<sup>[a]</sup> Thomas Schmalz,<sup>[b]</sup> Tobias Kraus,<sup>[b]</sup> Frank Haarmann,<sup>[c]</sup> Günter Motz,<sup>\*,[b]</sup> Rhett Kempe<sup>\*,[a]</sup>

**Keywords:** Alkanes; Aminopyridinato ligands; Copper; Cu-SiCN; Metal modification; Oxidation; Precursor ceramics

To be submitted

**Abstract.** A series of copper containing SiCN precursor ceramics (Cu-SiCN) was synthesised via molecular design using copper aminopyridinates. This molecular approach allowed the variation of the metal content in a wide range and even high metal contents up to 14% are reachable. These ceramics can be synthesised in very good ceramic yields. Elemental copper is present and depending on the metal content it is detectable by solid-state copper NMR. SEM micrographs clearly indicate the existence of copper particles in all ceramics. The Cu-SiCN ceramics containing higher amounts of copper show a broad distribution of particle sizes from micrometer-scale to nanometer-scale. However, only nanometer-scaled particles are found in less copper containing ceramics. Furthermore, a copper texture was found within the ceramics, which disappears with decreasing copper content. All ceramics show catalytical activity towards the oxidation of cycloalkanes by using air as oxidant. The selectivity of the reaction raises clearly with increasing copper content, whereas the turnover numbers decrease. The catalysts are recyclable and show only minor catalyst leaching. These results confirm the applicability of this new class of metal containing ceramics in catalysis.

## 7.1. Introduction

The selective oxidation of simple alkanes is one of the major challenges of today's chemistry.<sup>[1-3]</sup> Owing to the difficulties and high expenses associated with the handling and transportation of natural gas, large amounts remain unexploited.<sup>[4,5]</sup> Thus, there is great need for catalysts that are able to convert simple alkanes into the corresponding monooxidation products. An ideal catalyst should be robust, recyclable and inexpensive.

Interesting properties like high temperature stability, corrosion resistance or long term durability are provided by amorphous SiCN precursor ceramics derived from poly(organosilazanes). These ceramics are highly tunable and versatile materials because of the molecular pathway to these materials.<sup>[6-10]</sup> Furthermore, they are suitable for metal modification. Remarkable few pathways to metal modified precursor ceramics are described. Beside some less applicable approaches<sup>[6,11-19]</sup> metal alkyls like trimethylaluminum<sup>[20]</sup> or early transition metal amides<sup>[21]</sup> like amidotitanium complexes<sup>[8-10,22]</sup> have shown a certain potential to stronger interact with the ceramic precursor and increase ceramic yield. We recently reported the introduction of copper into ceramic material by the use of a copper aminopyridinate.<sup>[23]</sup> This material meets all demands of an ideal catalyst.

In this study we focus on an application of the ceramic as heterogeneous catalyst in the oxidation of alkanes. Furthermore, the dependency of the properties on the metal content of the copper containing precursor ceramic is presented.

## 7.2. Results and Discussion

### 7.2.1. Variation of the Metal Content

The recently published molecular approach was employed to obtain copper modified SiCN precursor ceramics that contain different amounts of copper.<sup>[23]</sup> Copper/Silicon ratios of 1/5, 1/10, 1/25, 1/50 and 1/100 were adjusted in the metal modified preceramic polysilazane. The ceramisation behaviour was investigated by thermogravimetical measurements. The ceramic yields range from 61% to 81% (Figure 1). The metal-free polysilazane provides 75% ceramic yield. Despite of liberation of large amounts of free ligand, quite good ceramic yields are achievable.

This is due to the contribution of the free ligand to the ceramic yield. In general, with increasing metal content, a decrease in ceramic yield is obtained.

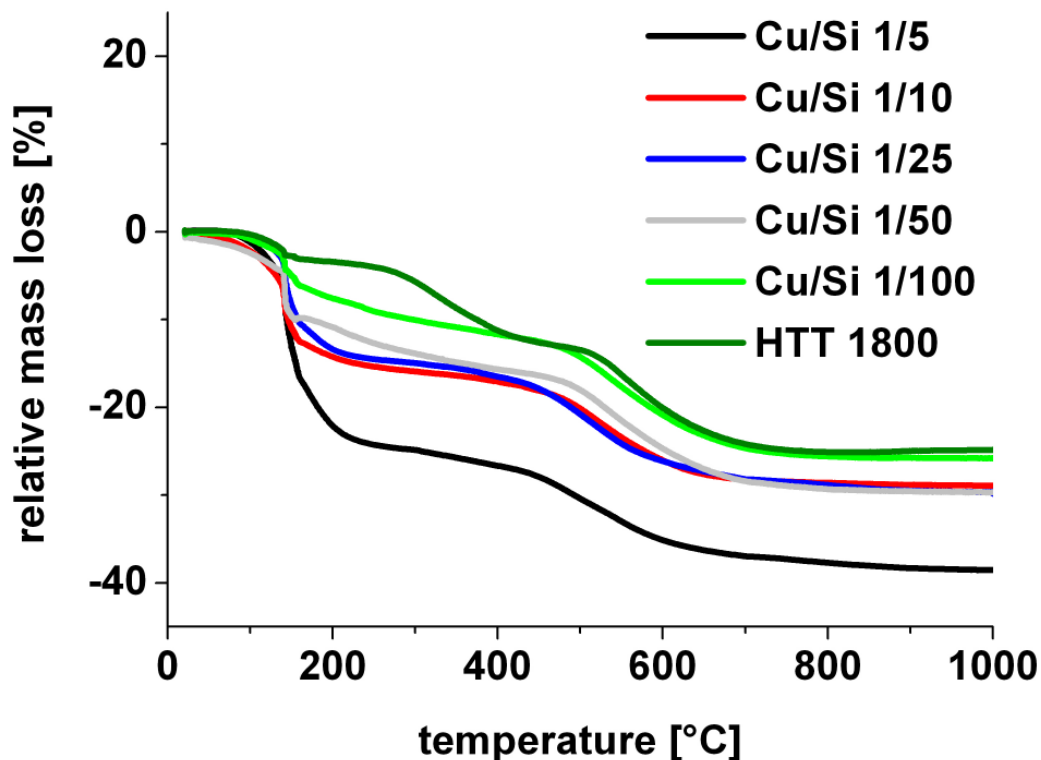


**Figure 1.** Thermogravimetric measurements of the ceramics containing different amounts of copper.

For further comparability, elemental analyses were carried out of each copper containing ceramic. Depending on the copper/silicon ratio found in the preceramic polymer, the metal content in the corresponding ceramic increases. Thereby, the content of silicon, carbon and nitrogen declines with increasing metal content. These results show that the metal content of the ceramic materials is tunable by addition of metal aminopyridinate and can be varied in a wide range.

**Table 1.** Elemental composition of the different copper containing SiCN ceramics. All values are given in wt%.

	1/5	1/10	1/25	1/50	1/100
<b>C</b>	15.0	15.1	16.6	18.4	17.6
<b>H</b>	0.7	0.6	0.7	0.6	0.5
<b>N</b>	21.8	23.8	22.8	24.1	23.8
<b>Si</b>	44.4	47.8	51.0	51.7	52.9
<b>Cu</b>	13.7	7.28	4.60	2.40	1.78
<b>O</b>	3.40	3.21	3.40	3.10	2.23

It was shown recently that elemental and crystalline copper particles are present in the ceramic containing copper.<sup>[23]</sup> The less copper containing ceramics are found to be completely amorphous (except very small amount of silicon nitride, which belongs to the ceramic matrix) indicating that copper is not crystalline in the less copper containing ceramics. In order to prove whether elemental copper or a copper compound is present, solid-state copper NMR investigations of the ceramics 1/10, 1/25, 1/50 and 1/100 were carried out (Figure 2).

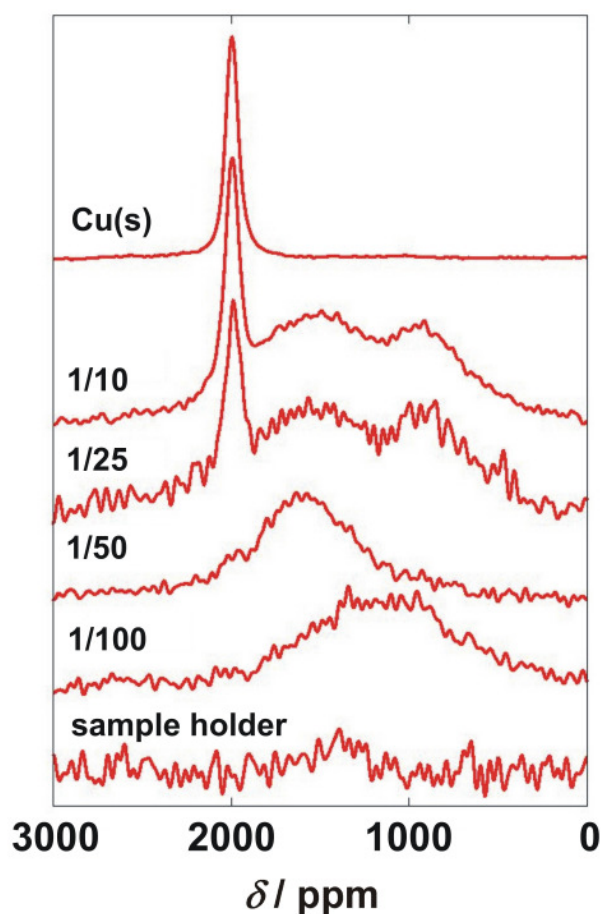


**Figure 2.** Solid-state copper NMR measurements of the different ceramics.

The results evidenced the presence of elemental copper in the 1/10 and 1/25 ceramic. Concerning the 1/50 and 1/100 ceramic, the solid-state copper NMR measurements do not allow an assignment to elemental copper. The observed, broad signals may indicate a fine-particle distribution of copper in the ceramic material.

More information about the kind of presence of copper in the ceramics was gained by SEM-micrographs. All ceramics contain copper particles and the number of particles increases with the copper content. In case of high copper amounts, a broad distribution of particle sizes was found. Micrometer-scaled as well as nanometer-scaled particles were obtained (Figure 3). Small (nanometer-scaled) particles could be obtained at low copper content.

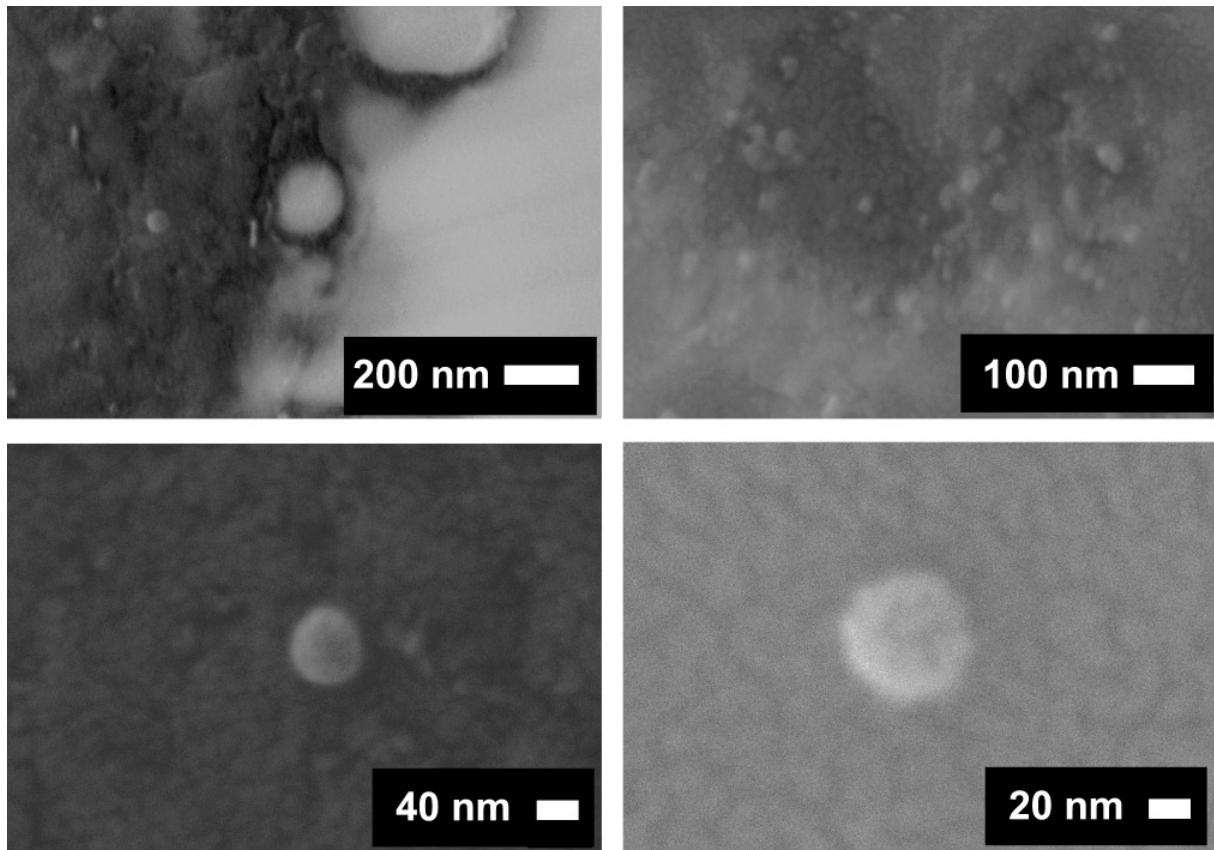


**Figure 3.** SEM-micrographs of different sized copper particles (ceramics 1/5 top left, 1/10 top right, 1/10 bottom left, 1/100 bottom right).

This finding can be explained by the lower tendency of agglomeration (because less copper is present). Thus, less and smaller particles are formed. Beside the particles, a texture of the ceramic matrix is obtained. The intensity and broadening of this texture decreases with decreasing copper content and disappears completely in case of the lowest copper content.

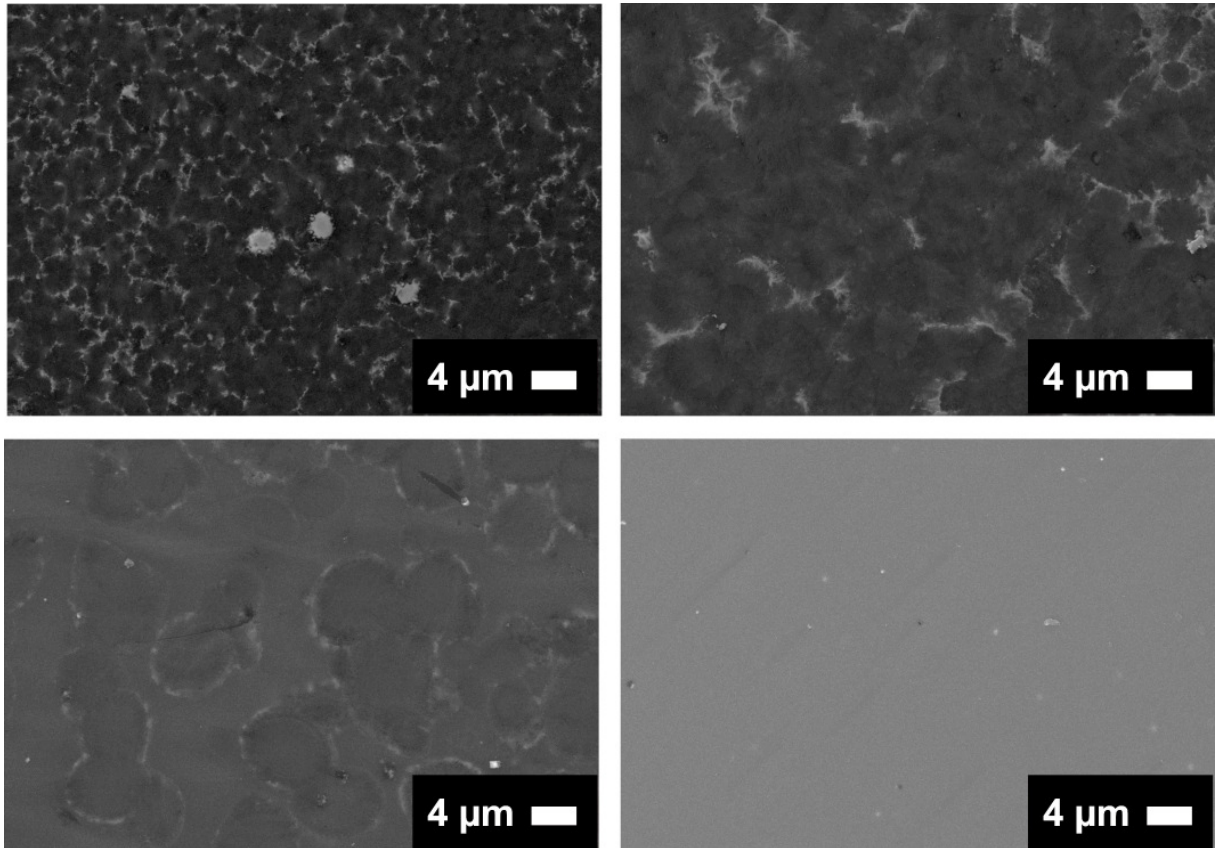


**Figure 4.** SEM-micrographs of different ceramics (top left: 1/5; top right: 1/10; bottom left: 1/50; bottom right: 1/100).

EDS-mappings of the 1/5 ceramic evidenced that the particles consist of elemental copper. It can clearly be seen that the amount and size of the particles decreases with decreasing copper content (Figure 5). Hence, no copper enriched areas could be found in case of less copper containing ceramics and a homogeneous distribution of copper could be found (Figure 5, right hand).

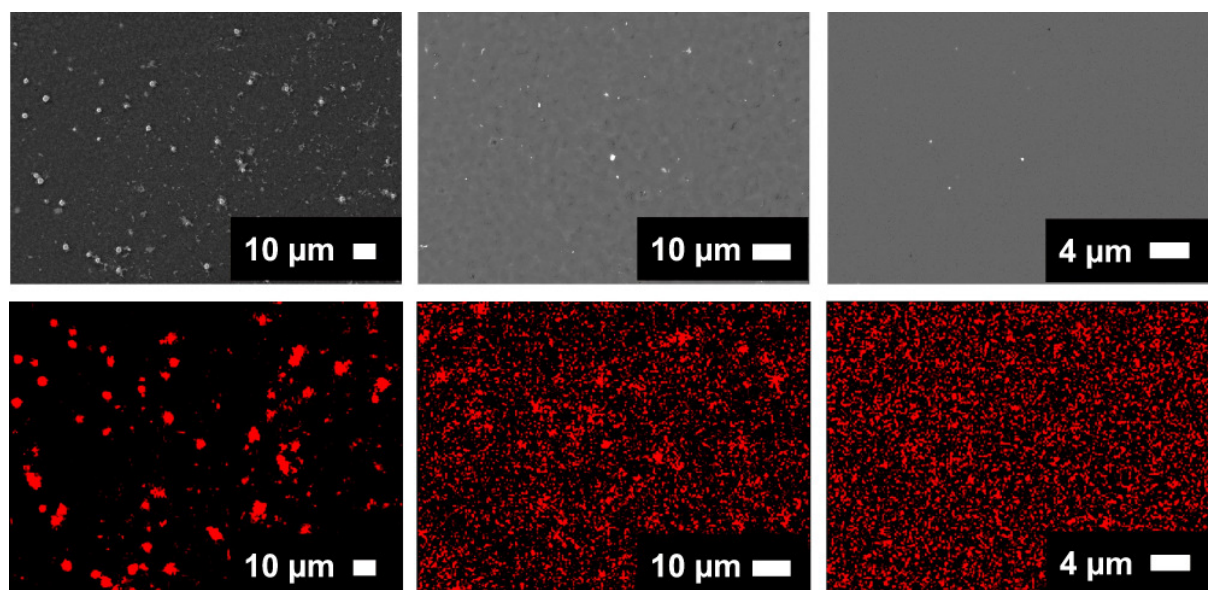


**Figure 5.** SEM-micrographs and corresponding copper EDS-mappings (left hand: 1/5; middle: 1/10; right hand: 1/100).

### 7.2.2. Catalytical Studies

Having compared the obtained copper containing SiCN precursor ceramics with respect to ceramic yield, elemental composition, solid-state copper NMR and SEM/EDS measurements, the catalytic properties of these ceramics were explored. The selective monooxidation of alkanes is a dream reaction and therefore, this reaction type has gained lot of research interest during the last years.<sup>[24,25]</sup> As a model system often cycloalkanes are employed. In the following, it is focused on the selective monooxidation of cycloalkanes only. In general, there are a few approaches, which differ in the way (homogeneously or heterogeneously) or in the oxidation agent (hydrogen peroxide, *tert*-butylhydroperoxide (TBHP), dioxygen or air). The homogeneous catalytic systems provide worse yields and selectivities than the heterogeneous systems. In case of using hydrogen peroxide or TBHP the yields are excellent (cyclohexane) in case of cobalt containing aluminophosphates<sup>[26]</sup> and even the selectivity are excellent (cyclohexanol) in case of titanium containing aluminophosphates.<sup>[27]</sup> But remarkable few systems are known to catalyse the selective oxidation of cycloalkanes using dioxygen as oxidant.<sup>[28-31]</sup>

We employed air as an oxidant for the oxidation of alkanes in this work. Cyclooctane was chosen as substrate. To prove the catalytic activity of copper containing SiCN precursor ceramics, blind controls were carried out (see Table 2). Neither TBHP only,

nor TBHP and copper free SiCN precursor ceramics together were able to catalyse the oxidation of cyclooctane. Furthermore, in no case a conversion was obtained when not TBHP was used. It can be concluded that TBHP is necessary as a radical initiator and a copper containing ceramic is needed as catalyst.

**Table 2.** Yields [%] observed in control experiments.

<b>catalyst</b>	<b>without TBHP</b>	<b>2mol% TBHP</b>
none	-	-
elemental copper <sup>b)</sup>	-	6.8
copper free ceramic <sup>c)</sup>	-	-
copper containing ceramic (1:10) <sup>c)</sup>	-	13.9

<sup>a)</sup> Reaction conditions: 1 mL cyclooctane, 2 mol% TBHP, 20 bar air, 80 °C, 75h.

<sup>b)</sup> An amount of 3mg of copper was used. This correlates to a multiple of the copper amount of 10mg of the most copper containing ceramic.

<sup>c)</sup> An amount of 10mg of ceramic material was used.

To investigate the role of the ceramic matrix, elemental copper was employed as catalyst. Elemental copper is able to catalyse the oxidation of cyclooctane, but the yield of products was considerably worse than by use of copper containing ceramics. Moreover, the selectivity is also much worse than observed for Cu-SiCN ceramics. The selectivity of the 1/100 ceramic is comparable to that of elemental copper.

**Table 3.** Yields [%] and turnover numbers of different Cu-SiCN catalysts achieved in oxidation of cyclooctan.<sup>a)</sup>

<b>ceramic</b>	<b>yield</b>	<b>TON<sup>b)</sup></b>
1/100	11.5	305
1/50	13.5	266
1/25	9.7	100
1/10	13.9	90
1/5	13.0	45

<sup>a)</sup> Reaction conditions: 1 mL cyclooctan, 10 mg ceramic, 2 mol% TBHP, 20 bar air, 80 °C, 75h.

<sup>b)</sup> Ratio of amount of products and amount of copper provided by the used catalyst.

With increasing copper content, the selectivity rises strongly up to 80% for cyclooctanone (Figure 6). Furthermore, the total yield tends to increase with growing copper content of the ceramic material but the turnover numbers (based on the copper content detected in elemental analyses) decrease with increasing copper content (see Table 3) Compared to known heterogeneous catalytic systems that use

dioxygen as oxidant, the presented Cu-SiCN ceramics are highly active and show similar or better selectivities.

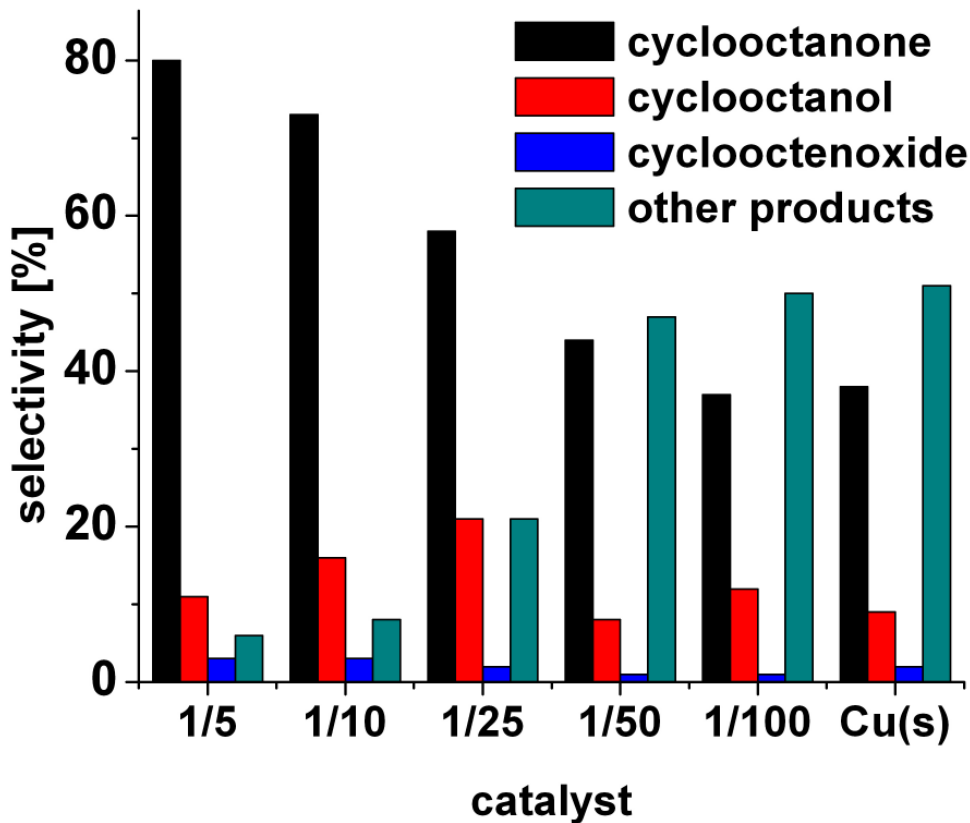


**Figure 6.** Selectivities [%] of different catalysts. Reaction conditions: 1 mL cyclooctane, 10 mg ceramic (or 3 mg copper), 2 mol% TBHP, 20 bar air, 80 °C, 75h.

One ceramic (1/10) was tested with regard to the recyclability. Actually, the Cu-SiCN ceramic is recyclable, when new substrate and new activator is added. However, the selectivity oscillates somewhat and the yields decrease slightly with increasing catalytic cycles, which is due to catalyst loss by filtration. In order to get evidence how general is the applicability of these ceramics in selective oxidation reactions, more cycloalkanes were employed as substrates (Table 5).

**Table 4.** Yields [%] and selectivities [%] achieved by recycling of the catalyst.<sup>a)</sup>

cycle	yield	Selectivity			
		ketone	alcohol	epoxide	Others
1	12.0	78	18	1	10
2	11.7	58	18	3	21
3	10.1	67	18	4	11

<sup>a)</sup> Reaction conditions: 1 mL cyclooctane, 2 mol% TBHP, 20 bar air, 80 °C, 50h. After every cycle, it was filtrated and new substrate and activator was added.

The smallest cycloalkane showed only minor conversion, but with increasing size of the rings, the yields are also increasing. The observed selectivity is quite constant for all cycloalkanes and is around 70% for the corresponding ketones.

**Table 5.** Yields [%] and selectivities [%] achieved by oxidation of different cycloalkanes.<sup>a)</sup>

substrate	yield	Selectivity		
		ketone	alcohol	Others
cyclohexane	1.0	n.d. <sup>b)</sup>	n.d. <sup>b)</sup>	n.d. <sup>b)</sup>
cycloheptane	6.0	68	25	7
cyclooctane	13.9	73	16	11
cyclodecane	16.0	74	19	7

<sup>a)</sup> Reaction conditions: 1 mL substrate, 10mg 1/10 ceramic, 2 mol% TBHP, 20 bar air, 80 °C, 75h.

<sup>b)</sup> Not determined.

### 7.3. Conclusion

A series of copper modified SiCN ceramics was synthesised and characterised. The copper content is tunable in a broad range. Even high copper amounts in the ceramic material are achievable. Elemental copper particles of different sizes are present in the ceramic material. The sizes of the particle depend on the copper content of the ceramic. Nanometer-scaled particles are present in all Cu-SiCN ceramics. The obtained ceramics are recyclable heterogeneous catalysts. As an example, they can be employed as catalysts for the selective oxidation of cycloalkanes under mild conditions. Due to the high tunability and the generalisability of the molecular approach to this new class of ceramics, further applications as heterogeneous catalysts can be expected.

**Acknowledgement.** Financial support from the DFG (SPP 1181 “Nanoskalige anorganische Materialien durch molekulares Design”) and the Fonds der Chemischen Industrie is acknowledged. We thank A. M. Dietel for lab assistance and

Dr. Ute Hörmann for preparing the samples for SEM investigations. Furthermore, we thank Clariant Advanced Materials GmbH for providing the precursor HTT 1800.

## 7.4. Experimental Section

### 7.4.1. General Procedures

The metal modification agent,  $[\text{Cu}_2(\text{Ap}^{\text{TMS}})_2]$  ( $\text{Ap}^{\text{TMS}}$  = 4-methyl-2-((trimethylsilyl)amino)pyridinate, was synthesised like reported previously.<sup>[23]</sup> All other chemicals were purchased from commercial vendors and used without further purification if not otherwise mentioned in the synthetic procedure.

The elemental analyses were carried out by Mikroanalytisches Labor Pascher, Remagen, Germany. Crosslinking and ceramisation was carried out under nitrogen (Nabertherm R70/9). Thermogravimetical analyses were carried out with a Linsers L81 A1550.

For SEM investigations, the ceramic material was embedded in an epoxy resin with added TiN particles and polished to a thickness of  $\sim 10 \mu\text{m}$ . The SEM measurements were performed with a Zeiss 1540EsB Cross beam, equipped with a Thermo Noran System Six EDS-system. GC analyses were carried out with a Agilent 6890N (column HP-5) using dodecane as internal standard.

### 7.4.2. Synthesis of the Ceramic Materials

The poly(organosilazane) HTT 1800 (6.435 g) was reacted with  $[\text{Cu}_2(\text{Ap}^{\text{TMS}})_2]$  (Cu:Si 1:5, 4.86 g, 10 mmol; Cu:Si 1:10, 2.43 g, 5mmol; Cu:Si 1:25, 971 mg, 2 mmol; Cu:Si 1:50, 486 mg, 1 mmol; Cu:Si 1:100, 243 mg, 0.5 mmol) in 10 mL of  $\text{Et}_2\text{O}$ . Furthermore, 129 mg (0.48 mmol) dicumylperoxide was added. During 30 min the reaction mixture turned from pale yellow to dark brown. The solvent was removed in vacuo yielding a viscous brown oil. The gained oil was taken into an oven under nitrogen. The temperature was raised to  $130^\circ\text{C}$  with a heating rate of 3 K/min. After holding for 30 min it was allowed to cool to room temperature. The aluminium bowl was removed from the solidified preceramic polymer and the temperature was raised to  $1000^\circ\text{C}$  (heating rate 3 K/min to  $300^\circ\text{C}$ ; 1 K/min to  $700^\circ\text{C}$ ; 3 K/min to  $950^\circ\text{C}$ ; 1 K/min to  $1000^\circ\text{C}$ ) and held for 30 min. Afterwards the sample was allowed to cool to

room temperature. The gained ceramic material was milled. Some fragments were taken out before and embedded in an epoxy resin for SEM investigations.

### 7.4.3. Catalytical Testings

A typical procedure: 10 mg of the ceramic were mixed together with 1 mL of cyclooctane and 2 mol% of TBHP (27.1  $\mu$ L of a 5.5 M solution in decane) in a glass tube. This was placed in a Parr autoclave and a pressure of 20 bar aer artificialis medicinalis (artificial air) was applied. At 80 °C the reaction mixture was stirred for 75h. Afterwards, it was diluted with THF and dodecane as internal standard was added. The yields and selectivities were determined by GC analyses.

## 7.5. References

- [1] G. Dyker, *Angew. Chem. Int. Ed.* **1999**, *38*, 1698-1712; *Angew. Chem.* **1999**, *111*, 1808-1822.
- [2] K. Godula, D. Sames, *Science* **2006**, *312*, 67-72.
- [3] F. Kakiuchi, N. Chatani, *Adv. Synth. Catal.* **2003**, *345*, 1077-1101.
- [4] J. A. Labinger, J. E. Bercaw, *Nature* **2002**, *417*, 507-514.
- [5] A. S. Goldman, A. H. Roy, Z. Huang, R. Ahuja, W. Schinski, M. Brookhart, *Science* **2006**, *312*, 257-261.
- [6] G. Motz, *Advances in Science and Technology* **2006**, *50*, 24-30.
- [7] G. Motz, T. Kabelitz, G. Ziegler, *Key Engineering Materials* **2004**, *264-268*, 481-484.
- [8] G. Motz, J. Hacker, G. Ziegler, "Design of SiCN - precursors for various applications" in: *Ceramic Materials for Engines* (Eds.: J. G. Heinrich, F. Aldinger), Wiley-VCH, Weinheim, **2001**, pp. 581-585.
- [9] G. Motz, G. Ziegler, *Key Engineering Materials* **2002**, *206-213*, 475-478.
- [10] G. Motz, J. Hacker, G. Ziegler, "Special modified silazanes for coatings, fibers and CMC's" in: *Ceramic Engineering and Science Proceedings*, Wiley, **2000**, vol. 21 (4, 24th Annual Conference on Composites, Advanced Ceramics, Materials and Structures: B), pp. 307-314.
- [11] X. Yan, X. Cheng, G. Han, R. Hauser, R. Riedel, *Key Engineering Materials* **2007**, *353-358*, 1485-1488.
- [12] X. Yan, X. Cheng, C. Li, R. Hauser, R. Riedel, *Mater. Sci. Forum* **2007**, *546-549*, 2269-2272.

- [13] H.-Y. Ryu, R. Raj, *J. Am. Ceram. Soc.* **2007**, *90*, 295-297.
- [14] P. Greil, *J. Eur. Ceram. Soc.* **1998**, *18*, 1905-1914.
- [15] P. Greil, *Adv. Eng. Mater.* **2000**, *2*, 339-348.
- [16] R. Petersen, D. A. Foucher, B.-Z. Tang, A. Lough, N. P. Raju, J. E. Greedan, I. Manners, *Chem. Mater.* **1995**, *7*, 2045-53.
- [17] R. Petersen, D. A. Foucher, A. Lough, N. Coombs, I. Manners, *Phosphorus, Sulfur Silicon Relat. Elem.* **1994**, *93-94*, 359-360.
- [18] M. Ginzburg, M. J. MacLachlan, S. M. Yang, N. Coombs, T. W. Coyle, N. P. Raju, J. E. Greedan, R. H. Herber, G. A. Ozin, I. Manners, *J. Am. Chem. Soc.* **2002**, *124*, 2625-39.
- [19] R. Hauser, A. Francis, R. Theismann, R. Riedel, *J. Mat. Sci.* **2008**, *43*, 4042-4049.
- [20] V. Salles, S. Foucaud, P. Goursat, "Ultrafine powders doped with aluminium in SiCN system" in: *Ceramic Engineering and Science Proceedings*, Wiley, **2000**, vol. 28 (2, Mechanical Properties and Performance of Engineering Ceramics and Composites III), pp. 65-75.
- [21] R. Kempe, *Angew. Chem.* **2000**, *112*, 478-504; *Angew. Chem. Int. Ed.* **2000**, *39*, 468-493.
- [22] N. Hering, K. Schreiber, R. Riedel, O. Lichtenberger, J. Woltersdorf, *Appl. Organomet. Chem.* **2001**, *15*, 879-886.
- [23] G. Glatz, T. Schmalz, T. Kraus, G. Motz, R. Kempe, unpublished results.
- [24] J. M. Thomas, R. Raja, *Top. Catal.* **2006**, *40*, 3-17.
- [25] J. M. Thomas, R. Raja, *Catal. Today* **2006**, *117*, 22-31.
- [26] P. Selvam, S. K. Mohapatra, *Microporous Microporous Mater.* **2004**, *73*, 137-149.
- [27] P. Selvam, S. K. Mohapatra, *J. Catal.* **2005**, *233*, 276-287.
- [28] K. Yamaguchi, N. Mizuno, *New J. Chem.* **2002**, *26*, 972-974.
- [29] R. Zhao, D. Ji, G. Lv, G. Qian, L. Yan, X. Wang, J. Suo, *Chem. Commun.* **2004**, 904-905.
- [30] Y.-J. Xu, P. Landon, D. Enache, A. F. Carley, M. W. Roberts, G. J. Hutchings, *Catal. Lett.* **2005**, *101*, 175-179.
- [31] N. Theyssen, Z. Hou, W. Leitner, *Chem. Eur. J.* **2006**, *12*, 3401-3409.

## 8. List of Publications

The following publications have been published, are submitted or to be submitted during the work on this thesis:

1. Germund Glatz, Torsten Irrgang, Rhett Kempe, *Z. Kristallogr. NCS* **2007**, *222(3)*, 261-262.  
“Crystal structure of tetra- $\mu_3$ -bromo-tetrakis(*tert*-butyl-(methylpyridin-2-yl)-amine)-tetracopper(I),  $\text{Cu}_4\text{Br}_4(\text{C}_{10}\text{H}_{16}\text{N}_2)_4$ ”
2. Germund Glatz, Torsten Irrgang, Rhett Kempe, *Z. Kristallogr. NCS* **2007**, *222(3)*, 265-266.  
“Crystal structure of (4-methyl-pyridin-2-yl)-(2,4,6-trimethyl-phenyl)-amine,  $\text{C}_{15}\text{H}_{18}\text{N}_2$ ”
3. Germund Glatz, Torsten Irrgang, Rhett Kempe, *Z. Kristallogr. NCS* **2007**, *222(3)*, 287-288.  
“Crystal structure of bis( $\mu$ -bromo)-tetrakis(*tert*-butyl-(4-methyl-pyridin-2-yl)-amine)-dicopper(I),  $\text{Cu}_2\text{Br}_2(\text{C}_{10}\text{H}_{16}\text{N}_2)_4$ ”
4. Germund Glatz, Rhett Kempe, *Z. Kristallogr. NCS* **2008**, *223(3)*, 307-308.  
“Crystal structure of bis- $\mu_3$ (*N,N'*-bis(trimethylsilyl)-pyridine-2-amine-6-amido)- $\mu_4$ (*N,N'*-bis(trimethylsilyl)-pyridine-2,6-diamido)-di-tetrahydrofuran-tetralithium,  $[(\text{C}_{11}\text{H}_{21}\text{N}_3\text{Si}_2)(\text{C}_{11}\text{H}_{22}\text{N}_3\text{Si}_2)_2(\text{C}_4\text{H}_8\text{O})_2\text{Li}_4]$ ”
5. Germund Glatz, Rhett Kempe, *Z. Kristallogr. NCS* **2008**, *223(3)*, 309-310.  
“Crystal structure of bis- $\mu_2$ (*N,N'*-bis-(trimethylsilyl)-pyridine-2-amine-6-amido)-bis- $\mu_5$ (*N,N'*-bis-(trimethylsilyl)-pyridine-2,6-diamido)-di-)bromo-tetracopper(I),  $[(\text{Cu}_4\text{Br})(\text{C}_{11}\text{H}_{22}\text{N}_3\text{Si}_2)(\text{C}_{11}\text{H}_{21}\text{H}_{21}\text{N}_3\text{Si}_2)]_2$ ”
6. Germund Glatz, Rhett Kempe, *Z. Kristallogr. NCS* **2008**, *223(3)*, 311-312.  
“Crystal structure of tetra- $\mu_3$ -bromo-tetrakis-(trimethylsilyl)-(4-methylpyridine-2-yl)-amine)-tetracopper(I),  $[\text{CuBr}(\text{C}_9\text{H}_{16}\text{N}_2\text{Si})]_4$ ”

7. Germund Glatz, Rhett Kempe, *Z. Kristallogr. NCS* **2008**, *223(3)*, 313-315.  
“Crystal structure of bis-(*N,N'*-bis-(trimethylsilyl)-pyridine-2-amine-6-amido)-(*N,N'*-bis-(trimethylsilyl)-pyridine-2,6-diamido)-di-cobalt(II),  
 $\text{Co}_2(\text{C}_{11}\text{H}_{22}\text{N}_3\text{Si}_2)_2(\text{C}_{11}\text{H}_{21}\text{N}_3\text{Si}_2)$ ”
8. Awal Noor, Winfried P. Kretschmer, Germund Glatz, Auke Meetsma, Rhett Kempe, *Eur. J. Inorg. Chem.* **2008**, 5088-5098.  
“Synthesis and Structure of Zirconium and Hafnium Polymerisation Catalysts Stabilised by Very Bulky Aminopyridinato Ligands”
9. Germund Glatz, Günter Motz, Rhett Kempe, *Z. Anorg. Allg. Chem.* **2008**, *634*, 2897-2902.  
“Synthesis and Structure of a Hexameric Silver and Tetrameric Gold Aminopyridinates”
10. Benoît Blank, Germund Glatz, Rhett Kempe, *Chem. Asian J.* **2009**, *4*, 321-327.  
“Single and Double C-Cl Activation of Methylene Chloride by P,N-ligand Coordinated Rhodium Complexes”
11. Anna M. Dietel, Christian Döring, Germund Glatz, Mikhail V. Butovskii, Oleg Tok, Falko M. Schappacher, Rainer Pöttgen, Rhett Kempe, *Eur. J. Inorg. Chem.* **2009**, 1051-1059.  
“Bimetallic Complexes of Ytterbium and Europium Stabilized by Sterically Demanding Dipyridylamides”
12. Germund Glatz, Günter Motz, Rhett Kempe, *Eur. J. Inorg. Chem.* **2009**, 1385-1392.  
“First row Transition Metal Aminopyridinates – the Missing Compounds”
13. Germund Glatz, Günter Motz, Rhett Kempe, *Z. Anorg. Allg. Chem.* **2009**, *635*, 811-814.  
“Trilithium Trisaminotriazinates”

14. Awal Noor, Germund Glatz, Robert Müller, Martin Kaupp, Serhiy Demeshko, Rhett Kempe, *Z. Anorg. Allg. Chem.* **2009**, 635, 1149-1152.  
“Metal-Metal Distances at the Limit: Cr-Cr 1.73 Å – the Importance of the Ligand and its Fine Tuning”
15. Awal Noor, Germund Glatz, Robert Müller, Martin Kaupp, Serhiy Demeshko, Rhett Kempe, *Nature Chem.* **2009**, 1, 322-325  
“Carboalumination of a Cr-Cr Quintuple Bond”
16. Sadaf Qayyum, Awal Noor, Germund Glatz, Rhett Kempe, *Z. Anorg. Allg. Chem.* **2009**, DOI: 10.1002/zaac.200900249.  
“Attempted Reduction of Divalent Rare Earth Iodo Aminopyridinates”
17. Germund Glatz, Thomas Schmalz, Tobias Kraus, Günter Motz, Rhett Kempe, *Chem. Mater.* (to be submitted).  
“Novel Cu-SiCN ceramics via molecular design – Part I: Synthesis and characterisation of Cu-SiCN”
18. Germund Glatz, Thomas Schmalz, Tobias Kraus, Frank Haarmann, Günter Motz, Rhett Kempe (to be submitted).  
“Novel Cu-SiCN ceramics via molecular design – Part II: The Selective Oxidation of Simple Alkanes Using Air”

## 9. Danksagung

Meinem verehrten akademischen Lehrer,

Prof. Dr. Rhett Kempe

danke ich für die Überlassung des sehr interessanten Themas, die hervorragenden Arbeitsmöglichkeiten, sein stetes Interesse am Fortgang der Arbeit, seine unermüdliche Diskussionsbereitschaft und die gewährte enorme wissenschaftliche Freiheit. Weiterhin möchte ich ihm dafür danken, dass er mich in die Welt der Einkristallröntgenstrukturanalyse eingeführt hat.

Besonders bedanken möchte ich mich bei Dr. Günter Motz und Dr. Thomas Schmalz für ihre Unterstützung, Diskussionen und Motivation.

Ein großes Dankeschön geht an die von mir betreuten Praktikanten Andreas Lang, Kathrin Inzenhofer, Marina Schmäzlein, Anja Göckel, Michaela Kersch, Nico Helfricht und vor allem Matthias Pischl für ihre Arbeit und Hilfe, sowie an Cornelia Spörlein für die in Rahmen ihres Praktikums und Bachelorarbeit geleistete Arbeit.

Bei Walter Kremnitz, Heidi Maisel, Marlies Schilling, Sandra Keller und Anna Dietel möchte ich mich für die Unterstützung bei Verwaltungsangelegenheiten und bei alltäglichen Labordingen bedanken.

Für das Korrekturlesen dieser Arbeit sowie der darin enthaltenen Publikationen bin ich Dr. Katja Bensmann, Benoît Blank, Dr. Aderoju Osowole, Dr. Torsten Irrgang und Prof. Dr. Glen Deacon zu großem Dank verpflichtet.

Meinen Laborkollegen Heidi Maisel, Dr. Awal Noor und Sadaf Qayyum gilt ein ganz besonder großer Dank für die ausgesprochen gute Arbeitsatmosphäre, Hilfsbereitschaft und Freundlichkeit, die in unserem Labor herrschte.

Meinen Arbeitskollegen Dr. Denise Friedrich, Christian Döring, Benoît Blank, Dr. Sebastian Proch, Justus Hermannsdörfer, Tobias Bauer und Heidi Maisel danke ich

ganz besonders für die gemeinsam verbrachte Zeit, die nicht immer nur den chemischen Fragen gewidmet war. Weiterhin bin ich ihnen gegenüber für ihre gewaltige Hilfsbereitschaft und tatkräftige Unterstützung in vielerlei Hinsicht zu Dank verpflichtet.

Den anderen Mitgliedern der Arbeitsgruppe Kempe, Dr. Winfried Kretschmer, Kathrin Kutlescha, Dr. Mikhail Butovskii und Dr. Torsten Irrgang danke ich für die immerwährende Diskussionsbereitschaft und Hilfe in vielen Dingen.

Weiterhin danke ich allen anderen, die am Lehrstuhl AC II arbeiten (besonders Julian Lang und Dr. Christine Denner), für die konstruktive und lustige Arbeitsatmosphäre.

Bei Dr. Jessica Benner, Dr. Stefan Hinrichs, Dr. Esteban Vöhringer-Martinez, Ole Revermann, Wiebke Heuer, Dr. Edith Wöltjen, Dr. Anna Sachse, Stefanie Jonas, Katja Petersen, Dominik Erhard, Dr. Markus Retsch, Dr. Felix Schacher, Bertram Barnickel, Dr. Marc Schrunner, Sonja Endres, Dr. Hanna Berkner und Dr. Stefan Prasch möchte ich mich für ihre Freundschaft und langjährige Unterstützung in meiner Zeit in Göttingen und Bayreuth bedanken.

Meinem bestem Freund und Mitbewohner Maximilian Hartl danke ich für die Aufmunterungen, vielen Diskussionen, die Joggingrunden, Fernsehabeude, spontanen Feiern und seine treue Freundschaft und Gesellschaft seit so vielen Jahren.

Meinen Schwestern Heidrun und Diemut gilt ein ganz außerordentliches Dankeschön für ihre ständige Unterstützung.

Desweiteren möchte ich mich bei meinen Eltern für ihre Motivation und Hilfe bedanken, auf die ich mich stets verlassen konnte.

Zuletzt aber möchte ich mich bei Katja für ihre grenzenlose Liebe, unendliche Geduld und zahllose Aufmunterungen bedanken, mit der sie mir besonders in der letzten Zeit weit mehr geholfen hat, als sie denkt.

## Acknowledgment

Firstly, I would like to express my deep gratitude to my supervisor,

Prof. Dr. Rhett Kempe

for the very interesting topic, the excellent working conditions, his continuous support, his indefatigable readiness to discuss and the great academic liberty. Furthermore I like to thank him for introducing me into the world of single crystal X-ray analysis.

A special thanks goes to Dr. Günter Motz and Dr. Thomas Schmalz for their support, discussions and motivation.

I am very thankful to my student apprentices Andreas Lang, Kathrin Inzenhofer, Marina Schmäzlein, Anja Göckel, Michaela Kersch, Nico Helfricht and especially Matthias Pischl for their work and help, and to Cornelia Spörlein for the work done during her Bachelor Thesis.

Thanks to Walter Kremnitz, Heidi Maisel, Marlies Schilling, Sandra Keller und Anna Dietel for their support in administration related things and everyday matters.

I am indebted to Dr. Katja Bensmann, Benoît Blank, Dr. Aderoju Osowole, Dr. Torsten Irrgang and Prof. Dr. Glen Deacon for proof-reading this thesis and the containing manuscripts.

Futhermore, I am very grateful to my lab colleagues Heidi Maisel, Dr. Awal Noor and Sadaf Qayyum for the very nice helping atmosphere and niceness in our lab.

I appreciate my colleagues Dr. Denise Friedrich, Christian Döring, Benoît Blank, Dr. Sebastian Proch, Justus Hermannsdörfer, Tobias Bauer and Heidi Maisel for their nice company and the time spent together, which was not always dedicated to chemistry. Moreover, I am grateful for their immense helpfulness and support concerning all kinds of things.

Thanks to the other group members, Dr. Winfried Kretschmer, Kathrin Kutlescha, Dr. Mikhail Butovskii and Dr. Torsten Irrgang for their discussions and help in all kinds of things.

Furthermore, I would like to thank all other people, who work at the chair of inorganic chemistry II (especially Julian Lang and Dr. Christine Denner), for the constructive and cheerful atmosphere.

I would like to express my gratitude to Jessica Benner, Dr. Stefan Hinrichs, Dr. Esteban Vöhringer-Martinez, Ole Revermann, Wiebke Heuer, Dr. Edith Wöltjen, Dr. Anna Sachse, Stefanie Jonas, Katja Petersen, Dominik Erhard, Dr. Markus Retsch, Dr. Felix Schacher, Bertram Barnickel, Dr. Marc Schrinner, Sonja Endres, Dr. Hanna Berkner and Dr. Stefan Prasch for their friendship and long-term support during my time in Göttingen and Bayreuth.

Special thanks to my best friend Maximilian Hartl for his encouragement, discussions, being a running partner, television evenings, spontaneous partys, his loyal friendship and company since so many years.

Finally I am exceptionally grateful to my sisters Heidrun und Diemut for their continuous support.

Furthermore I would like to thank my parents for their motivation and help I always could count on.

Last but not least, I would like to thank Katja for her endless love, neverending patience, and countless encouragement, which helped me more than she thinks, notably during the last time.

## 10. Declaration/Erklärung

Hereby I declare that I have written this work by myself and that I have not used any other sources except those mentioned in this work. Furthermore, I declare that this work has so far neither been submitted to the Faculty of Biology, Chemistry and Earth Sciences at the University of Bayreuth nor to any other scientific institution for the purpose of doctorate. I never finally failed a similar doctoral examination at any other university.

Hiermit erkläre ich, dass ich die Arbeit selbständig verfasst und keine anderen als die von mir angegebenen Quellen und Hilfsmittel benutzt habe.

Ferner erkläre ich, dass ich anderweitig mit oder ohne Erfolg nicht versucht habe, diese Dissertation einzureichen. Ich habe keine gleichartige Doktorprüfung an einer anderen Hochschule endgültig nicht bestanden.

---

Germund Glatz

## 11. Appendix

### General remarks

Unless mentioned otherwise, all manipulations were carried out under exclusion of oxygen and moisture by using standard Schlenk or glove box techniques. Non-halogenated solvents were distilled from sodium benzophenone ketyl and halogenated solvents from P<sub>2</sub>O<sub>5</sub>. Deuterated solvents were obtained from Cambridge Isotope Laboratories and were degassed, dried with molecular sieves and distilled prior to use. All chemicals were purchased from commercial sources and used without further purification unless mentioned otherwise in the synthetic procedure. NMR spectra were recorded with either a Varian INOVA 300 or a Varian INOVA 400 spectrometer. Chemical shifts are reported in ppm relative to the deuterated solvent. Elemental analyses were carried out on a Vario elementar EL III.

### Complex Synthesis and Characterisation

A number of additional transition metal aminopyridinato complexes were synthesised and characterised. These novel complexes are presented in the following.

#### Synthesis of [Pt(Ap<sup>TMS</sup>)<sub>2</sub>]

The platinum aminopyridinate [Pt(Ap<sup>TMS</sup>)<sub>2</sub>] (Figure 11.1) is obtained by a salt metathesis reaction with [PtCl<sub>2</sub>(cod)] and lithiated Ap<sup>TMS</sup> (cod = cyclooctadiene).

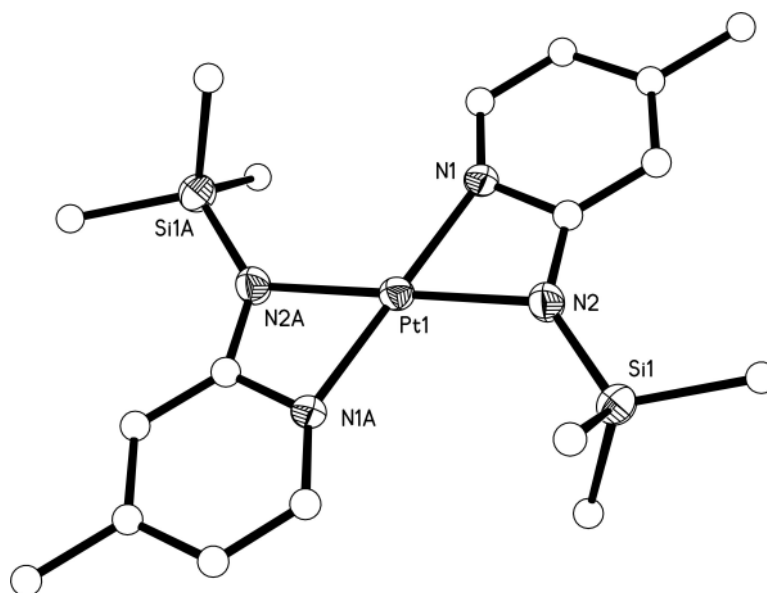


**Figure 11.1.** Molecular structure of  $[\text{Pt}(\text{Ap}^{\text{TMS}})_2]$  (ORTEP view, for clarity, only non-carbon atoms are drawn as 50% probability ellipsoids). Selected bond lengths [ $\text{\AA}$ ] and angles [ $^\circ$ ]: Pt1-N1 2.021(2), Pt1-N2 2.061(3), N1-Pt1-N2 64.72(11).

A solution of  $\text{Ap}^{\text{TMS}}\text{H}$  (721 mg, 4 mmol) in 30 mL of  $\text{Et}_2\text{O}$  was treated with 2.5 mL (1.6 M, 4 mmol) of  $n\text{BuLi}$  in hexanes at  $0\text{ }^\circ\text{C}$  and stirred for 30 min and then one hour at room temperature. The mixture turned from colourless to yellow. It was then added to a suspension of  $[\text{PtCl}_2(\text{cod})]$  (748 mg, 2 mmol) in 180 mL of thf at  $0\text{ }^\circ\text{C}$ . The orange solution was stirred overnight at room temperature. After removing the solvent, the residue was extracted four times with 40 mL of hexane, filtered and concentrated. Yellow crystals and a yellow precipitate were obtained after storage in a freezer at  $-30\text{ }^\circ\text{C}$ . Yield 958 mg (1.7 mmol, 87%).  $\text{C}_{18}\text{H}_{30}\text{N}_4\text{Si}_2\text{Pt}$  (553.71): calcd C 39.04, H 5.46, N 10.12; found C 39.28, H 5.39, N 9.94.  $^1\text{H}$  NMR (300 MHz, thf- $d_8$ , 296 K):  $\delta$  = 0.22 (s, 18 H, TMS), 2.13 (s, 6 H, ar- $\text{CH}_3$ ), 5.65 (s, 2 H), 5.94 (d,  $J_{\text{H,H}} = 5.7\text{ Hz}$ , 2 H), 7.45 (d,  $J_{\text{H,H}} = 5.7\text{ Hz}$ , 2 H) ppm.  $^{13}\text{C}$  NMR (300 MHz, thf- $d_8$ , 296 K):  $\delta$  = 2.06, 25.51, 109.12, 112.54, 143.70, 149.57, 179.53 ppm.  $^{29}\text{Si}$  NMR (300 MHz, thf- $d_8$ , 296 K):  $\delta$  = 2.92 ppm.  $^{195}\text{Pt}$  NMR (250 MHz,  $\text{CDCl}_3$ , 296 K):  $\delta$  = 2896 ppm.

### Synthesis of $[\text{Rh}(\text{Ap}^{\text{TMA}})(\text{cod})]$ and $[\text{Ir}(\text{Ap}^{\text{TMA}})(\text{cod})]$

In the case of rhodium and iridium, the customary ligand  $\text{Ap}^{\text{TMS}}$  could not be used with regard to the catalytic cleavage of the N-Si bond. Therefore, the only C-C and C-N bond containing ligand  $\text{Ap}^{\text{TMA}}$  was used to obtain rhodium and iridium

aminopyridinates, whose molecular structures are shown in Figure 11.2 and 11.3, respectively.<sup>[1]</sup>

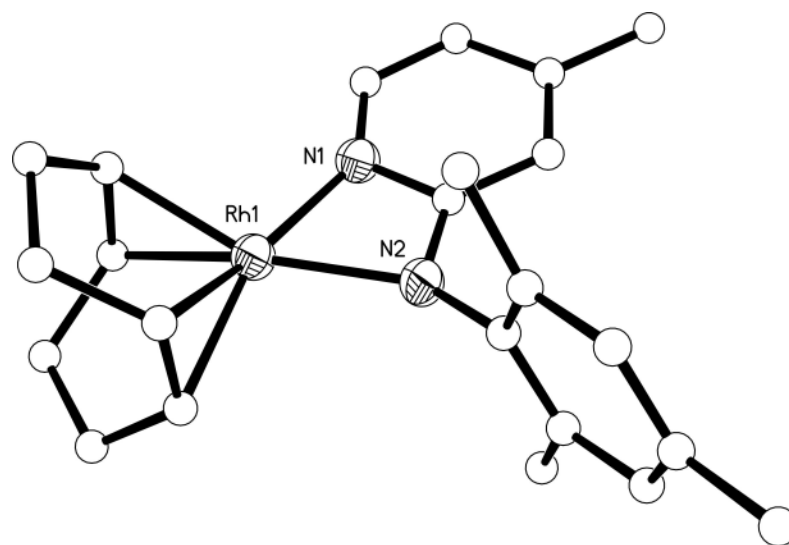


**Figure 11.2.** Molecular structure of  $[\text{Rh}(\text{Ap}^{\text{TMA}})(\text{cod})]$  (ORTEP view, for clarity, only non-carbon atoms are drawn as 50% probability ellipsoids). Selected bond lengths [Å] and angles [°]: Rh1-N1 2.090(3), Rh1-N2 2.077(2), N1-Rh1-N2 64.10(9).

**$[\text{Rh}(\text{Ap}^{\text{TMA}})(\text{cod})]$ .** A solution of  $\text{Ap}^{\text{TMA}}\text{H}$  (453 mg, 2 mmol) in 35 mL of  $\text{Et}_2\text{O}$  was treated with 1.25 mL (1.6 M, 2 mmol) of  $n\text{BuLi}$  in hexanes at 0 °C and stirred overnight at room temperature. It was then added to a solution of  $[\text{RhCl}(\text{cod})]_2$  (493 mg, 1 mmol) in 25 mL of thf at 0 °C and stirred again overnight at room temperature. After removing the solvent, the residue was extracted with 25 mL of hexane and concentrated to one third of the original volume. Yellow crystals and a yellow precipitate of  $[\text{Rh}(\text{Ap}^{\text{TMA}})(\text{cod})]$  could be obtained by storage in a freezer at -30 °C. Yield 665 mg (1.5 mmol, 76%).  $\text{C}_{23}\text{H}_{29}\text{N}_2\text{Rh}$  (436.40): calcd C 63.30, H 6.70, N 6.42; found C 63.14, H 6.82, N 6.33.  $^1\text{H}$  NMR (400 MHz, thf- $d^8$ , 296 K):  $\delta$  = 1.73 (s, br, 4 H, cod), 1.91 (s, 3 H, ar- $\text{CH}_3$ ), 2.17 (s, 3 H, ar- $\text{CH}_3$ ), 2.29 (s, 6 H, ar- $\text{CH}_3$ ), 2.40 (s, 4 H, cod), 3.63 (s, br, 2 H, cod), 4.09 (s, br, 2 H, cod), 5.04 (s, 1 H), 5.71 (d,  $J_{\text{H,H}} = 5.6$  Hz, 1 H), 6.75 (s, 2 H), 6.95 (d,  $J_{\text{H,H}} = 5.6$  Hz, 1 H) ppm.  $^{13}\text{C}$  NMR (400 MHz, thf- $d^8$ , 296 K):  $\delta$  = 18.98, 21.19, 21.79, 31.95, 77.14, 80.26, 104.97, 108.17, 129.52, 133.29, 134.89, 141.96, 144.17, 151.44, 176.34 ppm.

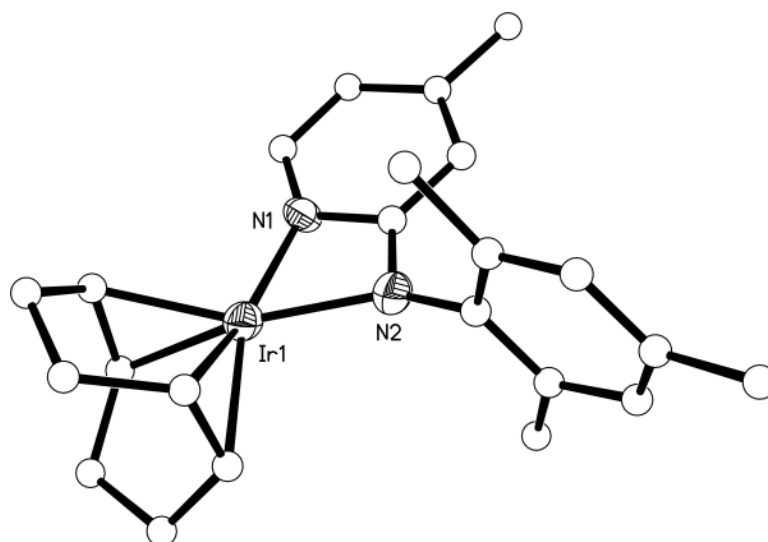


**Figure 11.3.** Molecular structure of  $[\text{Ir}(\text{Ap}^{\text{TMA}})(\text{cod})]$  (ORTEP view, for clarity, only non-carbon atoms are drawn as 50% probability ellipsoids and the second crystallographically independent molecule is not shown). Selected bond lengths [Å] and angles [°]: Ir1-N1 2.092(11), Ir1-N2 2.064(11), N1-Ir1-N2 63.6(4).

**$[\text{Ir}(\text{Ap}^{\text{TMA}})(\text{cod})]$ .** A solution of  $\text{Ap}^{\text{TMA}}\text{H}$  (453 mg, 2 mmol) in 60 mL of  $\text{Et}_2\text{O}$  was treated with 1.25 mL (1.6 M, 2 mmol) of  $n\text{BuLi}$  in hexanes at 0 °C and stirred overnight at room temperature. It was then added to a solution of  $[\text{IrCl}(\text{cod})]_2$  (671 mg, 1 mmol) in 100 mL of thf at 0 °C and stirred again overnight at room temperature. After removing the solvent, the residue was extracted with 40 mL of hexane. Orange crystals and a orange precipitate of  $[\text{Ir}(\text{Ap}^{\text{TMA}})(\text{cod})]$  could be obtained by storage in a freezer at -30 °C. Yield 444 mg (0.84 mmol, 42%).  $\text{C}_{23}\text{H}_{29}\text{N}_2\text{Ir}$  (525.71): calcd. C 52.55, H 5.56, N 5.33; found C 52.36, H 5.65, N 5.34.  $^1\text{H}$  NMR (300 MHz,  $\text{thf-d}^8$ , 296 K):  $\delta$  = 1.35 (s, br, 4 H, cod), 1.85 (s, 3 H, ar- $\text{CH}_3$ ), 2.01-2.23 (m, br, 13 H, cod, ar- $\text{CH}_3$ ), 3.41 (s, br, 2 H, cod), 3.72 (s, br, 2 H, cod), 4.97 (s, 1 H), 5.77 (d,  $J_{\text{H,H}} = 5.7$  Hz, 1 H), 6.68 (s, 2 H), 7.07 (d,  $J_{\text{H,H}} = 5.7$  Hz, 1 H) ppm.  $^{13}\text{C}$  NMR (300 MHz,  $\text{thf-d}^8$ , 296 K):  $\delta$  = 18.56, 21.02, 22.00, 23.99, 59.61, 64.75, 106.35, 109.64, 129.34, 134.24, 135.31, 140.30, 143.22, 153.19, 179.34 ppm.

### Synthesis of $[\text{Mo}(\text{Ap}^{\text{TMS}})_2(\text{dipi})_2]$ , $[\text{W}(\text{Ap}^{\text{TMS}})_2(\text{dipi})_2]$ and $[\text{Re}(\text{Ap}^{\text{TMS}})(\text{dipi})_3]$

Additional anionic ligands are necessary to stabilise molybdenum(VI), tungsten(VI) and rhenium(VII) aminopyridinates. For this purpose, 2,6-diisopropylphenyl-imido (dipi) was chosen as ligand due to the easy accessibility of corresponding molybdenum,<sup>[2]</sup> tungsten<sup>[2]</sup> and rhenium<sup>[3]</sup> compounds. Furthermore, dipi contains only carbon and

nitrogen, which is important with regard to the manufacture of metal-modified SiCN ceramics. The molecular structures of the molybdenum precursor, molybdenum aminopyridinate, tungsten aminopyridinate and rhenium aminopyridinate are shown in Figures 11.4, 11.5, 11.6 and 11.7, respectively.

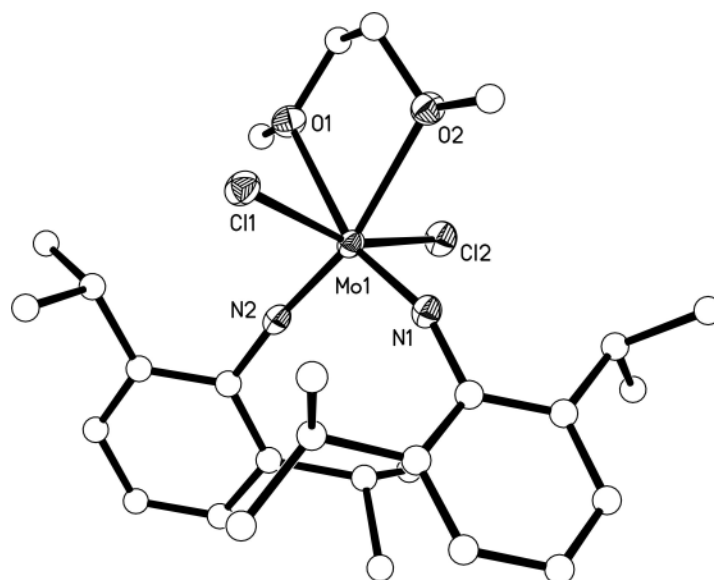


**Figure 11.4.** Molecular structure of  $[\text{MoCl}_2(\text{dme})(\text{dipi})_2]$  (ORTEP view, for clarity, only non-carbon atoms are drawn as 50% probability ellipsoids). Selected bond lengths [ $\text{\AA}$ ] and angles [ $^\circ$ ]: Mo1-N1 1.7495(17), Mo1-N2 1.7447(16), Mo1-Cl1 2.3953(5), Mo1-Cl2 2.4005(5), Mo1-O1 2.391(15), Mo1-O2 2.3119(14), Cl1-Mo1-Cl2 158.62(2), N1-Mo1-N2 105.27(8), O1-Mo1-O2 69.47(5).

**$[\text{MoCl}_2(\text{dme})(\text{dipi})_2]$ .** The molybdenum imido complex was synthesised according to a literature procedure.<sup>[2]</sup> The mother liquor was stored in a freezer at  $-30\text{ }^\circ\text{C}$  for a few weeks to yield dark red crystals of  $[\text{MoCl}_2(\text{dme})(\text{dipi})_2]$ .  $\text{C}_{28}\text{H}_{44}\text{N}_2\text{Cl}_2\text{MoN}_2\text{O}_2$  (607.51): calcd C 55.36, H 7.30, N 4.61; found C 54.96, H 7.85, N 4.65.  $^1\text{H}$  NMR (400 MHz,  $\text{C}_6\text{D}_6$ , 296 K):  $\delta$  = 1.26 (d,  $J_{\text{H,H}}$  = 6.8 Hz, 24 H,  $\text{CH}_3$ ), 3.20 (s, 4 H, dme), 3.45 (s, 6 H, dme), 4.30 (sept,  $J_{\text{H,H}}$  = 6.8 Hz, 4 H, CH), 6.90 (t,  $J_{\text{H,H}}$  = 6.8 Hz, 2 H), 7.01 (d,  $J_{\text{H,H}}$  = 6.8 Hz, 4 H) ppm.  $^{13}\text{C}$  NMR (400 MHz,  $\text{C}_6\text{D}_6$ , 296 K):  $\delta$  = 22.99, 25.44, 28.40, 62.82, 71.35, 123.76, 127.89, 145.31, 153.97 ppm.

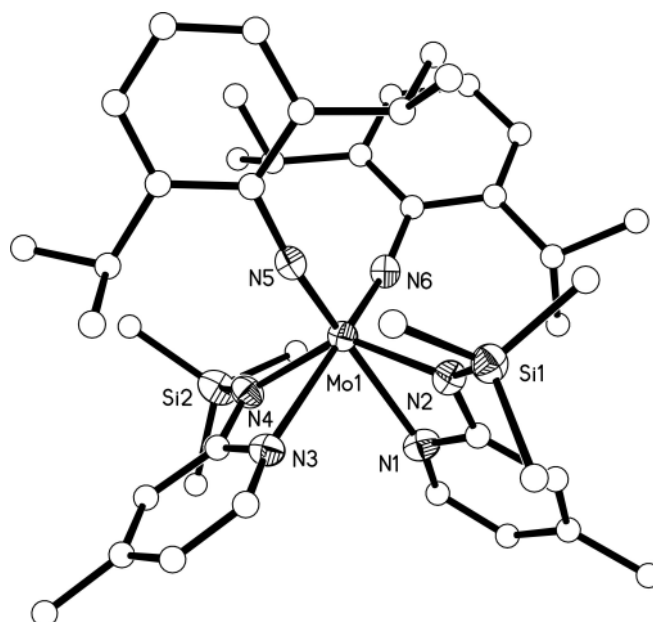


**Figure 11.5.** Molecular structure of  $[\text{Mo}(\text{Ap}^{\text{TMS}})_2(\text{dipi})_2]$  (ORTEP view, for clarity, only non-carbon atoms are drawn as 50% probability ellipsoids). Selected bond lengths [Å] and angles [°]: Mo1-N1 2.3217(17), Mo1-N2 2.1064(17), Mo1-N3 2.3334(18), Mo1-N4 2.1137(18), Mo1-N5 1.7627(17), Mo1-N6 1.7703(17), N1-Mo1-N2 60.36(7), N3-Mo1-N4 60.01(7), N5-Mo1-N6 102.27(8).

**$[\text{Mo}(\text{Ap}^{\text{TMS}})_2(\text{dipi})_2]$ .** A solution of  $\text{Ap}^{\text{TMS}}\text{H}$  (721 mg, 4 mmol) in 40 mL of  $\text{Et}_2\text{O}$  was treated with 2.5 mL (1.6 M, 4 mmol) of  $n\text{BuLi}$  in hexanes at 0 °C and stirred overnight at room temperature. It was then added to a solution of  $[\text{MoCl}_2(\text{dme})(\text{dipi})_2]$  (1.215 g, 2 mmol) in 29 mL of thf at 0 °C and stirred again overnight at room temperature, whereupon the colour changed from red to red-brown. After removing the solvent, the residue was extracted with 40 mL of hexane. Concentration and storage in a freezer at -30 °C afforded dark red crystals and a dark red precipitate of  $[\text{Mo}(\text{Ap}^{\text{TMS}})_2(\text{dipi})_2]$ . The yield may be increased by further concentration of the mother liquor. Yield 172 mg (0.21 mmol, 11%).  $\text{C}_{42}\text{H}_{64}\text{N}_6\text{Si}_2\text{Mo}$  (805.11): calcd C 62.66, H 8.01, N 10.44; found C 62.36, H 8.02, N 10.14.  $^1\text{H}$  NMR (400 MHz,  $\text{C}_6\text{D}_6$ , 296 K):  $\delta$  = 0.51 (s, 18 H, TMS), 0.85 (d,  $J_{\text{H,H}} = 6.8$  Hz, 12 H,  $\text{CH}_3$ ), 1.29 (d,  $J_{\text{H,H}} = 6.8$  Hz, 12 H,  $\text{CH}_3$ ), 1.86 (s, 6 H, ar- $\text{CH}_3$ ), 3.59 (sept,  $J_{\text{H,H}} = 6.8$  Hz, 4 H, CH), 5.97 (d,  $J_{\text{H,H}} = 5.2$  Hz, 2 H), 6.39 (s, 2 H), 6.86 (t,  $J_{\text{H,H}} = 7.6$  Hz, 2 H), 6.99 (d,  $J_{\text{H,H}} = 7.6$  Hz, 4 H), 7.93 (d,  $J_{\text{H,H}} = 5.2$  Hz, 2 H) ppm.  $^{13}\text{C}$  NMR (400 MHz,  $\text{C}_6\text{D}_6$ , 296 K):  $\delta$  = 3.06, 21.67, 24.50, 25.06, 28.53, 112.70, 114.07, 123.44, 124.63, 142.71, 143.58, 149.58, 155.74, 170.10 ppm.  $^{29}\text{Si}$  NMR (300 MHz,  $\text{C}_6\text{D}_6$ , 296 K):  $\delta$  = 6.61 ppm.

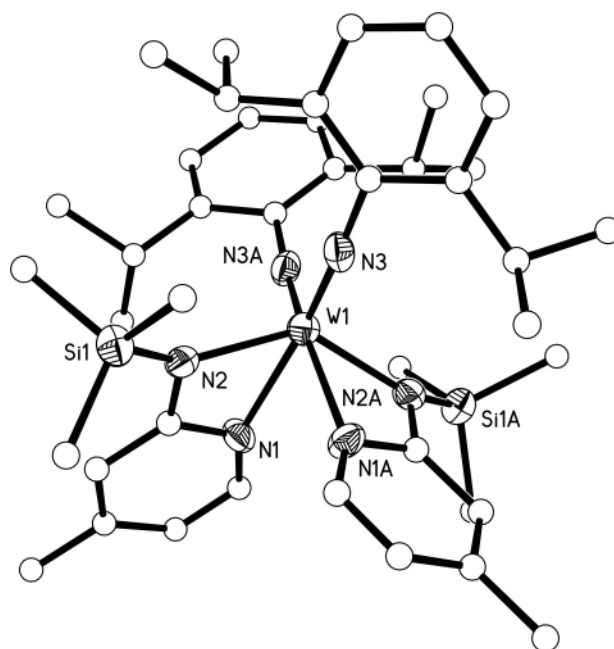


**Figure 11.6.** Molecular structure of  $[W(\text{Ap}^{\text{TMS}})_2(\text{dipi})_2]$  (ORTEP view, for clarity, only non-carbon atoms are drawn as 50% probability ellipsoids and the second crystallographically independent molecule is not shown). Selected bond lengths [Å] and angles [°]: W1-N1 2.280(10), W1-N2 2.104(10), W1-N3 1.780(10), N1-W1-N2 61.4(4), N3-W1-N3A 102.2(6).

**$[W(\text{Ap}^{\text{TMS}})_2(\text{dipi})_2]$ .** A solution of  $\text{Ap}^{\text{TMS}}\text{H}$  (1.44 g, 8 mmol) in 30 mL of  $\text{Et}_2\text{O}$  was treated with 5 mL (1.6 M, 8 mmol) of  $n\text{BuLi}$  in hexanes at 0 °C and stirred overnight at room temperature. It was then added to a solution of  $[W\text{Cl}_2(\text{dme})(\text{dipi})_2]^{[2]}$  (2.78 g, 4 mmol) in 25 mL of thf at 0 °C and stirred again overnight at room temperature. After removing the solvent, the residue was extracted with 50 mL of hexane. Concentration and storage in a freezer at -30 °C afforded orange crystals and an orange precipitate of  $[W(\text{Ap}^{\text{TMS}})_2(\text{dipi})_2]$ . The yield may be increased by further concentration of the mother liquor. Yield 307 mg (0.34 mmol, 9%).  $\text{C}_{42}\text{H}_{64}\text{N}_6\text{Si}_2\text{W}$  (893.01): calcd C 56.49, H 7.22, N 9.41; found C 56.39, H 7.57, N 9.14.  $^1\text{H}$  NMR (400 MHz,  $\text{C}_6\text{D}_6$ , 296 K):  $\delta$  = 0.50 (s, 18 H, TMS), 0.89 (d,  $J_{\text{H,H}} = 6.8$  Hz, 12 H,  $\text{CH}_3$ ), 1.32 (d,  $J_{\text{H,H}} = 6.8$  Hz, 12 H,  $\text{CH}_3$ ), 1.82 (s, 6 H, ar- $\text{CH}_3$ ), 3.58 (sept,  $J_{\text{H,H}} = 6.8$  Hz, 4 H, CH), 5.97 (d,  $J_{\text{H,H}} = 5.6$  Hz, 2 H), 6.36 (s, 2 H), 6.85 (t,  $J_{\text{H,H}} = 7.6$  Hz, 2 H), 7.09 (d,  $J_{\text{H,H}} = 7.6$  Hz, 4 H), 7.94 (d,  $J_{\text{H,H}} = 5.6$  Hz, 2 H) ppm.  $^{13}\text{C}$  NMR (400 MHz,  $\text{C}_6\text{D}_6$ , 296 K):  $\delta$  = 3.03, 21.81, 24.74, 25.02, 28.31, 113.63, 114.58, 123.08, 123.48, 142.52, 143.03, 150.17, 154.35, 168.81 ppm.  $^{29}\text{Si}$  NMR (400 MHz,  $\text{C}_6\text{D}_6$ , 296 K):  $\delta$  = 7.68 ppm.

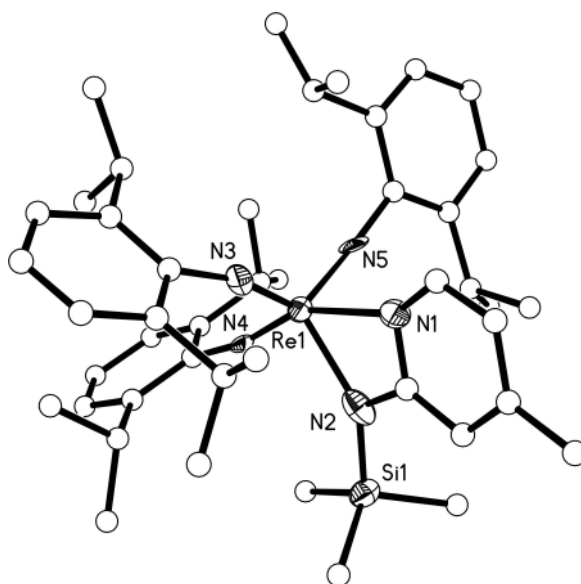


**Figure 11.7.** Molecular structure of  $[\text{Re}(\text{Ap}^{\text{TMS}})(\text{dipi})_3]$  (ORTEP view, for clarity, only non-carbon atoms are drawn as 50% probability ellipsoids and the second crystallographically independent molecule is not shown). Selected bond lengths [ $\text{\AA}$ ] and angles [ $^\circ$ ]: Re1-N1 2.345(8), Re1-N2 2.059(8), Re1-N3 1.680(8), Re1-N4 1.721(8), Re1-N5 1.690(8), N1-Re1-N2 59.7(3), N3-Re1-N4 102.2(3), N3-Re1-N5 116.8(3), N4-Re1-N5 109.5(3).

**$[\text{Re}(\text{Ap}^{\text{TMS}})(\text{dipi})_3]$ .** A solution of  $\text{Ap}^{\text{TMS}}\text{H}$  (0.902 g, 5 mmol) in 25 mL of  $\text{Et}_2\text{O}$  was treated with 3.13 mL (1.6 M, 5 mmol) of  $n\text{BuLi}$  in hexanes at  $0\text{ }^\circ\text{C}$  and stirred overnight at room temperature. It was then added to a solution of  $[\text{ReCl}(\text{dipi})_3]^{[3]}$  (3.74 g, 5 mmol) in 25 mL of thf at  $0\text{ }^\circ\text{C}$  and stirred again overnight at room temperature. After removing the solvent, the residue was extracted with 50 mL of hexane. Concentration and storage in a freezer at  $-30\text{ }^\circ\text{C}$  afforded very dark red (almost black) crystals and a black precipitate of  $[\text{Re}(\text{Ap}^{\text{TMS}})(\text{dipi})_3]$ . The yield may be increased by further concentration of the mother liquor. Yield 1.58 g (1.8 mmol, 36%).  $\text{C}_{45}\text{H}_{66}\text{N}_5\text{SiRe}$  (891.33): calcd C 60.64, H 7.46, N 7.86; found C 60.28, H 7.95, N 7.64.  $^1\text{H}$  NMR (400 MHz,  $\text{C}_6\text{D}_6$ , 296 K):  $\delta$  = 0.38 (s, 9 H, TMS), 1.12 (d,  $J_{\text{H,H}}$  = 6.8 Hz, 36 H, CH<sub>3</sub>), 1.79 (s, 3 H, ar-CH<sub>3</sub>), 3.75 (sept,  $J_{\text{H,H}}$  = 6.8 Hz, 6 H, CH), 6.07 (d,  $J_{\text{H,H}}$  = 5.6 Hz, 1 H), 6.55 (s, 1 H), 6.89 (t,  $J_{\text{H,H}}$  = 7.6 Hz, 3 H), 7.09 (d,  $J_{\text{H,H}}$  = 7.6 Hz, 6 H), 7.96 (d,  $J_{\text{H,H}}$  = 5.6 Hz, 1 H) ppm.  $^{13}\text{C}$  NMR (400 MHz,  $\text{C}_6\text{D}_6$ , 296 K):  $\delta$  = 2.92, 21.82, 24.35, 28.64, 112.75, 116.23, 122.74, 126.05, 141.85, 143.58, 149.53, 155.13, 166.74 ppm.  $^{29}\text{Si}$  NMR (400 MHz,  $\text{C}_6\text{D}_6$ , 296 K):  $\delta$  = 13.77 ppm.

- [1] G. Glatz, T. Irrgang, R. Kempe, *Z. Kristallogr. NCS* **2007**, *222(3)*, 265-266.
- [2] R. R. Schrock, R. T. DePue, J. Feldman, K. B. Yap, D. C. Yang, W. M. Davis, L. Park, M. DiMare, M. Schofield, J. Anhaus, E. Walborsky, E. Evitt, C. Krüger, P. Betz, *Organometallics* **1990**, *9*, 2262-2275.
- [3] D. S. Williams, R. R. Schrock, *Organometallics*, **1993**, *12*, 1148-1160.